Scuola di Ingegneria Industriale e dell'Informazione

Corso di Laurea Magistrale in
Energy for Development

POLITECNICO
MILANO 1863

Techno-economic design of an advanced generation plant equipped with an MPC controller in a 4th generation district heating network

Relatore: Prof. Luigi Pietro Maria COLOMBO

Correlatore: Ing. Andrea ROSSETTI

Tesi di Laurea di:

Michele PRAOLINI Matr. 854626

Anno Accademico 2017 - 2018

Ringraziamenti

In questo piccolo frammento di tesi desidero ringraziare tutti coloro che, direttamente o indirettamente, hanno contribuito alla sua realizzazione ed al coronamento di questo difficile traguardo.

Anzitutto vorrei ringraziare il mio relatore, il professor Luigi Colombo, per la sua grande disponibilità e per i preziosi consigli che mi ha fornito.

Un ringraziamento speciale va al mio tutor e correlatore, l'ing. Andrea Rossetti, che mi ha dato la possibilità di svolgere questa tesi e che, con pazienza ed amicizia, ha saputo guidarmi durante il tirocinio, dimostrando tutta la sua competenza e professionalità.

Colgo l'occasione per ringraziare anche Luigi Mazzocchi, Carmen Valli e tutti i nuovi amici e colleghi di R.S.E. che ho avuto il piacere di conoscere grazie a questa opportunità, oltre che l'azienda stessa.

Ringrazio tutta la mia splendida e numerosa famiglia, per aver creduto in me e per avermi sempre sostenuto. Mi sento fortunato ad essere circondato da persone così straordinarie, e la vostra presenza rappresenta un porto sicuro nella mia vita su cui potrò sempre fare affidamento. In particolare ringrazio mia mamma, Anna, mio papà, Alfredo, e mia sorella, Lisa. Ringrazio mia nonna Luisa, da sempre grande esempio di vita e fonte di ispirazione, e mia nonna Ucci che, anche da lassù, ha sempre vegliato su di me durante questo cammino impegnativo.

Ringrazio i miei amici Vittorio, Cesare, Francesco, Davide e tutti i colleghi di università con cui ho condiviso gli anni di studi, che sono stati di enorme conforto in questi anni. Ringrazio specialmente Giacomo, che con la sua incrollabile fiducia mi ha incoraggiato a proseguire durante i periodi più ardui di questo percorso.

Per concludere, ringrazio anche me stesso, per aver stretto i denti e non aver mai mollato fino alla fine.

Alla nonna Ucci

Da qualche parte,
qualcosa di incredibile è
in attesa di essere scoperto.
(Carl Sagan)

Gli ingegneri amano risolvere i problemi.
Se non hanno problemi a portata di mano,
li creano subito.
(Scott Adams)

Table of contents

List of figures

List of tables

Nomenclature and acronyms

EU	European Union
MPC	Model Predictive Control
DHN	District Heating Network
WTE	Waste-to-energy
RES	Renewable Energy Sources
CHP	Combined Heat and Power
4GDH	4th Generation District Heating
TMY2	Typical Meteorological Year Version 2
NFRC	National Fenestration Rating Council
COND	Condominium
COM	Company
PF	Physical person
HP	Heat Pump
ICE	Internal Combustion Engine
GT	Gas Turbine
NPV	Net Present Value
NCF	Net Cash Flows
MGP	Mercato del Giorno Prima
PZ	Prezzo Zonale
PUN	Prezzo Unico Nazionale
SEN	Strategia Energetica Nazionale
MSD	Mercato dei Servizi di Dispacciamento

Abstract

This thesis work focused on the design of the generation section of a 4th generation district heating system in order to maximize its synergies with the electric system, as well as the economic result. A TRNSYS model has been used to simulate the reference district heating network of Canavese (MI). To comply with the objective of this work, an optimization and control tool based on Model Predictive Control has been developed within a Matlab environment. This optimizer uses a simplified model of the reference network to predict its response to any set of the generators' state, over a certain time horizon, and it minimizes the operational costs of heat generation. The developed tool has been subsequently used to identify the economically optimal plant configuration for a given set of generation technologies, under four different electricity price scenarios, future and actual. The generators selected were a gas-fuelled internal combustion engine, a gas turbine and a groundwater heat pump. At last, a sensitivity analysis was performed on the most important parameters.

The results showed that the internal combustion engine technology is the preferable solution, because it allows exploiting the high prices for the sale of electricity during peak hours. This translates into a beneficial stabilizing effect on the electrical network. Moreover, simultaneous participation of the plant in both day-ahead and ancillary services markets is highly desirable, since it allows maximizing the economic advantages given by the fact that thermal energy demand results anti-cyclical compared to electrical energy one. The coupling of a combustion engine and a heat pump seems to be competitive only for a rather small size of the latter, which allow it to run entirely with the electricity produced by the engine.

Keywords: District heating system, model predictive control.

Sommario

Questa tesi si è focalizzata sulla progettazione della sezione di generazione di un sistema di teleriscaldamento di quarta generazione, al fine di massimizzarne le sinergie con il sistema elettrico, nonché il risultato economico. Un modello TRNSYS è stato utilizzato per simulare la rete di teleriscaldamento di riferimento di Canavese (MI). Per soddisfare l'obiettivo di questo lavoro, è stato sviluppato in ambiente Matlab uno strumento di ottimizzazione e controllo basato sul Model Predictive Control. Questo ottimizzatore si avvale di un modello semplificato della rete di riferimento per prevederne la risposta ad ogni possibile combinazione degli stati dei generatori in un dato orizzonte temporale, con l'obiettivo di ridurre al minimo i costi operativi della generazione di calore. Questo strumento è stato successivamente utilizzato per identificare la configurazione d'impianto economicamente ottimale per un determinato insieme di tecnologie di generazione, in quattro diversi scenari di prezzo dell'elettricità. I generatori selezionati sono stati un motore a combustione interna a gas, una turbina a gas e una pompa di calore geotermica. Infine, è stata effettuata un'analisi di sensitività sui parametri più importanti.

I risultati hanno indicato la tecnologia dei motori a combustione interna come la soluzione preferibile, consentendo lo sfruttamento dei prezzi elevati di vendita dell'elettricità nelle ore di punta del sistema elettrico. Questo si traduce in un favorevole effetto stabilizzante sulla rete elettrica. Inoltre, la partecipazione contemporanea dell'impianto sia al mercato del giorno prima che in quello di bilanciamento è altamente auspicabile, in quanto consente di massimizzare i vantaggi economici derivanti dalla anti-ciclicità della domanda termica rispetto a quella elettrica. L'accoppiamento di un motore a combustione e di una pompa di calore risulta essere competitivo solo per una taglia piuttosto ridotta di quest'ultima, che gli permette di funzionare interamente con l'elettricità prodotta dal motore.

Parole chiave: Teleriscaldamento, model predictive control.

Chapter 1

Introduction

Starting from the beginning of the 20th century, a progressive increase in the average temperature of the Earth's surface has been observed. This phenomenon is better known as global warming. Many eminent members of the international scientific community, including the appointed United Nation group of experts of the Intergovernmental Panel on Climate Change, agree to attribute this increase to the growth in the emission of greenhouse gases in the atmosphere due to the intensification in human activities derived from the Second Industrial Revolution [1].

Over the last decades, growing public awareness about the issues of sustainable development and climate change has led many countries to undertake i17

International commitments and treaties, bounding themselves to reduce the emissions of climate-altering substances. Following the 2015 United Nations Climate Change Conference - COP 21, 184 of 197 signatory Parties ratified the Paris Agreement [2], setting individual emission reduction targets, with the long-term aim to contain the global average temperature rise within 2°C compared to pre-industrial levels.

As highlighted by the European Commission, heating and cooling represent the most relevant segment in the energy sector of the European Union (EU), being alone responsible for a half of the total European energy consumption [3]. Nevertheless, as reported in the "EU Energy in figures - Statistical pocketbook 2018" [4], only 19% of the energy consumed for this purpose comes from renewable energy sources. Consequently, in order to fulfil the commitments pledged with COP 21, the European Union has paid particular attention to this sector. The importance of district heating and cooling technology has been emphasized in the European Directive 2012/27/EU [5], which

mentions it as still largely under-used in the EU but highly beneficial in terms of primary energy savings compared to non-centralised heat generation. Moreover, in [3], the issue of its synergic integration with others energy networks, in particular the electricity production sector, has been identified, in such a way as to increase the efficiency and flexibility of the entire energy system. This integration can be achieved both by means of cogeneration/trigeneration and power-to-heat systems and of the use of renewable energy sources, which are fundamental in view of the decarbonisation objective of this sector.

It is in this context that this thesis is framed, as part of a wider research project carried out by RSE S.p.A. in the field of Demand Management ("*Gestione della domanda*") and as part of the "*Ricerca di Sistema*" activities. During the 2015 research period, a project was conceived to develop a simulation model for an actual district heating network, able to simulate its behaviour in response to a variation in users demand.

The "*Milano Est*" network, owned by A2A S.p.A. and consisting of two networks (*Canavese* and *Linate*), has been used as a reference for the construction and validation of the model. Even though the two branches have been recently interconnected, the available data are not enough to provide for a reliable validation tool of an integrated model: consequently, the model focuses only on the section of *Canavese*. The modelling process has been carried out in a TRNSYS 17 environment and the data supplied by the provider for the 2014 operating year has been used for its validation.

1.1 Objectives

This thesis work focused on the design of the generation section of a 4^{th} generation district heating system in order to maximize its synergies with the electric system, as well as the economic result. At the same time, the satisfaction of the users' thermal demand has been set as an essential constraint to the optimization. To achieve this goal, an optimizer based on Model Predictive Control (MPC) has been developed within a

Matlab environment. This tool is recalled directly by TRNSYS during the network simulation in order to optimize the operation of the currently selected generator set, on the base of predictions about demand, electricity prices and weather conditions and of actual plant conditions. A wide number of generation technologies and electricity price scenarios were considered in order to pursue the objective of the thesis, which can be summarised as follows:

- The evaluation of the optimal plant configuration of a 4th generation district heating network and the assessment of its possible synergies with the electricity grid, for a selected range of electricity price scenarios, both actual and future.

1.2 Thesis outline

In **Chapter 2**, the theme of district heating is briefly presented, with an overview of the technologies adopted and their advantages and disadvantages.

Chapter 3 provides a more detailed description of the district heating network represented in the model: the *Canavese* section of the "*Milano Est*" system.

Chapter 4 describes both instruments employed for the subsequent analysis: the network model and the optimizer. With regard to the latter, the development process, its main characteristics and the assumptions made were presented.

In **chapter 5**, the possible exploitation of synergies between district heating and electricity networks are investigated. First, a description of the methodology used and of the scenarios considered is provided. Afterwards, the results of the analysis are presented, highlighting the optimal solutions for each scenario. Lastly, a sensitivity analysis was carried out on some of the main parameters in order to determine their influence on the results.

As a final point, in **chapter 6**, the conclusions of the thesis are drawn and the possible future developments of the project are identified.

Chapter 2

District heating and 4th generation plants

This chapter provides a brief overview of the operation and evolution of district heating technology. First, a brief analysis of this technology and its advantages is offered. In particular, the benefits arising from the use of combined heat and power generation is highlighted. Afterwards, a description of the near future of this technology is presented with the presentation of the fourth generation district heating plants.

2.1 Basic concepts on district heating networks

The main idea at the base of District Heating Networks (DHN) technology is the generation and subsequent distribution of thermal energy for urban heating and domestic hot water production purposes. Heat is transferred from a central production plants through a network of insulated pipes by means of a fluid carrier, typically water, and then it is delivered to each building connected to the grid. The size and extension of district heating networks can be greatly variable: they range from small networks that meet the demand of a small group of buildings to very large ones, able to meet the heating need of an entire city. Figure 1 shows a simple scheme describing the operation of a district heating system.

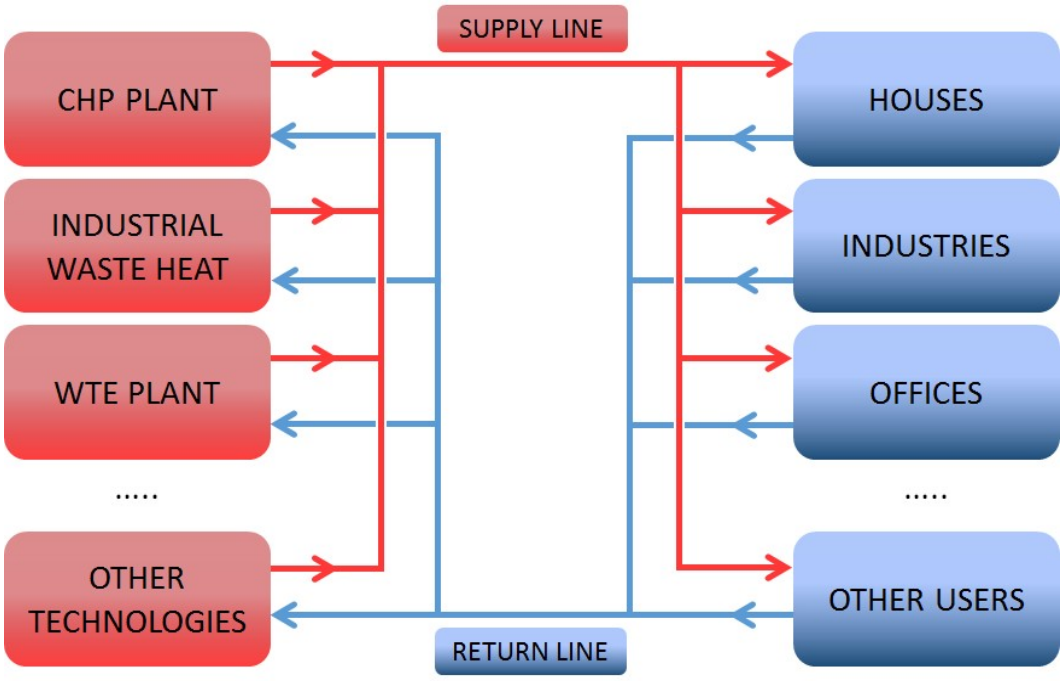

Figure 1: Operating diagram of a district heating system

The heat generation process occurs in one or more central plants and it generally exploits numerous energy sources, employing several different technologies simultaneously. This variety of sources and technologies is one of the main strengths of district heating, as it allows the use of hybrid systems that combine traditional methods of producing energy from fossil fuels with the use of alternative, more modern energy sources. These systems allow operating in compliance with the principles of:

- Energy security: since, frequently, the alternative sources employed are the most easily available at local level, such as biomasses, urban waste incineration (Waste To Energy - WTE), other Renewable Energy Sources (RES), etc.
- Energy efficiency: as it is possible, for instance, to exploit Combined Heat and Power (CHP) plants or to recover thermal wastes arising from industrial processes, in order to better employ primary energy.
- Environmental sustainability: since part of the energy mix of district heating systems can be made up of RES, such as biomasses, geothermal energy, solar thermal energy, etc.
- Emissions reduction: thanks again to the possibility to use waste heat or RES and to adopt CHP technologies.

Figure 2 shows a diagram summarizing the main technologies adopted. There are two macro-categories: technologies that provide heat only and technologies that produce both thermal and electrical energy.

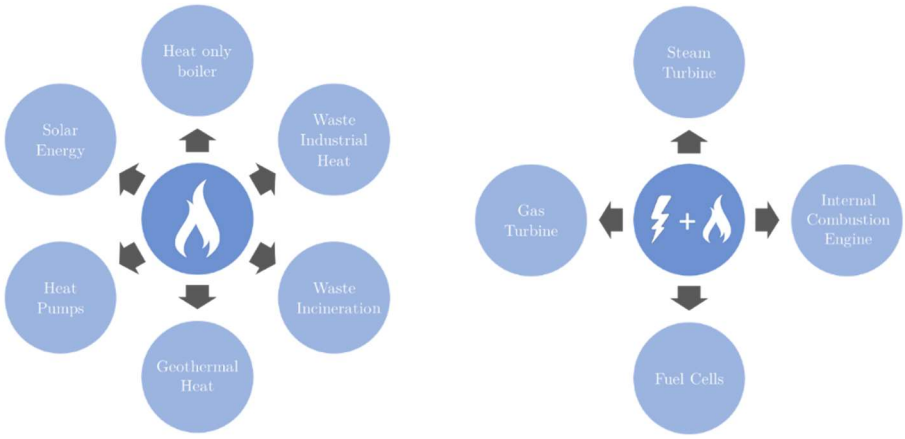

Figure 2: Generation technologies for district heating systems

To date, CHP systems represent an especially attractive option in district heating field, because they can deliver a variety of energy, environmental and economic benefits. As pointed out in Figure 3, this technology allows the production of electrical energy, reducing wasted heat and allowing a more efficient use of the primary fuel supply, thus lowering CO_2 emissions. In fact, if we assume a reference electrical efficiency of 40% for a generic power plant and a reference thermal efficiency of 85% of a generic boiler, it can be seen how the same energy output can be obtained by the CHP with a higher global efficiency. This means that it is possible to reduce fuel consumption, providing all the economic and environmental benefits that this entails. Consequently, cogeneration in CHP plants is a highly desirable technology in DHN.

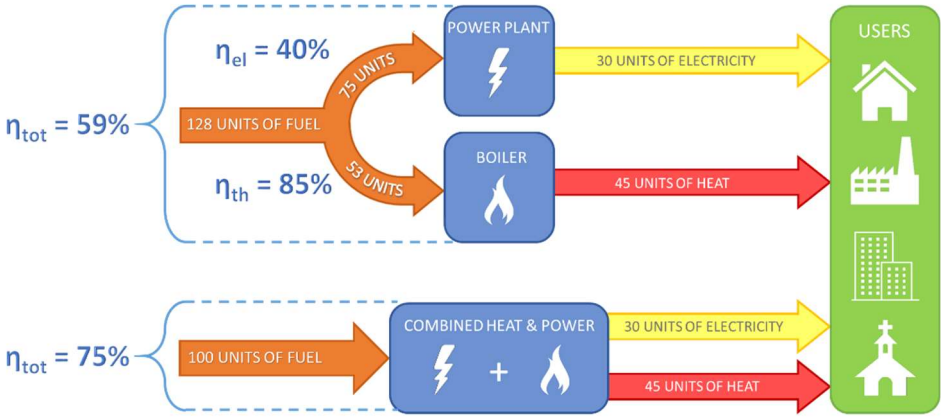

Figure 3: Global efficiency of separate production of heat and electricity vs. CHP

2.2 4th Generation District Heating

In the next future, the achievement of a sustainable energy system will be also linked to the integration of different networks, such as the electric grid, district heating and cooling systems, the gas network, the transport sector, etc. [6]. This integration process will result eventually in the creation of a smart energy system, where the potential synergies between each sector will be exploited allowing for an optimal operation of both the individual subsystems and the system as a whole [7]. In this context, district heating plays an important role in the implementation of future sustainable energy systems. However, in order for it to meet the challenge, district heating technology needs to advance to a new level and change radically its operation: this new concept is summarized by the term 4$^{\text{th}}$ Generation District Heating (4GDH).

In order to respond to the challenges posed by the development of a sustainable energy system, the future evolution of district heating must be based on the following five cornerstones [8]:

1. Reduction of the supply temperature of the network. (30 - 70 °C)
2. Reduction of the heat losses of the network.
3. Integration of renewable energy sources and low-temperature waste heat sources into the energy mix of the system. (smart thermal network)
4. Integration of the district heating system within a comprehensive smart energy system, so that it can work together with other networks.
5. Ability to implement suitable planning, cost and motivation structures in relation to the design and operation of the system.

The fulfilment of these objectives is subject to the implementation of technological and operational progress on several fronts, such as: the improvement of the energy performance of buildings and of the water distribution system, the refurbishment or replacement of the generation technologies, a careful demand management, the use of better measurement and control systems, and many others.

For instance, the improvement in the energy performances of new or renovated buildings is able to contribute to the achievement of each point of the list. In fact, a better insulation enables to reduce the supply temperature without compromising thermal comfort. Because of lower supply temperatures, the network thermal losses would result lower too. Furthermore, the decrease of energy use for space heating allows improving the balance of energy needs between summer and winter operation: this makes it easier for low-temperature RES and heat recycling to be employed in the network. In addition, even a possible district cooling system would equally benefit from an increase in the energy performance of buildings.

At the same time, an improvement of the space heating systems and of the domestic hot water supply system, in addition to an intelligent control of the heating operation, allows to decrease even further the supply water temperature.

To conclude, a comprehensive definition 4GDH is reported in [8] as follows:

> *"The 4th Generation District Heating system is consequently defined as a coherent technological and institutional concept, which by means of smart thermal grids assists the appropriate development of sustainable energy systems. 4GDH systems provide the heat supply of low-energy buildings with low grid losses in a way in which the use of low-temperature heat sources is integrated with the operation of smart energy systems. The concept involves the development of an institutional and organisational framework to facilitate suitable cost and motivation structures."*

Chapter 3

A2A Milano district heating

This chapter focuses on the description of the district heating system of Canavese (*Milano*), which will be used as reference in the construction and validation of the MPC-based optimizer in Chapter 4.

3.1 Structure and model of *Canavese* district heating network

Starting from the 1990s, district heating in Milan has been developed by the utility company A2A S.p.A.. To date, a 200 kilometres, double-piped network serves approximately 3000 buildings, providing heat also to historical edifices like the city's cathedral (the *Duomo*), the city hall (*Palazzo Marino*) and *La Scala* Theatre. As reported in Figure 4, Milan's district heating system is made up of three separated networks: *Milano Est*, *Milano Nord* and *Milano Ovest*.

Milano Est system is made up of 54.1 kilometres of thermally insulated double pipes - one for the supply and one for the return of water, the thermal carrier - and it consists of two sub-networks, *Canavese* and *Linate*. Until 2017, despite these two sub-systems had been recently connected by a new line, they still worked independently.

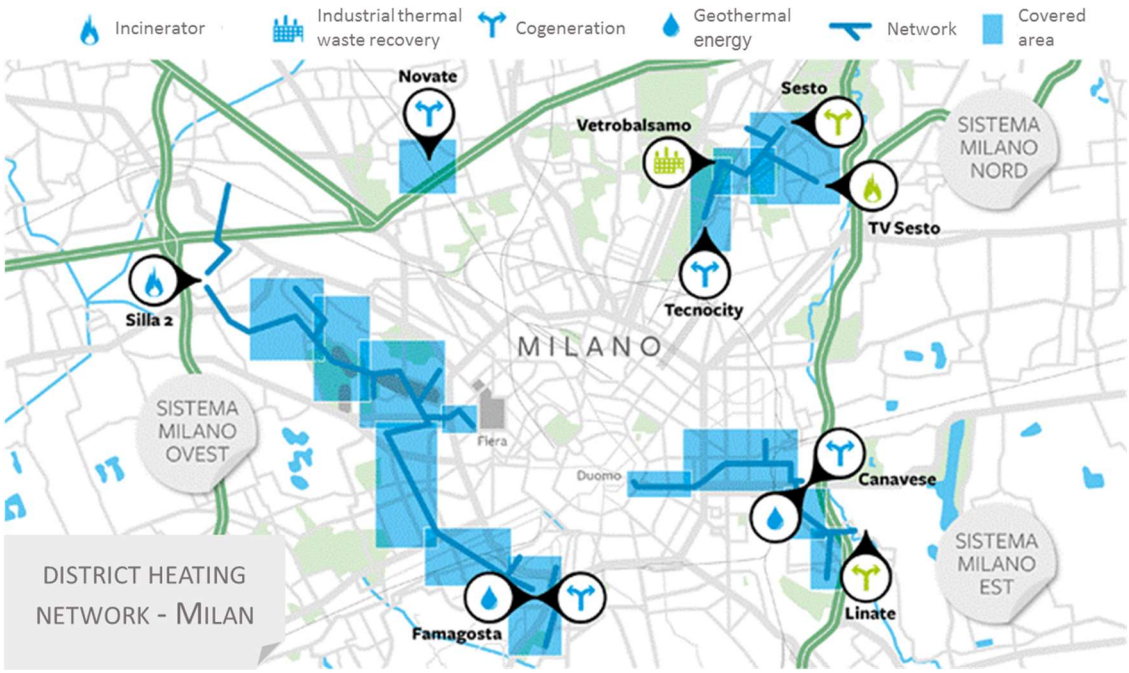

Figure 4: Scheme of Milan's district heating network

Figure 5, which reports the topography of *Canavese*, shows that the network spreads over the eastern part of the city, with some branches that ramifies towards the innermost part, eventually reaching *Piazza del Duomo*.

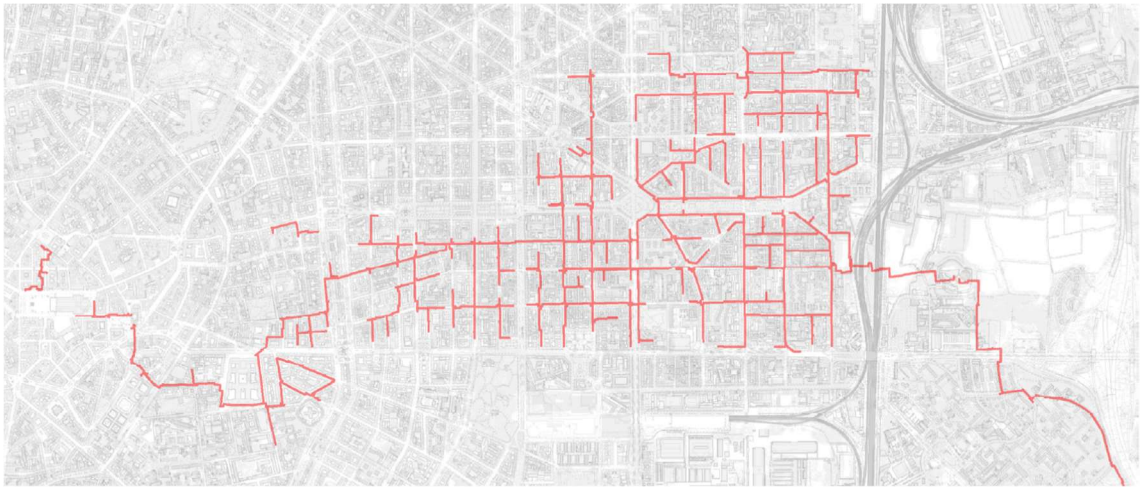

Figure 5: Topography of Canavese network (Milano Est)

Canavese power plant, which entered into service in 2007-2008, feeds the homonymous network with the hot water required by its users, satisfying both space heating and domestic hot water needs. The operation period of the network in 2014 (the considered year of operation) starts the 15th of October and it ends the 15th of April.

At present day, the plant adopts the following technologies to operate:

- 1 heat pump with a heating capacity of 15 MW_t that uses groundwater (~14°C) as cold heat source.
- 3 CHP, natural gas-fuelled internal combustion engines, each one with a nominal capacity of 5.04 MW_e of electric power and 4.4 MW_t of thermal power.
- 3 backup boilers, natural gas-fuelled, each one with a nominal capacity of roughly 15 MW_t.
- 2 thermal energy storage tanks with a capacity of 1000 m^3 each that allows to decouple hot water production from consumption and to cover peak demand.

The electricity produced by the CHP engines is partly used to run the heat pump and to satisfy the needs of the plant's auxiliaries, while the remaining part is introduced in the electricity grid.

The water comes back from the network to the plant with a temperature around 60°C, after having transferred the required heat to the users of the system. Then, the thermal energy obtained by the parallel operation of the plant's machines is used to heat the water up to 90°C.

The control logic of the plant defines a set point of 90°C for the supply water temperature. The mass flow rate of water that feeds the network varies together with the thermal needs of the users, with the aim of keeping a constant temperature difference of 30°C between the supply and return water. The generators are switched on and off on the base of the value of the controlled variable. As soon as the flow temperature falls below 90°C, the CHP and the heat pump are progressively switched on. If this is not sufficient, the thermal storage is exploited. Eventually, the backup boilers are gradually switched on in the event that the supply temperature falls below the 85°C.

As already reported in the introduction, in order to comply with the purpose of this thesis and to simulate the network operation, a model of the *Canavese* DHN has been developed by RSE S.p.A. [9] The model, built in a TRNSYS 17 environment, was then validated using the operational data of 2014, supplied by A2A S.p.A. The validation

process proved the model to be generally in accordance with the experimental data, both from the point of view of the production of thermal energy and for its overall consumption by users. The major discrepancies found have resulted from causes that cannot be predicted in the model, such as the failure of a generator or its stop for maintenance. Another source of error was the mismatch between the number of users accounted for by A2A and those actually connected to the network at the time of construction of the model.

Despite these inconveniences, the good results provided by the model make it a valuable and reliable tool to simulate the network and plant behaviour. Hence, this tool will be adopted as starting point for the development of the model of the advanced 4^{th} generation district heating system, described in Chapter 4.

Chapter 4

Modelling of an advanced district heating plant with a model predictive controller

The aim of this chapter is to describe the development of a tool based on model predictive control that allows the optimal design and operation of the generation section of a multi-generator district heating system. The first section presents the main features of MPC and explains how this control system has been integrated into the case study. In the second part, a description of the TRNSYS model of the district heating network and the generation plant is provided. After, the third section will present the development of the simplified model of the DHN that the MPC control system will use for the forecasting of the system's operation.

4.1 Structure and features of the TRNSYS-Matlab model of a 4GDH plant with MPC controller

MPC is an advanced instrument of control systems that allows following the given set point of a process while respecting a set of constraints and rejecting the system's disturbances. This feedback-loop control method has a wide range of applications, especially in the field of industrial processes where the main application is in the petrochemical industry. MPC is particularly useful to face multivariable control problems of dynamic systems and to handle the constraints on both the manipulated and the controlled variable.

Model predictive control is also known as receding (or moving) horizon control, making use of an explicit dynamic model of the system to predict the influence of the

future input variables on the optimal control signal, which is obtained by minimizing the operating cost function of the system. The receding horizon mechanism is the most important feature of MPC, since it allows adapting the future control actions on the base of the effects given by the current control actions and of the correctness of the available predictions of the system disturbances. The operation logic of a MPC-based controller can be summed up with the following four steps:

1. The first phase is the collection of current state data, which is the starting point for the subsequent modelling and optimization phase. The controller receives in input all the data needed to assess the present situation of the system.
2. The MPC controller solves a constrained optimization problem over a certain time-horizon, forecasting the system behaviour on the base of a physical model and of predictions of future disturbances.
3. The optimal solution, found at point 2, is applied to the system.
4. At the following sampling time, the process is repeated from point 1 allowing the correction of the control action.

A simple scheme of the moving horizon mechanism is shown in Figure 6:

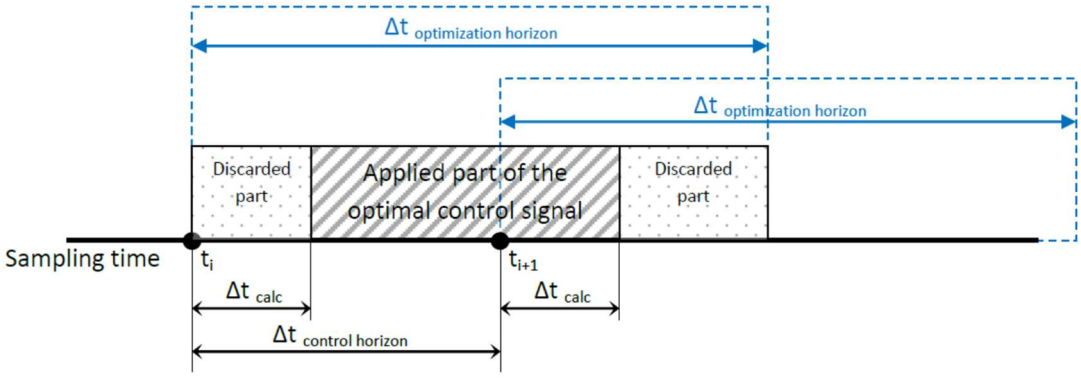

Figure 6: Operating principle of Model Predictive Control

In the figure, time t_i is the current sampling time, while time t_{i+1} is the subsequent one. After reading the current state variables at time t_i (step 1), the MPC controller solves the optimization problem taking time Δt_{calc} (step 2). Starting from time $t_i + \Delta t_{calc}$, the optimal control variables are applied to the system (step 3), but only up to the time $t_{i+1} + \Delta t_{calc}$, where the next optimal solution is applied. In fact, at

time $t_{i+1} + \Delta t_{calc}$ the controller solves again the optimization problem, taking into account any variation given by the effects of the application of the previous control action and by a change in the disturbances forecast. This means that only a portion of the optimal signal resulting from each optimization problem is used, while the rest is discarded. This allows the controller to adjust and correct its action, allowing for a better set-point tracking.

The application of the MPC operating principles in the case study has been implemented using a TRNSYS-Matlab co-simulation environment. While the TRNSYS model simulate the DHN behaviour throughout the year, its thermal power plant represents the process to control. The Matlab script acts as both the controller and the optimizer of the generation plant at the same time. The entire process is represented in Figure 7, where the information flows are highlighted.

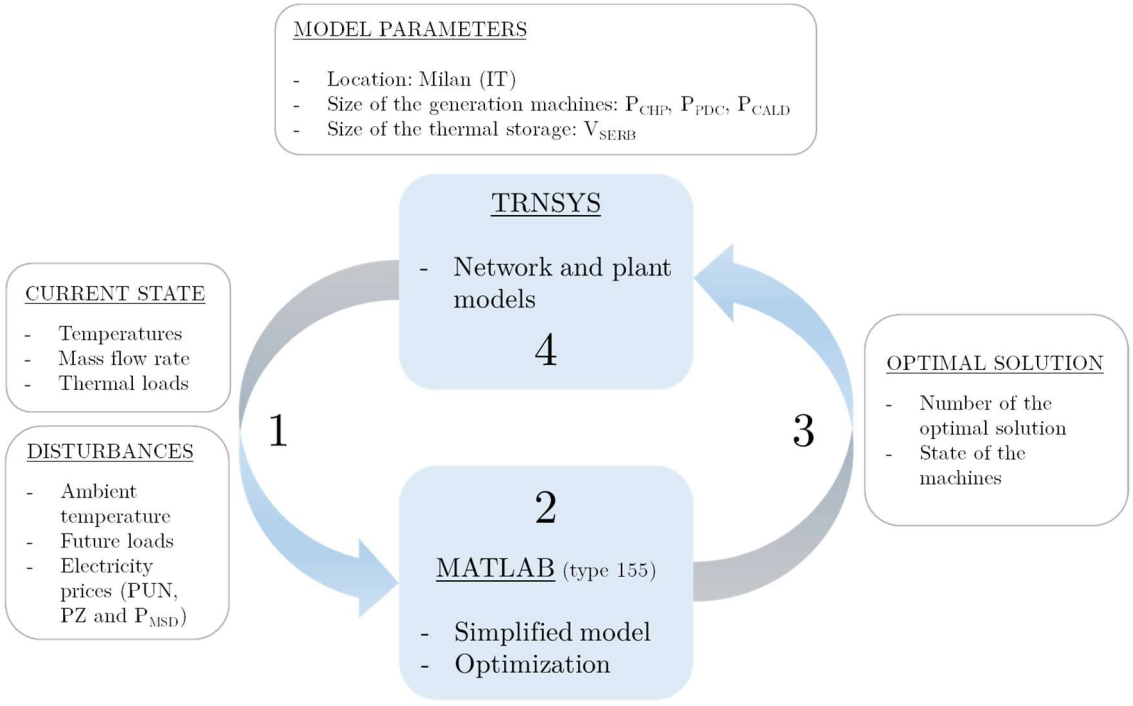

Figure 7: Scheme of operation of the optimization process

The control and optimization process implemented with Matlab is called at each time-step during the TRNSYS simulation. The process makes use of MPC in order to find the optimal on/off status of the currently evaluated set of generation technologies over a certain time-horizon. The optimization is economic and it is based on the

minimization of a cost function representing the operating cost of the plant over the entire optimization horizon. The sampling time interval of the control process has been set to 1 hour, while the optimization horizon is identified by the variable $stepM$, which can be defined by the user.

The first phase of the control process starts with the assessment of the system's state. The Matlab component in TRNSYS receives as inputs the current state variables, which are:

1. The temperature of water from each section of the system.
   $T_{\sup st}$, $T_{ret\ st}$, $T_{avg\ st}$, $T_{in\ load}$, $T_{out\ load}$, $T_{ret\ tank}$, $T_{\sup tank}$
2. The mass flow rate of water running through the system.
   $\dot{m}$
3. The thermal energy currently required by the three types of users.
   C_{cond} , C_{soc} , C_{pf}

The script also receives hourly-predicted values of the system disturbances over the optimization horizon ($stepM$). In the model, the disturbances taken into account are the following:

1. The ambient temperature, which is employed to compute the thermal losses of the DHN and of the storage tanks towards the environment.
   $T_{amb}(k)$ $\qquad k = 1, \dots, stepM$
2. The thermal energy required by the users over the entire time-horizon. This is needed to calculate the temperature drop across the load section.
   $C_{cond}(k)$, $C_{soc}(k)$, $C_{pf}(k)$ $\qquad k = 1, \dots, stepM$
3. The electricity buying and selling prices, that are required to compute the cost function for the optimization problem. Different price forecasts, according to different scenarios, will be considered during the analysis of the case study.
   $P_{acq}(k)$, $P_{ven}(k)$ $\qquad k = 1, \dots, stepM$

Making use of a simplified model of the network, which will be better described in section 4.3, the script is able to predict the network's future conditions, in terms of system temperatures, during each hour of the considered time-horizon. The prediction

takes into account the current state, the forecasted disturbances and the state of the machines at each hour of the horizon. This means that the correctness of the control action will not only be a function of the simplified model physical consistency, but also of the disturbances forecasts accuracy. The optimization has been based on the minimization of the operational costs of the plant over the prediction horizon: thus, the objective function of the problem comes in the form of a cost function.

The optimal on/off-state combination of the machines over the horizon $stepM$, during each optimization process, is evaluated through a cyclical simulation of all the possible combinations of the machines' state. This system allows finding always the optimal combination but, on the other hand, it also needs a simplification of the model because it requires a large amount of computational resources, since the number of possible solutions to assess is very high. The number of generators considered depends on each evaluated configuration and it is represented with the variable $Nmacchine$. The cycler has been programmed to generate a matrix S_M of $(stepM \times Nmacchine)$ dimension containing the states of the machines (0;1). The value of the matrix elements is temporary: once the optimizer has evaluated the impact on the system of the current combination and the cost function, the cycler overwrites S_M with the subsequent combination. A univocal number identifies every sequence: the number 0 designates the first case, a matrix of zeros, and the number $(numeroM - 1)$ indicates the last case, a matrix of ones. The number of possible combinations for the system under consideration is given by the variable $numeroM$, whose value is computed as follows. The variable $nstati$, whose value indicates the number of possible states, is equal to two. The ordered selection of the possible states for each hour of operation is then given by the variable $casiM$, computed as $nstati$ to the power of $Nmacchine$. Variable $numeroM$ represents the ordered selection of the combinations of each hour of the time-horizon.

$$nstati = 2 \qquad casiM = nstati^{Nmacchine} \qquad numeroM = casiM^{stepM}$$

The cost function has been defined taking into account the operating costs of each different technology. The selection of the optimal solution is determined by the comparison between the cost functions of the current combination and the previous one.

The satisfaction of the thermal needs of the users has been set as a constraint for the problem in the form of a lower and an upper limit to the supply temperature of the water. The upper boundary has been fixed at 115°C and the lower one at 65°C. Furthermore, if the temperature read from the current state exceeds the upper limit the program skips the optimization process and shuts down all the generators for the next hour. Vice versa, if the lower limit is trespassed, all the machines switch on. This is especially necessary during the first hours of the simulation, since the entire system faces a cold-start and it takes some time to enter into full operation.

After the optimal solution has been determined, the control signal is transferred to the TRNSYS environment. The variables delivered are the following:

1. The number that univocally identifies the optimal combination.
   $numOPT$
2. The value of the predicted optimal cost function for the next hour.
   $FCoraria$
3. The optimal control signals for the operation of the next hour.
   $S_M(1,1), \dots, S_M(1,N), \dots$ $N = 1, \dots, nMacchine$

The optimal status of the machines is maintained for the duration of the subsequent hour of simulation, which is just the first one of the optimization horizon *stepM*. After this time, the entire process is carried out again, updating the state variables and the forecasts of the disturbances to the current state.

4.2 Description of the TRNSYS model of plant and network

The models of *Canavese* district heating network and its power plant have been developed in a TRNSYS 17 environment. This program is a component-based simulation software that allows to model the behaviour of a dynamic thermal system. In the first place, it was conceived expressly for the energy field allowing the user to perform the simulation of thermal and electrical transient systems. The software comes with a vast library of validated components, named "types", each one modelling a specific element of energy systems, with different levels of detail. At present, TRNSYS can be employed in the analysis of a generic dynamic problem, thanks to the possibility to create new, ad hoc, user-defined components. The choice to use this software derived from its ability to interface with other programs, from the availability of a large number of energy systems components and from the flexibility in the choice of the simulation time-step and time-horizon. This model was developed by RSE within a research project in the field of smart cities [9]. The validation process has been performed by means of the real 2014 operational data of the system. The complete model is reported in Figure 8 (see App. A for better view).

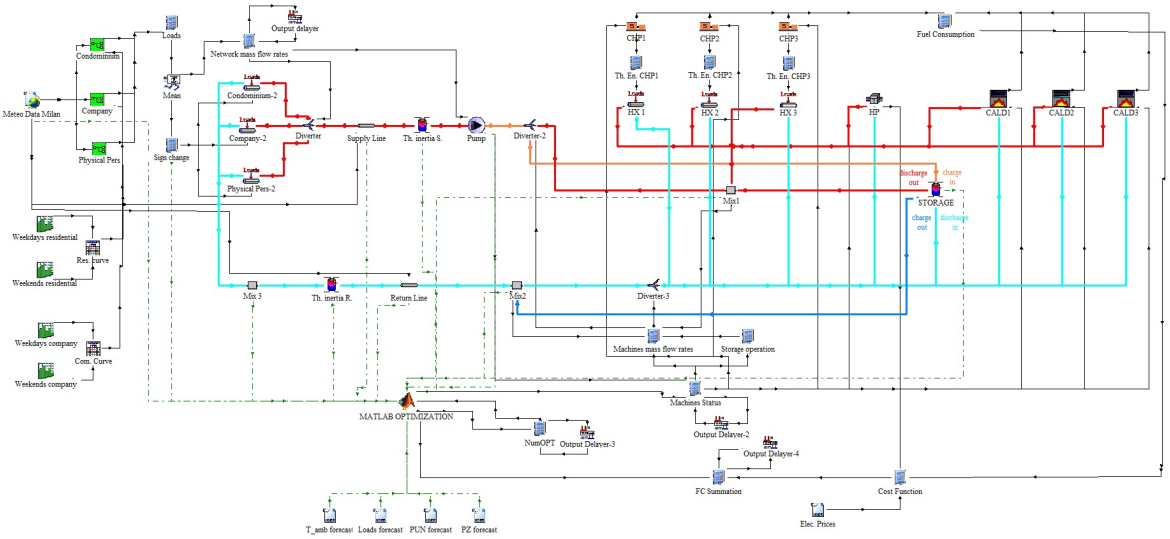

Figure 8: TRNSYS model of Canavese DHN

The elements representing the users of the system and their thermal needs lie in the left part of the scheme, while the ones representing the power plant stand in the

upper right section. The central part represents the network of the district heating: the red colour denotes the supply line and the light blue ones denotes the return line. Lastly, the lower section performs the functions of controller and optimizer of the system operation. The data that the Matlab optimizer receives from the DHN model are reported here with dash-dotted, green lines. The following paragraphs will focus on the first three sections of the model, while the last part will be better described in Chapter 4.3.

Model of users demand

The users of the network under consideration are of three main kinds: condominiums, companies and physical persons. The data concerning the thermal need of the system have been provided by A2A.

Most of the load is to be attributed to the condominium type, since it features the highest number of connected buildings. The number of buildings and the total thermal demand of the three types of user is reported in Table 1.

Canavese DHN		
User type	**Number of users [-]**	**Load required [kWh]**
Condominium	515	71,873,088
Company	16	1,306,178
Physical person	11	1,048,724
Total	542	74,227,990

Table 1: Users number and thermal load required

To better explain the operation of the model, Figure 9 reports a focus on this section.

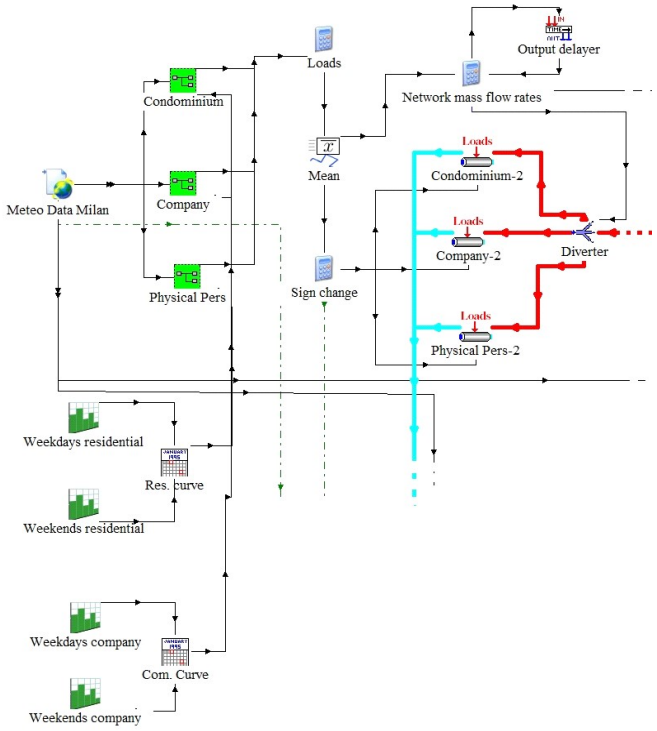

Figure 9: Users section of the model

In order to capture the different characteristics of each user, their load has been modelled through the definition of a corresponding "type building". The daily profiles, which represent the use of the heating system by each user, have been reported in Figure 10.

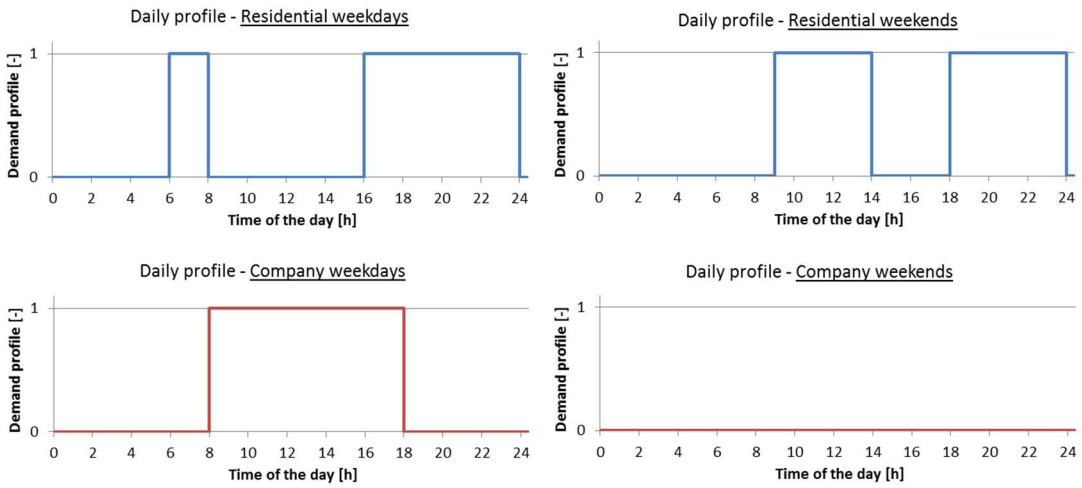

Figure 10: Daily profile curves of the users

The meteorological data for the model derives from the element *Meteo Data Milan* (*type 15*). This component is a weather data processor that reads a Typical Meteorological Year Version 2 (TMY2) file and interpolates its data to make them available for the other TRNSYS components. The file contains the most relevant weather data for a given location, including environmental temperatures, wind velocity, atmospheric pressure and radiation data.

The type building models are encased in the macro-elements named after the related user-type: *Condominium*, *Physical Pers.* and *Company*. As visible in Figure 11, these components are made of four elements each: *Building*, *Windows*, *Heating Control* and *Previous Temp*.

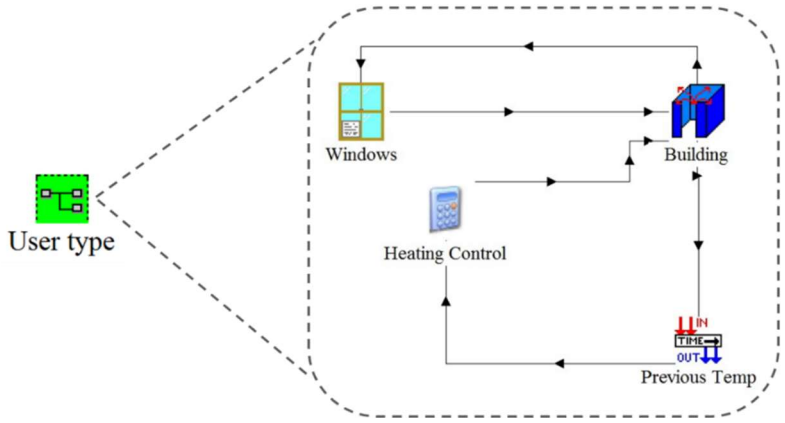

Figure 11: Structure of the user type

The first one uses *type 759* that models the temperature and humidity level of a lumped capacitance building. The element can include many different effects, such as infiltration and ventilation or internal loads and gains. There is also the possibility to incorporate user-defined miscellaneous energy gains or losses, in order to better simulate the building behaviour. The model requires both geometrical and heat transfer parameters, as well as the thermal capacitance of the building.

As the name suggests, the second element represents the windowed surface of the building making use of *type 687*. This component allows computing the amount of solar energy and illumination that is transmitted through the considered windowed surface. The parameters required are the geometrical properties of the windows, the number of

identical units present, the temperatures and radiation data and the National Fenestration Rating Council (NFRC) label data. The latter express the heat transfer properties of the window in the form of three ranking parameters: a thermal loss coefficient (Q_L), which denotes the overall energy loss coefficient per unit of area, the "Solar Heat Gain Coefficient" (SHGC), which represents the fraction of incident solar radiation admitted through the glass, and the "Visible Transmittance" (VT), which is the transmittance of the surface at the radiation of the visible spectrum. The resulting overall thermal power exchanged through the window is then sent to the building component as one of the miscellaneous energy gains. The main parameters used for the characterization of the buildings and the windows models are reported in Table 2 and Table 3 respectively.

Symbol	Description	Value	Units
V_{COND}	Volume of the condominium building	3,060	m^3
C_{COND}	Thermal capacitance of the condominium building	721,244	kJ K^{-1}
$(UA)_{COND}$	Heat transfer coefficient of the condominium building	1,722	kJ h^{-1} K^{-1}
V_{COM}	Volume of the company building	1,339	m^3
C_{COM}	Thermal capacitance of the company building	424,402	kJ K^{-1}
$(UA)_{COM}$	Heat transfer coefficient of the company building	3,038	kJ h^{-1} K^{-1}
V_{PP}	Volume of the physical person building	419	m^3
C_{PP}	Thermal capacitance of the physical person building	106,787	kJ K^{-1}
$(UA)_{PP}$	Heat transfer coefficient of the physical person building	701	kJ h^{-1} K^{-1}

Table 2: Main parameters for the users' buildings model

Symbol	Description	Value	Units
A_{COND}	Area of the condominium windows	2	m^2
N_{COND}	Number of units of the condominium windows	60	-
$Q_{L,\ COND}$	Thermal loss per unit area of the condominium windows	5	W m^{-2}
A_{COM}	Area of the company windows	3.6	m^2
N_{COM}	Number of units of the company windows	30	-
$Q_{L,\ COM}$	Thermal loss per unit area of the company windows	9	W m^{-2}
A_{PP}	Area of the physical person windows	2	m^2
N_{PP}	Number of units of the physical person windows	10	-
$Q_{L,\ PP}$	Thermal loss per unit area of the physical person windows	3.5	W m^{-2}
SHGC	Solar heat gain coefficient for each user type	0.41	-
VT	Visible transmittance for each user type	0.7	-

Table 3: Main parameters of the users' windows model

Model of generators

Figure 12 shows in detail the generation section of the model.

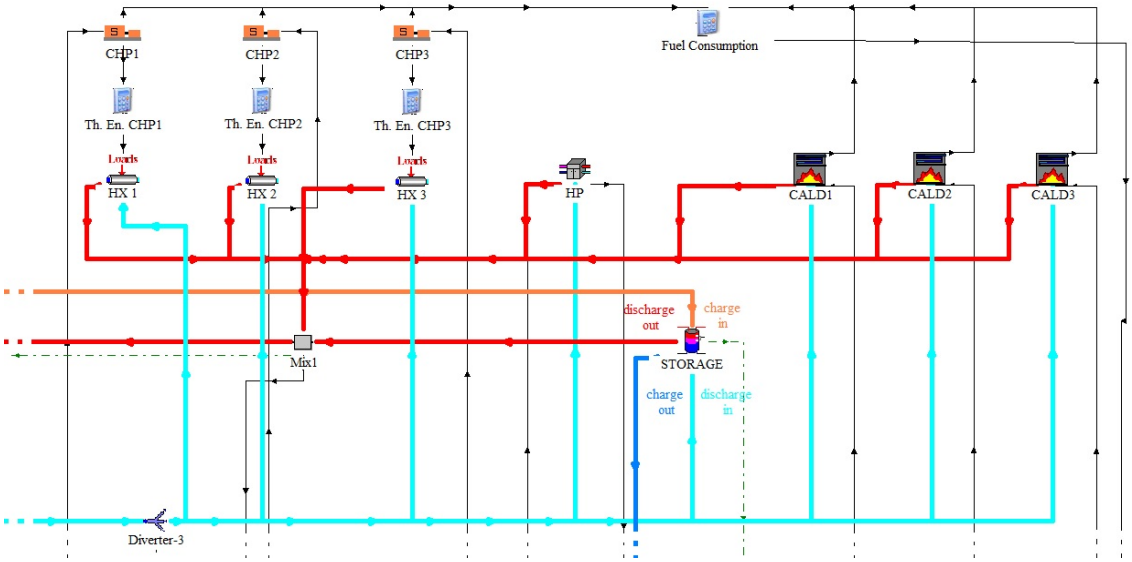

Figure 12: Generation section of the model

This section represents the thermal power plant of the district heating network. As in the physical plant, the machines considered are of three kinds: CHP internal

combustion engines, heat pump and thermal heaters. Moreover, the thermal energy storage model has been included, since it acts like an additional generator during the discharge phase. All the machines run with a parallel operation, receiving cold water from the return line, heating it up and delivering it to the supply line after a mixing process.

The three CHP internal combustion engines have been represented with *type 120*, which is the static model of a Diesel Engine Generator System (DEGS). The component requires setting as parameter the kind of fuel and the maximum and minimum electrical power generated. Furthermore, it allows the user to establish the fuel consumption curve in the form of an empirical, first-order polynomial expression that links the fuel consumed with the electric power production. Hence, the model is able to determine the power output, the fuel consumption rate and the performances of the generator in terms of electrical efficiency. Since *type 120* only models the electric generator part, in order to model a CHP system three components named *Th.En.CHP* have been added in order to compute the heat recovered from the engine, with the assumption of a constant thermal efficiency. Eventually, the thermal power is delivered to the network by means of three *type 682* components that are named HX (as for heat exchangers) but, in reality, simply model the imposition of a certain load on a fluid stream, computing the outlet conditions.

Table 4 reports the main data of the three internal combustion engines.

Description	Value	Units
Manufacturer brand	Rolls-Royce	-
Machine model	B35:40V-12AG	-
Type of generator	ICE - CHP	-
Type of fuel	Natural gas	-
Working fluid	Water	-
Nominal electric power	5.04	MW_e
Electrical efficiency	0.44	-
Thermal efficiency	0.37	-

Table 4: Main parameters of the ICE generators

The heat pump has been represented with type 927 that represents the static model of a reversible, single-stage, water-to-water heat pump. Therefore, the component can work both in heating mode, as a heat pump, or in cooling mode, as a refrigerator. Naturally, in the current case study, only the first option is allowed. The type requires two user-supplied files, containing the power consumption and the heating and cooling performance data, as function of the inlet temperatures and mass flow rates of both the source and load fluids. The model then performs a double interpolation on the data in order to assess the current heat pump working conditions, which are determined by the current value of the two fluids temperatures and mass flow rates. The output parameters are the source and load outlet temperatures, the power consumption, the heat transfer rates and the coefficient of performance. The component is directly linked with the network model, receiving water from the return line and providing the heated one to the mixing valve.

The characteristics of the modelled heat pumps are reported in Table 5.

Description	Value	Units
Manufacturer brand	Friotherm AG	-
Machine model	Unitop FY-81611 U	-
Type of generator	Groundwater HP	-
Type of fuel	Electricity	-
Working fluids	Water \ R134A	-
Nominal thermal power	15	MW_t
Coefficient of performance [ref. conditions (*)]	2.624	-

Table 5: Main parameters of the HP generator

(*) Reference conditions for the HP: $T_{return,load} = 65$ °C , $T_{supply,load} = 85$ °C , $V'_{load} = 648$ m³/h
$T_{supply,source} = 15$ °C , $V'_{source} = 1150$ m³/h

The thermal heaters have been represented using three *type 700* components, which models a simple boiler. The main parameters required by the component are the

rated heating power, the boiler efficiency and the combustion efficiency. In addition, the user may also specify the set point temperature of the fluid stream exiting the device. Then, given the current working conditions, the model computes the part load ratio as the heat required to raise the fluid temperature up to the set point one over the heating capacity of the boiler. If the heat required exceeds the heating capacity (part load ratio higher than 1), the outlet temperature of the fluid cannot reach the set point and it is computed using the boiler capacity. The heated fluid is subsequently sent to the mixing valve.

The main parameters of the given thermal heaters are reported in Table 6.

Description	Value	Units
Manufacturer brand	BONO energia	-
Machine model	Oil-Matic	-
Type of generator	Thermal heater	-
Type of fuel	Natural gas	-
Working fluids	Water	-
Nominal thermal power	16.12	MW_t
Thermal efficiency	0.93	-

Table 6: Main parameters of the boilers

The two thermal energy storage tanks have been considered as a single 2000 m^3 capacity tank in order to simplify the model. The tank has been designed to preserve the same amount of thermal losses towards the environment of the two separate storages. The component used to represent the equivalent storage is *type 60*, which models a vertical cylindrical storage tank with four openings: two inlet sections and two outlet sections. *Type 60* models a stratified fluid storage tank with the possibility to include optional internal heaters and optional internal heat exchangers. In addition, the type accounts for fluid stratification effect and it models uniform thermal losses through the external surface, allowing the value of a tank loss coefficient. In terms of operation, the tank can have two possible configurations: charge and discharge phase. During the charge phase, the storage intakes hot water (orange colour) coming from the supply line, through

the diverting valve *Diverter-2*, releasing colder water (dark blue colour) to the return line. This allows increasing the tank average temperature. the discharge phase works exactly the opposite way: hot water is sent to the mixing valve *Mix1*, while cold water is drawn from the return line, through *Diverter-3*. Since the storage behaves like a generator during this phase, the colours of inlet and outlet streams are the same as the others: red for the supply and light blue for the return.

Model of network

The network of the district heating stands in the central part of the TRNSYS project. A clearer view of this section is reported in Figure 13:

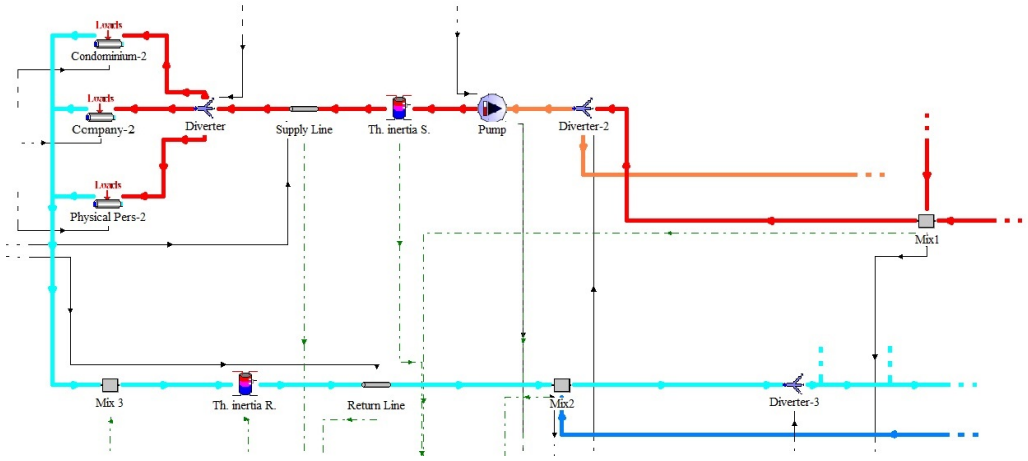

Figure 13: Network section of the model

In order to simplify the model, the network of the district heating system has been represented with three blocks of elements, neglecting the meshed structure and the real topology of the network. The two components named *Th. inertia S.* and *Supply Line* belong to the first block, which represents the supply line of the system. The second block, which denotes the return network, has been similarly structured with the two elements *Th. inertia R.* and *Return Line*. The first component of each block accounts for the thermal inertia of the system and it has been modelled as a thermal storage tank with a capacity of 1500 m^3 using *type 60*. On the other hand, the second part represents

the network of pipelines as a single equivalent tube, keeping constant the amount of thermal losses. The pipes have been modelled using *type 31*, which allows simulating the thermal behaviour of a fluid flowing in a pipeline. The model considers the tube as partitioned into smaller segments, each one characterized by its own temperature and thermally interacting with the environment. The fluid entering pushes the subsequent segments forward during each time-step. This method allows to simulate both the thermal losses towards the environment and the physical time taken by the water to flow through the pipelines. At last, the third block is composed of the elements named *Condominium-2*, *Company-2* and *Physical Pers-2*. They represents the heat extraction from the network by each kind of user and they have been modelled with *type 682* components, as like as in the CHP generators case.

Model of controller and optimizer

The lower section of the model is related to the implementation of the optimization and control strategies of the system. Figure 14 shows it in details.

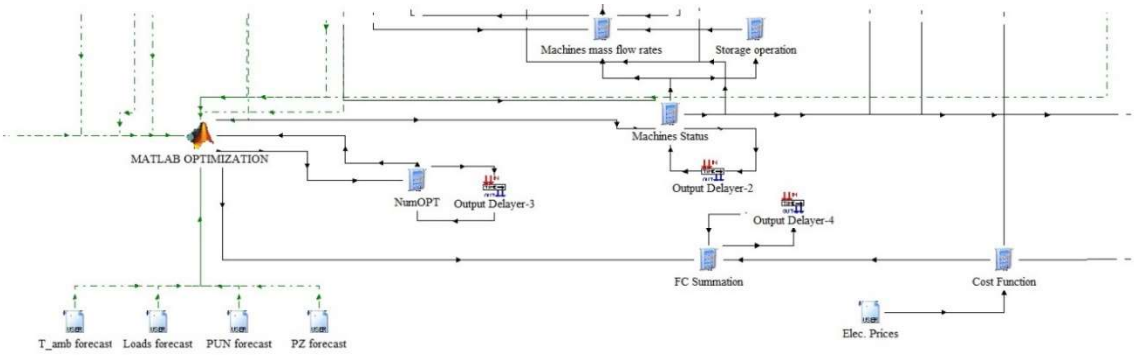

Figure 14: Optimization and control section of the model

As already reported, the MPC optimizer has been developed in a Matlab environment. The predictions of the system disturbances used in MPC strategy are supplied to the optimizer from external files containing forecasts over the optimization

time-horizon of the environmental temperature, the thermal loads and the electricity prices. So, in this study, perfect forecasts are considered.

The *numOPT* equation stores the number that identifies the current optimal set of the generators status and, then, it sends the number back to Matlab as an input. The optimal on/off configuration is delivered to the equation Machines Status that uses them to control the generators.

4.3 Development and validation of a simplified model for MPC controller

A simplified model of the district heating network has been developed for the forecast optimization process, in the MPC controller. The model has to predict, over the entire optimization horizon, the state of the system in terms of temperatures and mass flow rates, taking into account the forecasted disturbances.

The network, as reported in Figure 15, has been modelled with five main components: the generation block, the load section, the thermal storage and the supply and return lines.

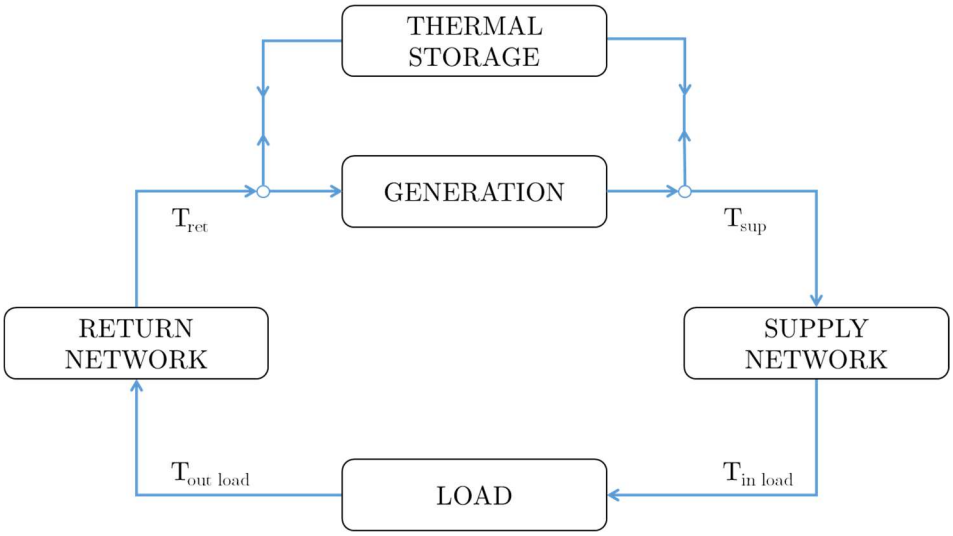

Figure 15: Simplified model of the network implemented as Matlab code

4.3.1 Model of generators

The generation section of the network includes all the technologies selected for the current configuration, connected in parallel.

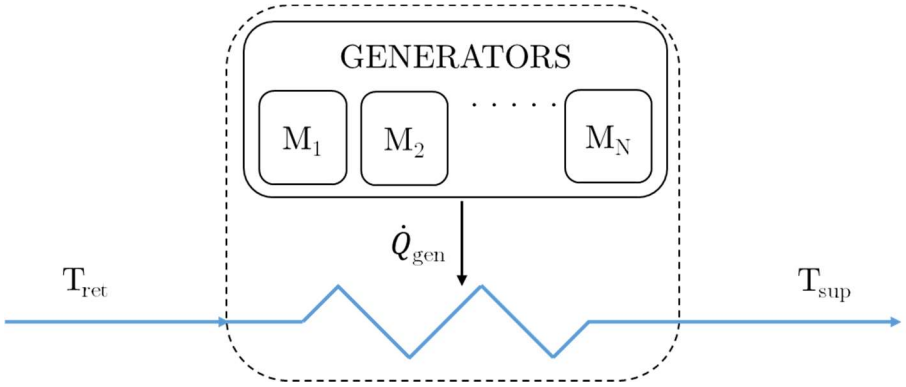

Figure 16: Simplified model of the generation section

As reported in Figure 16, the entire section has been modelled as a single block introducing heat $\dot{Q}_{gen}$ into the flow, heating the water up from T_{ret} to T_{man} according to the following equations:

$$\dot{Q}_{gen}(k) = \dot{Q}_M(1) * S_M(k,1) + \dot{Q}_M(2) * S_M(k,2) + \ \dots + \dot{Q}_M(N) * S_M(k,N) + \ \dots$$

$$T_{sup}(k) = T_{ret}(k) + \frac{\dot{Q}_{gen}(k)}{\dot{m}_{gen}(k) * c_w} \qquad k = 0,1,\dots,stepM \qquad N = 1,\dots,Nmacchine$$

The state of each generator at every optimization step k is given by the value of the corresponding element in the S_M matrix. The model calculates the power introduced into the system during each hour of the optimization for every possible combination of the generators state. Afterwards, it computes the supply temperature T_{sup} starting from the return temperature and making use of the first law of thermodynamics and of the definition of water specific heat c_w. The mass flow rate $\dot{m}_{gen}$ running through the generation section depends on the current state of the thermal storage.

4.3.2 Model of users demand

The load section model, which is reported in Figure 17, represents the synthesis of the thermal needs of the three kind of user considered: condominium (COND), company (COM) and physical person (PF).

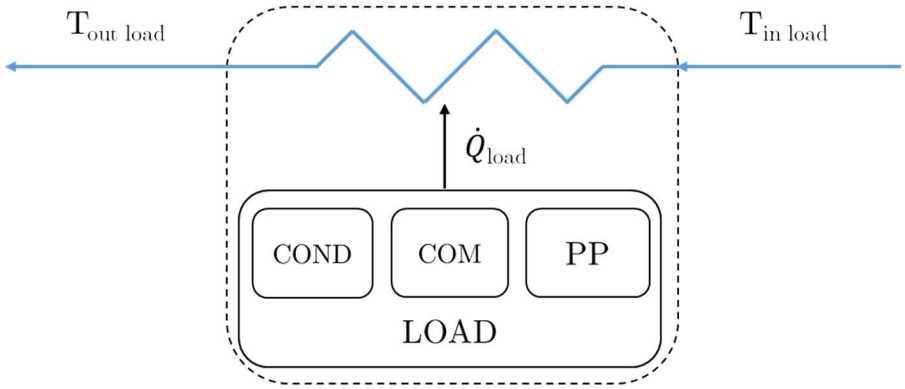

Figure 17: Simplified model of the users section

Similarly to the generation section, the three loads has been condensed into a single block that extracts the heat $\dot{Q}_{load}$ from the flow, cooling the water down from $T_{in\ load}$ to $T_{out\ load}$. The adopted formulae are analogous to the ones of the generators block.

$$\dot{Q}_{load}(k) = \dot{Q}_{COND}(k) + \dot{Q}_{COM}(k) + \dot{Q}_{PP}(k)$$

$$T_{out\ load}(k) = T_{in\ load}(k) - \frac{\dot{Q}_{load}(k)}{\dot{m}(k)\, c_w} \qquad k = 0,1, \dots, stepM$$

The heat required by each type of load for every step of the optimization has to be known, thus representing one of the disturbances of the MPC.

4.3.3 Model of plant storages

Another important element of the network is the thermal energy storage section. The storage has been represented, like in the TRNSYS project, as a 2000 m^3 tank connected in parallel with the generation block. The tank is continuously connected to the system and its available status are two: charge, represented by a value of 0 in the S_M matrix, and discharge, represented by a value of 1.

Hereafter, Figure 18 represents both the storage operation status.

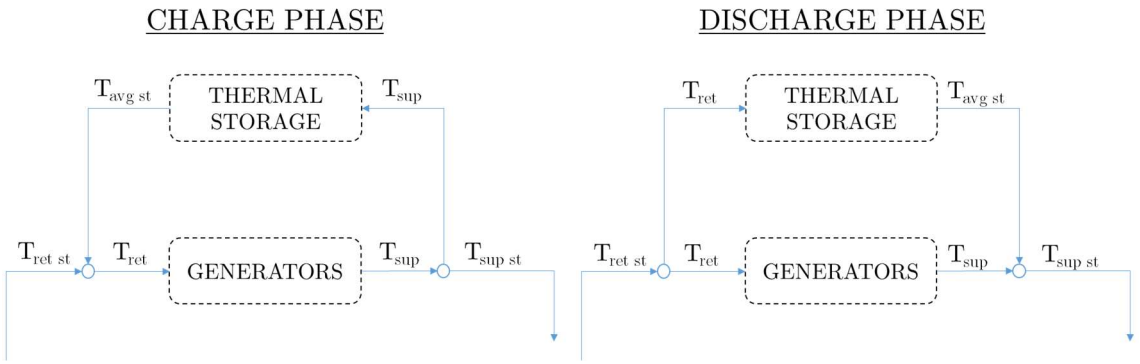

Figure 18: Simplified model of the thermal storage section

During the charging phase, the tank receives hot water at T_{sup} from the supply line releasing the same amount of water at $T_{avg\ st}$ to the return line. The intake water undergoes a mixing process with the one stored in the tank, thus progressively increasing the average temperature. The opposite situation occurs during the discharge phase: the tank receives cold water at T_{ret} from the return line and releases the same rate of stored water to the supply network, thus behaving like an additional generator. The heat loss towards the environment have been neglected in the model, since it is negligible compared to the thermal energy that flows during each phase.

The following equations have been used to model the behaviour of the thermal storage:

CHARGE PHASE

$$T_{ret}(k) = \frac{\dot{m}_{st} * T_{avg\ st}(k-1) + \dot{m}(k) * T_{ret\ st}(k-1)}{\dot{m}(k) + \dot{m}_{st}}$$

$$\dot{m}_{gen}(k) = \dot{m}(k) + \dot{m}_{st}$$

$$T_{sup\ st}(k) = T_{sup}(k)$$

$$T_{avg\ st}(k) = \frac{\dot{m}_{st}*\Delta t*T_{sup}(k)+(M_{st}-\dot{m}_{st}*\Delta t)*T_{avg\ st}(k-1)}{\dot{m}_{st}*\Delta t + (M_{st}-\dot{m}_{st}*\Delta t)} \qquad k = 0,1,\dots,stepM$$

DISCHARGE PHASE

$$T_{ret}(k-1) = T_{ret\,st}(k-1)$$

$$\dot{m}_{gen}(k) = \dot{m}(k) - \dot{m}_{st}$$

$$T_{sup\,st}(k) = \frac{\dot{m}_{st} * T_{avg\,st}(k-1) + \dot{m}_{gen}(k) * T_{sup}(k)}{\dot{m}(k)}$$

$$T_{avg\,st}(k) = \frac{\dot{m}_{st}*\Delta t*T_{ret}(k-1)+(M_{st}-\dot{m}_{st}*\Delta t)*T_{avg\,st}(k-1)}{\dot{m}_{st}*\Delta t + (M_{st}-\dot{m}_{st}*\Delta t)} \qquad k = 0,1,\dots,stepM$$

The initial values for the return temperature and the average storage temperature are given as an input by the TRNSYS simulation ($T_{ret\,st}(-1) = T_{ret\,st\,read}$ and $T_{avg\,st}(-1) = T_{avg\,st\,read}$), while the subsequent ones are given by the results of the other sections for each step of the optimization.

4.3.4 Model of network

In the TRNSYS model, the two networks of pipes that distributes and then recollects water have been condensed into two equivalent single pipes: one for the supply line and one for the return line. The simplified model of the two lines needs not only to simulate the thermal inertia given by the mass of water that is filling the tubes, but also the heat loss towards the environment $\dot{Q}_{loss}$ and the transport effect.

The thermal inertia of each line has been represented, like in the TRNSYS model, as a tank with a capacity of 1500 m^3, where the flowing water and the one currently stored in the network undergo a mixing process. This process takes the temperature of water from $T_{sup\,st}$ to $T_{sup\,tank}$ and from $T_{out\,load}$ to $T_{ret\,tank}$ respectively, according to the following equations:

$$T_{\mathrm{sup}\,tank}(k) = \frac{\dot{m}(k) * \Delta t * T_{sup\,st}(k) + (M_{ntw} - \dot{m}(k) * \Delta t) * T_{sup\,tank}(k-1)}{\dot{m}(k) * \Delta t + (M_{ntw} - \dot{m}(k) * \Delta t)}$$

$$T_{ret\,tank}(k) = \frac{\dot{m}(k) * \Delta t * T_{out\,load}(k) + (M_{ntw} - \dot{m}(k) * \Delta t) * T_{ret\,tank}(k-1)}{\dot{m}(k) * \Delta t + (M_{ntw} - \dot{m}(k) * \Delta t)}$$

The heat losses and transport effect have been modelled with another block, whose functioning is explained in Figure 19. The supply and return pipes have been divided into a great number of elements ($n_{el} = 100$). Starting from the knowledge of the mass flow rate running through the system, the velocity of the water is calculated, allowing the computation of the number of elements overpassed during each hour of the optimization horizon. This allows computing the heat loss and, hence, the temperature of each "set" of elements passed, thus simulating both the effects occurring.

The equations describing this model are the following:

$v(k) = \frac{\dot{m}(k)}{A_{tubo}}$ -> velocity of the flow at step k

$x_{el} = \frac{l_{rete}}{n_{el}}$ -> length of one element

$m_{el} = \frac{M_{ntw}}{n_{el}}$ -> mass of water of one element

$n_{el\ passed} = \frac{v(k) * \Delta t}{x_{el}}$ -> number of elements overpassed during time Δt

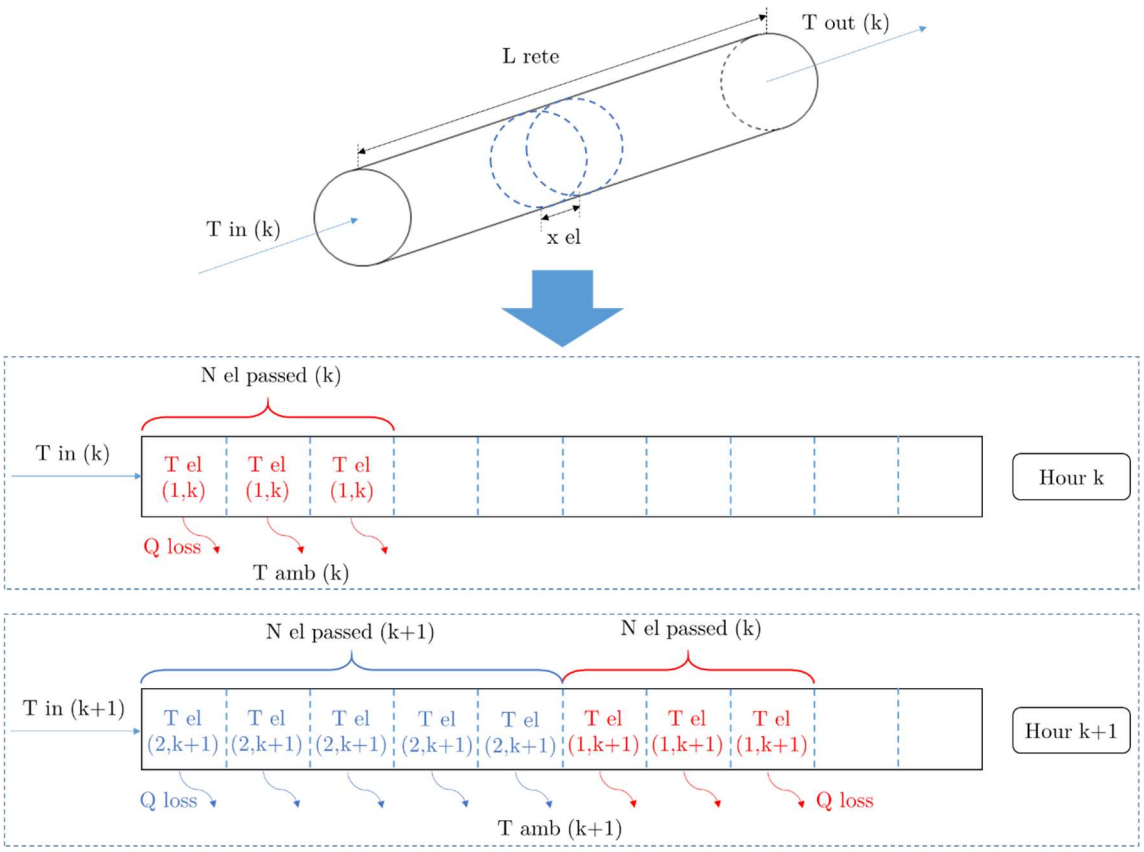

Figure 19: Scheme of operation of the network model

SUPPLY LINE

$$T_{sup\ el}(j,k) = T_{sup\ tank}(k) - \frac{U*A_{el}*\Delta t}{m_{el}*c_w} * (T_{sup\ tank}(k) - T_{amb}(k))$$

$$T_{sup\ el}(i,k) = T_{sup\ el}\big((i - n_{el\ passed}),(k-1)\big) - \frac{U*A_{el}*\Delta t}{m_{el}*c_w} * (T_{sup\ el}\big((i - n_{el\ passed}),(k-1)\big) - T_{amb}(k))$$

$$T_{in\ load}(k) = T_{sup\ el}(n_{el},k) \qquad j = 1,\dots,n_{el\ passed} \qquad i = n_{el\ passed}+1,\dots,n_{el}$$

RETURN LINE

$$T_{ret\ el}(j,k) = T_{ret\ tank}(k) - \frac{U*A_{el}*\Delta t}{m_{el}*c_w} * (T_{ret\ tank}(k) - T_{amb}(k))$$

$$T_{ret\ el}(i,k) = T_{ret\ el}\big((i - n_{el\ passed}),(k-1)\big) - \frac{U*A_{el}*\Delta t}{m_{el}*c_w} * (T_{ret\ el}\big((i - n_{el\ passed}),(k-1)\big) - T_{amb}(k))$$

$$T_{ret\ st}(k) = T_{ret\ el}(n_{el},k) \qquad j = 1,\dots,n_{el\ passed} \qquad i = n_{el\ passed}+1,\dots,n_{el}$$

It is not possible to determine the initial temperature value of each element of the supply and return lines both in the simulation and in the real plant. The only known values are the inlet and outlet initial temperatures, respectively $T_{sup\ tank}(-1)$ and $T_{in\ load}(-1)$ for the supply network and $T_{ret\ tank}(-1)$ and $T_{ret\ st}(-1)$ for the return one. Hence, the assumption of a linear distribution of temperatures between the inlet and the outlet section of the pipes has been made.

The consistency check and calibration of this simplified model has been performed through the knowledge of the initial system states, in the form of temperatures, mass flow rates, user demand and generated power, during the reference year of operation. A set of fifteen, uniformly distributed reference days has been considered for the calibration: one day every ten in the interval (10^{th} – 90^{th} day of the year) and one day every ten in the interval (310^{th} – 360^{th}). The system states at the hour 00:00 of each selected day is given as input to the simplified model, along with the correct "predictions" over the following 24 hours for the user demand, the generated power, the environmental temperature and the storage status. Afterwards, the simplified model has been implemented and the resulting temperatures have been collected in a graphical form in order to compare the forecasted values with the actual ones. To provide an example of the results, the following Figure 20 reports the comparison between the actual and the predicted values for the four main temperatures of the system ($T_{sup\ st}, T_{ret\ st}, T_{in\ load}, T_{out\ load}$) during two days characterized by different environmental temperatures: day 10 (10^{th} Jan.) and day 90 (31^{st} Mar.).

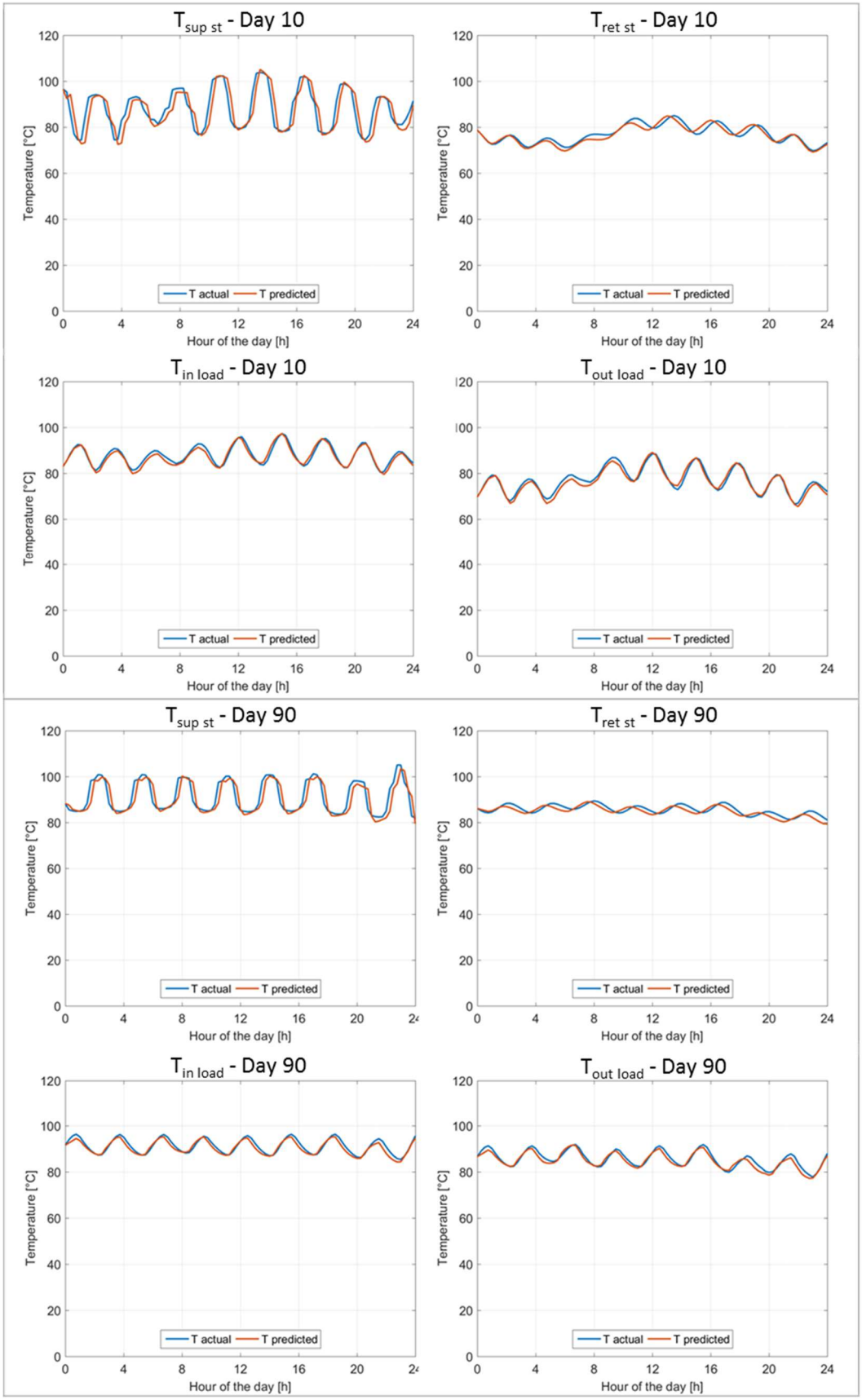

Figure 20: Comparison between actual and predicted temperatures

The predicted values (orange line) are quite adherent to the real ones (blue line) for the entire prediction horizon (24 hours). This fact is confirmed also by the value of the average prediction error, computed as follows:

$$\bar{E} = \frac{\sum_{i=1}^{N} \left| T_{actual,i} - T_{predicted,i} \right|}{N}$$

The average errors of each day are reported in the following Table 7.

	AVERAGE PREDICTION ERROR [°C]				
Day	10 (10th Jan)	20 (20th Jan)	30 (30th Jan)	40 (9th Feb)	50 (19th Feb)
$T_{sup\ st}$	3.31	3.47	3.49	3.66	3.56
$T_{ret\ st}$	1.14	1.44	1.53	1.62	1.69
$T_{in\ load}$	1.00	1.23	1.31	1.42	1.53
$T_{out\ load}$	1.11	1.38	1.42	1.53	1.63
Day	60 (1st Mar)	70 (11st Mar)	80 (21st Mar)	90 (31st Mar)	310 (6th Nov)
$T_{sup\ st}$	3.21	3.22	2.91	2.43	3.01
$T_{ret\ st}$	1.42	1.61	1.47	1.22	1.53
$T_{in\ load}$	1.21	1.31	1.11	0.96	1.16
$T_{out\ load}$	1.34	1.41	1.18	1.02	1.21
Day	320 (16th Nov)	330 (26th Nov)	340 (6th Dec)	350 (16th Dec)	360 (26th Dec)
$T_{sup\ st}$	3.62	3.56	3.49	3.07	3.64
$T_{ret\ st}$	1.95	1.77	1.39	1.51	1.57
$T_{in\ load}$	1.78	1.60	1.14	1.13	1.61
$T_{out\ load}$	1.79	1.70	1.30	1.16	1.62

Table 7: Average errors in the temperature predictions

Since the average errors assessed for each day considered results sufficiently low, the calibration of the simplified model can be regarded as completed.

Chapter 5

Evaluation of the synergy of thermal district heating network and electrical network

The main goal of this thesis is the evaluation of the synergy between a thermal district heating system and the electrical network. The methodology used for this purpose is described in the first section, where the main assumptions and parameters adopted during the study are also illustrated. The subsequent section presents the various scenarios considered during the simulation, both in terms of electricity prices and in terms of generation technologies adopted. Afterwards, the results of each individual scenario were presented and a comparative analysis of the optimal solutions derived was performed. Lastly, a sensitivity analysis on these results has been carried out.

5.1 Methodology

The development of the DHN model and of the optimizer has been the starting point to perform the deeper analysis of the synergy between the electrical network and a generic district heating network. In order to perform this evaluation, the tool created has been used to control and optimize the operation of the district heating network under a large number of scenarios, where different prices for the purchase and sale of electricity and different generation plant configurations have been considered. Each case has been implemented and simulated using the TRNSYS-Matlab tool and the results have been collected for the analysis, with the aim of determining the economically optimal plant

configurations. A sensitivity analysis has been carried out both on economic and physical variables in order to understand their effects on the results of the simulation.

Concerning the sale and purchase of electricity, four price scenarios have been considered. In addition, among all the possible technologies for the DH generation plant, four were selected: a groundwater Heat Pump (HP), a CHP natural gas-fuelled reciprocating Internal Combustion Engine (ICE), a CHP natural gas-fuelled Gas Turbine (GT) and three backup boilers. In addition, a thermal energy storage was considered as part of the generation section for each configuration. The reason behind this choice is given by the fact that these technologies are well-established in the energy sector, they have a large availability of supplier companies and they usually present a high degree of flexibility during operation, which allows to better work in synergy with the DHN. Steam turbines and combined cycle plants were not considered due to their lack of flexibility during operation and due to the high costs of investments that make them attractive only when they are already available on site (typically, when they operate as base-load electric power plants and heat is only a by-product of the process). Similarly, being waste heat coming from industrial processes a by-product by definition, it is possible to consider this source only when available on site.

The optimal configuration, in terms of technology and sizing of the generators, has been found through an economic analysis aimed at determining the Net Present Value (NPV) of the district heating system modelled. The NPV has been computed, according to its definition, as the sum over the system lifetime (T) of the Net Cash Flows (NCF) discounted at their present value through the discount rate (i). The NPV mathematical expression is reported in the following equation:

$$NPV = \sum_{t=0}^{T} \frac{NCF_t}{(1+i)^t}$$

The annual NCF of the network has been computed as the difference between the revenues and the costs associated with the system. The revenues are generated by the sale of thermal energy to the users (R_{TH}) and, in presence of CHP technology, by the sale

of electricity (R_{EL}); their sum is indicated as operating revenues (R_{OP}). The costs can be divided into two categories: the investment costs (C_{INV}) of the generators and the thermal storage, and the operating costs (C_{OP}). The latter can be split into operation and maintenance costs ($C_{O\&M}$) of the machines and fuel costs (C_F).

Naturally, the revenues from the sale of heat to the users are approximately constant and independent from the price scenario and machines configuration, since the demand remains the same and it is bound to be satisfied by the constraint. The thermal energy withdrawn by the users has been valued at an assumed constant price of 0.08 €/kWh$_t$, taking as reference the average prices set by A2A for domestic users [10]. On the other hand, the revenues from the eventual sale of electricity and the costs associated with the fuel (including the eventual purchase of electricity from the grid to run the heat pump) are both condensed into a single net cash flow in the form of the cost function that results from the optimization, changed of sign. In fact, the cost function has been implemented as the sum of all the fuel costs that arises from the use of the generators minus the possible revenues from the sale of electricity. In addition, if both a CHP and a heat pump are present in the configuration, the system is given the option to self-consume the electricity produced or, instead, to sell it to the grid. The possibility to buy and sell electricity simultaneously is also allowed. Two conditions are required for the heat pump to self-consume electricity from the CHP: both systems must be turned on at the same time and the buying price (P_{ACQ}) must be higher than the selling price (P_{VEN}). The difference between the electricity purchase and sale price is determinant: if P_{ACQ} is lower than P_{VEN}, then each kWh of electricity used for self-consumption generates a net loss of money equal to (P_{VEN} - P_{ACQ}). On the contrary, if P_{ACQ} is higher than P_{VEN}, each kWh of electricity self-consumed produces a saving of money equal to (P_{ACQ} – P_{VEN}). Thus, the difference between these two prices represents the opportunity cost for the self-consumption decision.

Figure 21 is useful to clarify this concept, allowing a direct picture of the cash and energy flows in each one of the three possible conditions.

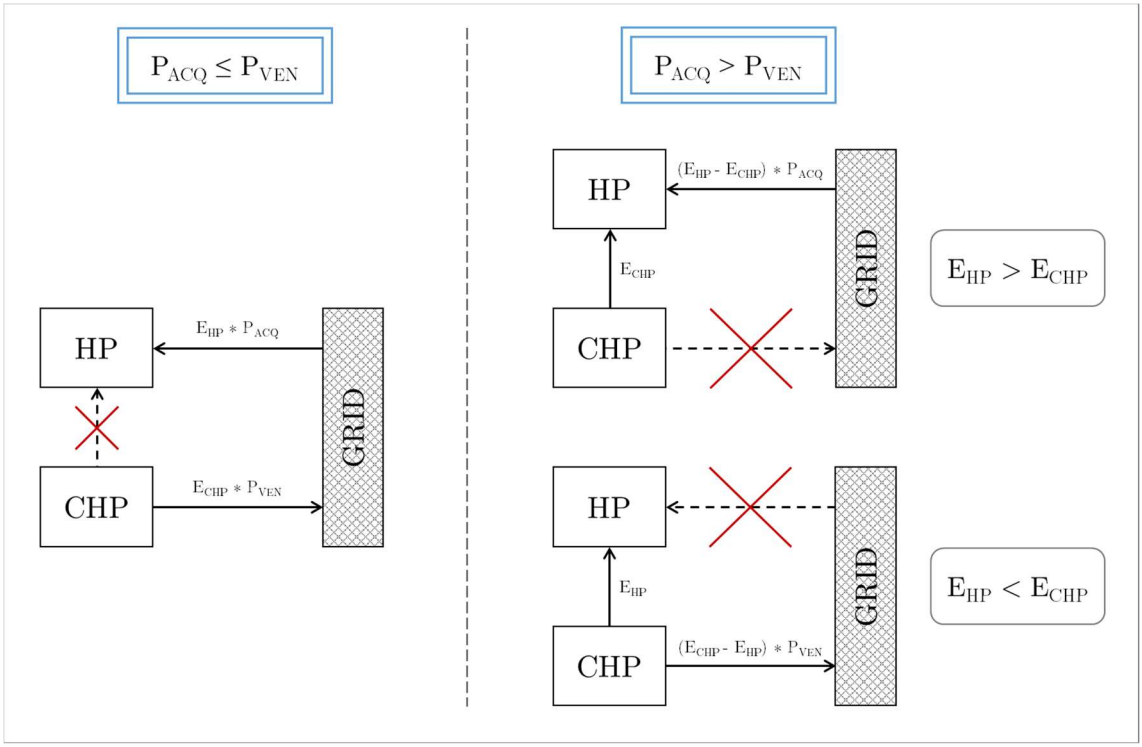

Figure 21: Alternative options for the optimizer with a cogenerative system

The investment cost per unit of capacity for the ICE has been assumed as variable with the nominal electrical power of the machines, according to the *Catalog of CHP Technologies* published by the U.S. Environmental Protection Agency [11]. In addition, the same source reports the O&M costs for the different sizes of the machine as dependent from the electricity production. The estimation of the costs outside the considered interval has been performed using logarithmic interpolation of the available data, while inside the interval a linear interpolation has been used. Figure 22 reports a synthesis of the data for the ICE.

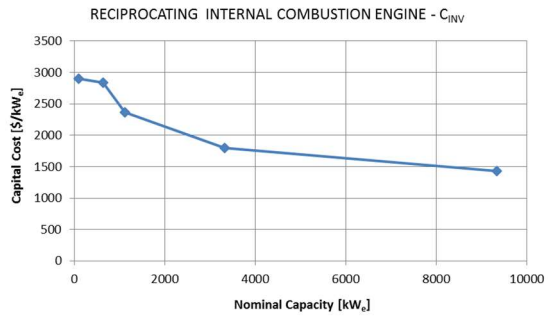

Capacity [kW]	100	633	1.121	3.326	9.341
C_{INV} [k€]	218	1.350	1.994	4.504	10.064

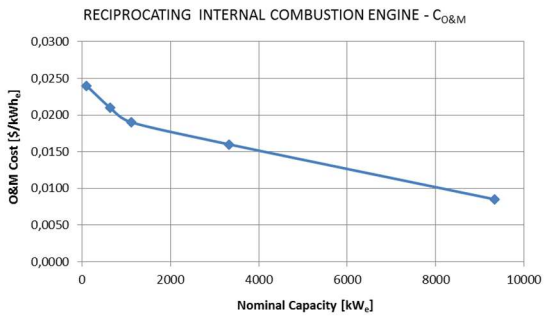

Capacity [kW]	100	633	1.121	3.326	9.341
$C_{O\&M}$ [€/kWh]	0,0180	0,0158	0,0143	0,0120	0,0064

Figure 22: Internal combustion engine cost curves

The same catalogue provides also the data for the investment and O&M costs for the gas turbine. The procedure used to assess the costs for the GT is identical to the one used with the ICE. Figure 23, hereafter, summarizes the results.

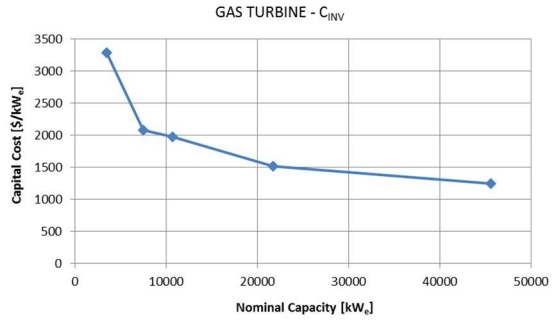

Capacity [kW]	3.510	7.520	10.680	21.730	45.607
C_{INV} [k€]	8.659	11.761	15.867	24.802	42.795

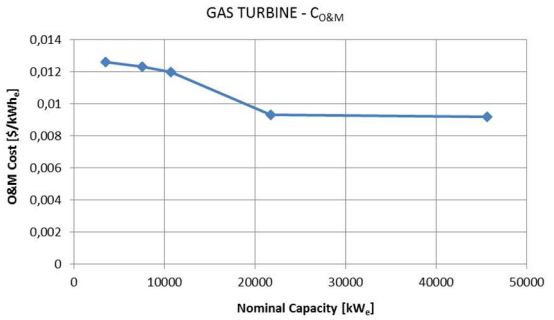

Capacity [kW]	3.510	7.520	10.680	21.730	45.607
$C_{O\&M}$ [€/kWh]	0,0095	0,0092	0,0090	0,0070	0,0069

Figure 23: Gas turbine cost curves

The investment costs per unit of heating capacity of the heat pump has been set to the constant value of 166 €/kW$_t$ [12]. On the other hand, for the operation and maintenance costs an annual fixed value has been considered, depending on the nominal capacity of the machine [13]. A logarithmic interpolation of these data has been implemented in order to determine the costs for the capacities outside the given interval. Figure 24 reports the assumed data for the heat pump.

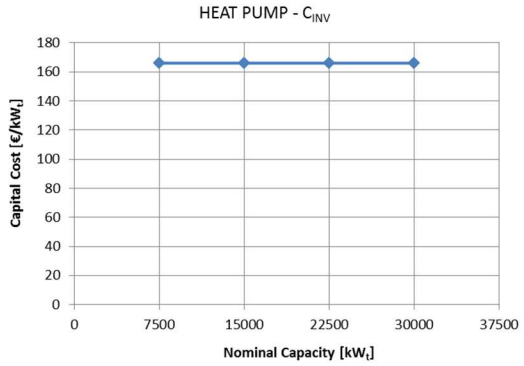

Capacity [kW]	7.500	15.000	22.500	30.000
C_{INV} [k€]	1.245	2.490	3.735	4.980

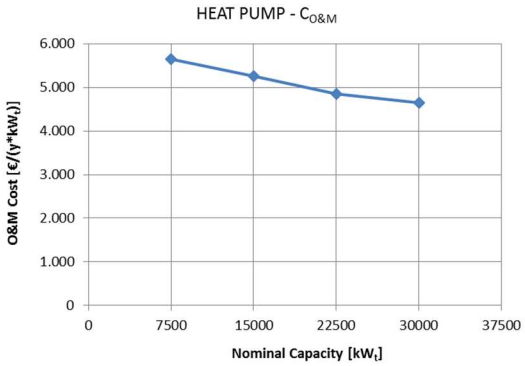

Capacity [kW]	7.500	15.000	22.500	30.000
$C_{O\&M}$ [k€/y]	42	79	109	139

Figure 24: Heat pump cost curves

The investment cost per unit of thermal power for the backup boilers has been set at the constant value of 90 €/kW$_t$ [14]. The cost has been then re-proportioned for each configuration on the base of the actual number of operating hours of the boilers.

The operation and maintenance costs have been computed as a fraction of the investment cost equal to the 3.5%.

At last, for the thermal storage just the investment cost has been taken into account. Its value is assumed variable with the capacity [15], expressed in terms of volume of water. Figure 25 reports the storage investment cost.

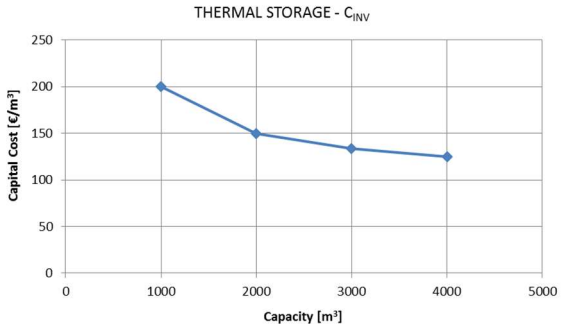

Capacity [m^3]	1.000	2.000	3.000	4.000
C_{INV} [k€]	200	300	400	500

Figure 25: Thermal storage cost curve

The economic lifetime of each technology has been assumed equal to 15 years, which thus represents also the lifetime of the investment for the computation of the NPV. The set lifetime value approximately holds true for each of the considered technologies, except from the gas turbine that can safely operate up to 20 years. Hence, in order to compare the configurations in a fair way and to use the same time-horizon, the investment cost of the GT has been reduced by 25%, which represent the ratio between the difference of lifetime (5 y) and the actual one of the machine (20 y).

Concerning the definition of the prediction horizon, the value of *stepM* has been set to 3 hours. This time interval, in fact, has proved sufficiently accurate in order to comply with the purpose of this thesis, which focuses on the assessment of the benefits from the possible synergies with the electricity grid.

The discount rate for the computation of the NPV has been set to 5%. Its value correspond to the Weighted Average Cost of Capital, which measures the rate that a company is expected to pay on average to all its security holders to finance its assents. The relevance of this parameter on the economic evaluation has been further investigated during the sensitivity analysis.

As regards the price for gas, its value has been set to a plausible 0.25 € sm^{-3} for all the considered scenarios. A study of the impact of this value on the optimal configuration has been carried out during the sensitivity analysis.

5.2 Scenarios

As already mentioned, in order to find the optimal configuration and design for the DHN generation plant four electricity price scenarios were selected. This choice was made to try to give a comprehensive overview of the possible situations that may happen during the operation of a district heating plant interacting with the electrical network. The price scenarios are named as follows: *BASE*, *2017*, *SEN* and MSD.

The *BASE* scenario refers to the electricity prices that A2A used for the year 2014. The buying price is the result of a bilateral agreement with the supplier and it is fixed at a constant level of 140 € MWh^{-1} for the entire year. On the contrary, the selling price comes from the Italian electricity day-ahead market, as known as *Mercato del Giorno Prima* (MGP). During every hour of the day the MGP forms a price, called *Prezzo Zonale* (PZ), for each one of the geographical zones of the national power grid. Since Milan falls under its influence, the *NORD* zone has been considered for the selection of the selling price.

The *2017* scenario is similar to the previous one with the exception that, this time, both the prices are variable and formed by the MGP. The reference year for the data of this scenario is 2017. One more time, the selling price is set equal to the PZ formed during each session. On the other hand, the value to be considered for the buying is called *Prezzo Unico Nazionale* (PUN) that is the single national price at which electricity can be purchased from the network and it is computed as the average of zonal prices weighted for the purchases.

The *SEN* scenario refers to the attainment of the goals contained in the national energy strategy of 2017 (*Strategia Energetica Nazionale*), which aims the overcoming of the objectives about the share of renewable energy set in the European directive 2009/28/CE. While the directive requires reaching the 17% of renewable energy in final consumption by 2020, the SEN policy set 19-20% as a goal. [16]

At last, the *MSD* scenario is the same as *2017* one, except that, this time, a certain portion of the CHP generators is devoted to the participation in selling to the Italian ancillary services market, as known as *Mercato dei Servizi di Dispacciamento* (MSD). The MSD market has the purpose of resolving grid congestions, keeping the system balanced in real time, and it takes place in the form of a mandatory auction at the end of which the winning offers are paid-as-bid. In order to simulate the participation in the MSD market, the electricity price has been set equal to the average bidders selling price accepted during each hour of the day. [17] To date, the MSD market is still in progress and is therefore subject to continuous changes by the Italian energy regulator, ARERA. Therefore, in this thesis, the rules in force in the reference year 2017 have been taken into account.

The share of electric capacity devoted to the MSD market has been fixed to 25% of the nominal electric power of the CHP. To model the partialisation of the machine during the simulation, the CHP is considered as made by two distinct machines: one dedicated to the MGP market with a power of 75% of the nominal and the other to the MSD market with the remaining 25% power.

As a rule of thumb, the buying and selling prices of electricity generally increase with the reference year. The MSD-market price is much more volatile: it can be as null as it can be much higher than the PZ price. To give an idea of this tendency, the graphs representing the electricity prices trend on two representative days are shown in Figure 26.

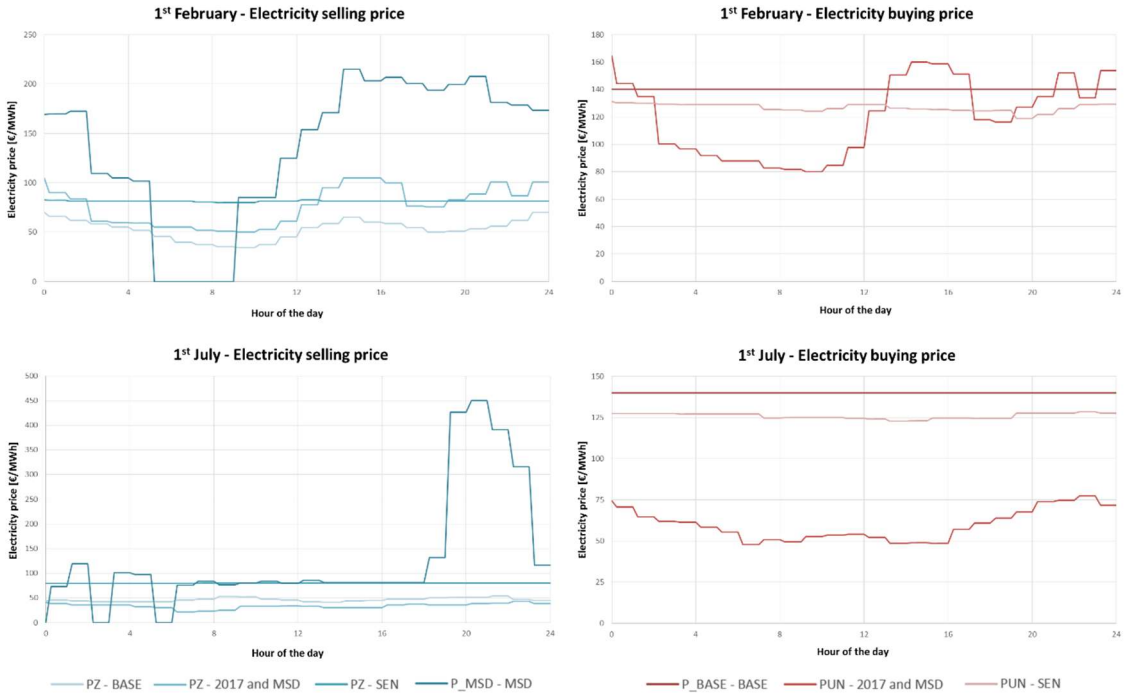

Figure 26: Electricity price trends for two representative days of the year

Each price scenario has been analysed taking in consideration many different plant configurations and sizes of the machines. Among the four technologies selected, only one has been maintained in each configuration and this is the thermal heater. In fact, the boilers were selected as the backup generators, ready to integrate the other machines during peak demand hours or to take their place whenever it is necessary, like when facing a failure or when maintenance operations occurs. Since the boilers serves as the backup technology and their investment cost specific to the thermal power is quite low with respect to the other technologies, their size has been dimensioned to face the peak demand and it has been kept constant across each configuration.

The other three technologies have been analysed considering four different plant configurations, named as follows: *ICE*, *HP*, *GT* and *CHP+HP*. As the names suggest, the first three plants are devoted to study each single technology, while the last one confronts with the interrelationship between the CHP and the HP technologies. This allows not only to study the effects of interfacing each single technology with the electricity grid, but also to assess the possible synergies arising from the interaction between a CHP and a HP in the same framework.

In addition to the variation of electricity prices and technology selection, another degree of freedom in the analysis has been the size of each generator. In order to understand the decision process that was made during the study, figure 1 has been reported below.

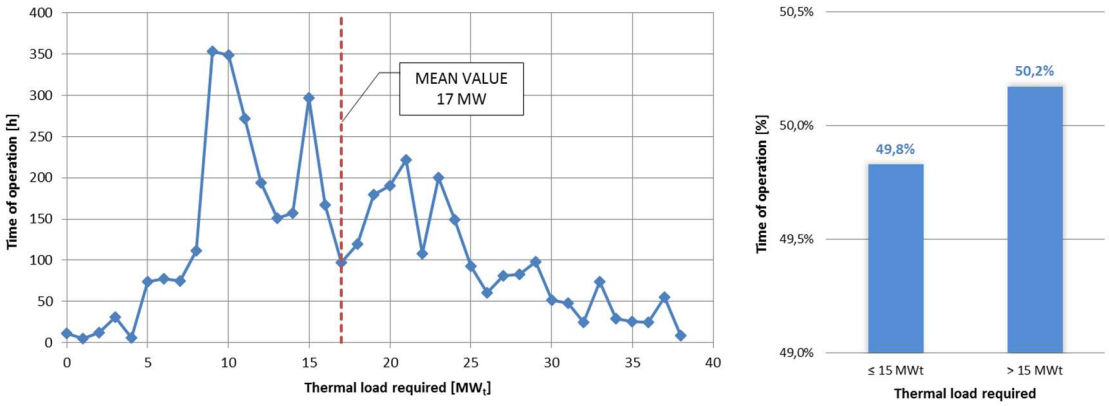

Figure 27: Amount of operating time during which a given thermal load is required by the users

The figure reports graphically the amount of time, in terms of hours of operation of the system, during which the users approximately require a certain level of thermal load. This allows us to recognize that the maximum demand faced by the system stands around a value of 38 MW and that the average load, weighted for the hours of operation, is approximately 17 MW. One more thing that can be noticed is the fact that during about half of the time of system operation, the load required is lower or equal than 15 MW. Considering this, a rational starting point for the machines size is precisely the one currently in place in *Canavese* plant. Each one of the base technologies has been dimensioned to a size of 15 MW, which is very close to the mean value. On the other hand, the backup boilers have been sized to 15 MW each (45 MW in total), in order to be able to face the maximum load and any other unexpected peak on their own. At last, concerning the thermal storage, a base size of 2000 m^3 has been selected, which is exactly the dimension of the actual plant.

Once the base sizes have been selected, the following step consisted in their systematic variation in order to search for the optimal plant configuration. As a first attempt, the variation consisted in the multiplication of the base size by a factor of 0.5,

1.5 and 2. If the optimal solution found within this interval is questionable, additional factors are considered. In order to clarify, the following Table 8 reports the technologies considered and their sizes within the base variation factors set.

			Multiplication factor			
			BASE	0.5	1.5	2
Machines size	ICE	[MW]	15	7.5	22.5	30
	HP	[MW]	15	7.5	22.5	30
	GT	[MW]	15	7.5	22.5	30
	STORAGE	[m^3]	2000	1000	3000	4000
	BOILERS	[MW]	45	-	-	-

Table 8: Base set of variation factors of the generators nominal power

As mentioned before, the *ICE* configuration consists of an internal combustion engine for the cogeneration of electricity and heat, a thermal storage and a set of three backup boilers. Hence, the number of simulations to be performed, coherently with the base variation factors set, is 16 since we may have any composition of CHP and storage sizes. The *HP* and the *GT* configurations are very similar in to the *ICE* one, except that the base technology added to the thermal storage and the backup boilers are a heat pump and a CHP gas turbine respectively.

Table 9 represents the initial set of configurations for these scenarios.

ICE configuration																	
CONFIGURATION		CF1	CF2	CF3	CF4	CF5	CF6	CF7	CF8	CF9	CF10	CF11	CF12	CF13	CF14	CF15	CF16
Boilers	[MW]	45	45	45	45	45	45	45	45	45	45	45	45	45	45	45	45
Internal Combustion Engine	[MW]	15	7.5	22.5	30	15	7.5	22.5	30	15	7.5	22.5	30	15	7.5	22.5	30
Thermal Storage	[m^3]	2000	2000	2000	2000	1000	1000	1000	1000	3000	3000	3000	3000	4000	4000	4000	4000
HP configuration																	
CONFIGURATION		CF17	CF18	CF19	CF20	CF21	CF22	CF23	CF24	CF25	CF26	CF27	CF28	CF29	CF30	CF31	CF32
Boilers	[MW]	45	45	45	45	45	45	45	45	45	45	45	45	45	45	45	45
Heat Pump	[MW]	15	7.5	22.5	30	15	7.5	22.5	30	15	7.5	22.5	30	15	7.5	22.5	30
Thermal Storage	[m^3]	2000	2000	2000	2000	1000	1000	1000	1000	3000	3000	3000	3000	4000	4000	4000	4000
GT configuration																	
CONFIGURATION		CF33	CF34	CF35	CF36	CF37	CF38	CF39	CF40	CF41	CF42	CF43	CF44	CF45	CF46	CF47	CF48
Boilers	[MW]	45	45	45	45	45	45	45	45	45	45	45	45	45	45	45	45
Gas Turbine	[MW]	15	7.5	22.5	30	15	7.5	22.5	30	15	7.5	22.5	30	15	7.5	22.5	30
Thermal Storage	[m^3]	2000	2000	2000	2000	1000	1000	1000	1000	3000	3000	3000	3000	4000	4000	4000	4000

Table 9: Initial set of configurations for the ICE, HP and GT scenarios

Lastly, the *CHP+HP* configuration consists on the concurrent presence of both a CHP technology and a heat pump in addition to the thermal storage and the backup

boilers. The CHP technology selected for this scenario depends on the results of the comparison between the *ICE* and the *GT* configurations: the choice falls on the best option in terms of NPV. The set of initial possible combinations for this scenario is 64, which is much higher than the other configurations one since this time the selected machines are three. Table 10 reports this initial set of combinations for the *CHP+HP* scenario.

CHP+HP configuration																	
CONFIGURATION		CF49	CF50	CF51	CF52	CF53	CF54	CF55	CF56	CF57	CF58	CF59	CF60	CF61	CF62	CF63	CF64
Boilers	[MW]	45	45	45	45	45	45	45	45	45	45	45	45	45	45	45	45
Heat Pump	[MW]	15	7.5	22.5	30	15	7.5	22.5	30	15	7.5	22.5	30	15	7.5	22.5	30
Combined heat and power	[MW]	15	15	15	15	7.5	7.5	7.5	7.5	22.5	22.5	22.5	22.5	30	30	30	30
Thermal Storage	[m^3]	2000	2000	2000	2000	2000	2000	2000	2000	2000	2000	2000	2000	2000	2000	2000	2000
CONFIGURATION		CF65	CF66	CF67	CF68	CF69	CF70	CF71	CF72	CF73	CF74	CF75	CF76	CF77	CF78	CF79	CF80
Boilers	[MW]	45	45	45	45	45	45	45	45	45	45	45	45	45	45	45	45
Heat Pump	[MW]	15	7.5	22.5	30	15	7.5	22.5	30	15	7.5	22.5	30	15	7.5	22.5	30
Combined heat and power	[MW]	15	15	15	15	7.5	7.5	7.5	7.5	22.5	22.5	22.5	22.5	30	30	30	30
Thermal Storage	[m^3]	1000	1000	1000	1000	1000	1000	1000	1000	1000	1000	1000	1000	1000	1000	1000	1000
CONFIGURATION		CF81	CF82	CF83	CF84	CF85	CF86	CF87	CF88	CF89	CF90	CF91	CF92	CF93	CF94	CF95	CF96
Boilers	[MW]	45	45	45	45	45	45	45	45	45	45	45	45	45	45	45	45
Heat Pump	[MW]	15	7.5	22.5	30	15	7.5	22.5	30	15	7.5	22.5	30	15	7.5	22.5	30
Combined heat and power	[MW]	15	15	15	15	7.5	7.5	7.5	7.5	22.5	22.5	22.5	22.5	30	30	30	30
Thermal Storage	[m^3]	3000	3000	3000	3000	3000	3000	3000	3000	3000	3000	3000	3000	3000	3000	3000	3000
CONFIGURATION		CF97	CF98	CF99	CF100	CF101	CF102	CF103	CF104	CF105	CF106	CF107	CF108	CF109	CF110	CF111	CF112
Boilers	[MW]	45	45	45	45	45	45	45	45	45	45	45	45	45	45	45	45
Heat Pump	[MW]	15	7.5	22.5	30	15	7.5	22.5	30	15	7.5	22.5	30	15	7.5	22.5	30
Combined heat and power	[MW]	15	15	15	15	7.5	7.5	7.5	7.5	22.5	22.5	22.5	22.5	30	30	30	30
Thermal Storage	[m^3]	4000	4000	4000	4000	4000	4000	4000	4000	4000	4000	4000	4000	4000	4000	4000	4000

Table 10: Initial set of configurations for the CHP+HP scenario

Concerning the model of each generator, the ICE, the HP and the boilers were selected so to have the same operating parameters of the ones modelled in Chapter 4.2.2 and reported in Table 4, Table 5 and Table 6.

The SGT-400 gas turbine model by Siemens has been selected as a reference model for the GT configuration. [18] The main parameters of this generator are reported in Table 11.

Description	Value	Units
Manufactorer brand	Siemens	-
Machine model	SGT-400	-
Type of generator	Gas turbine	-
Type of fuel	Natural gas	-
Nominal electric power	12,9	MW_e
Electrical efficiency	0.348	-
Heat rate	10355	kJ/kWh
Turbine speed	9500	rpm
Exhaust gas flow	39.4	kg/s
Exhaust gas temperature	555	°C
Compressor pressure ratio	16.8:1	-

Table 11: Main parameters of the GT

At last, the most important parameters set for the operation of the model have been reported in Table 12.

Description	Value	Units
TRNSYS simulation time step	0.25	h
TRNSYS simulation tolerance convergence	0.001	-
MPC optimization horizon	3	h

Table 12: Main parameters of the simulation

5.3 Results

5.3.1 Results and analysis of *BASE* scenario

Since the *BASE* scenario has been the first one to be modelled, its results have been employed to extract important indications for the implementation of the other price scenarios. This allowed reducing the number of significant variables and, by consequence, the number of simulations to perform. The cost function resulting of the starting set of configurations for this scenario is represented in Figure 28.

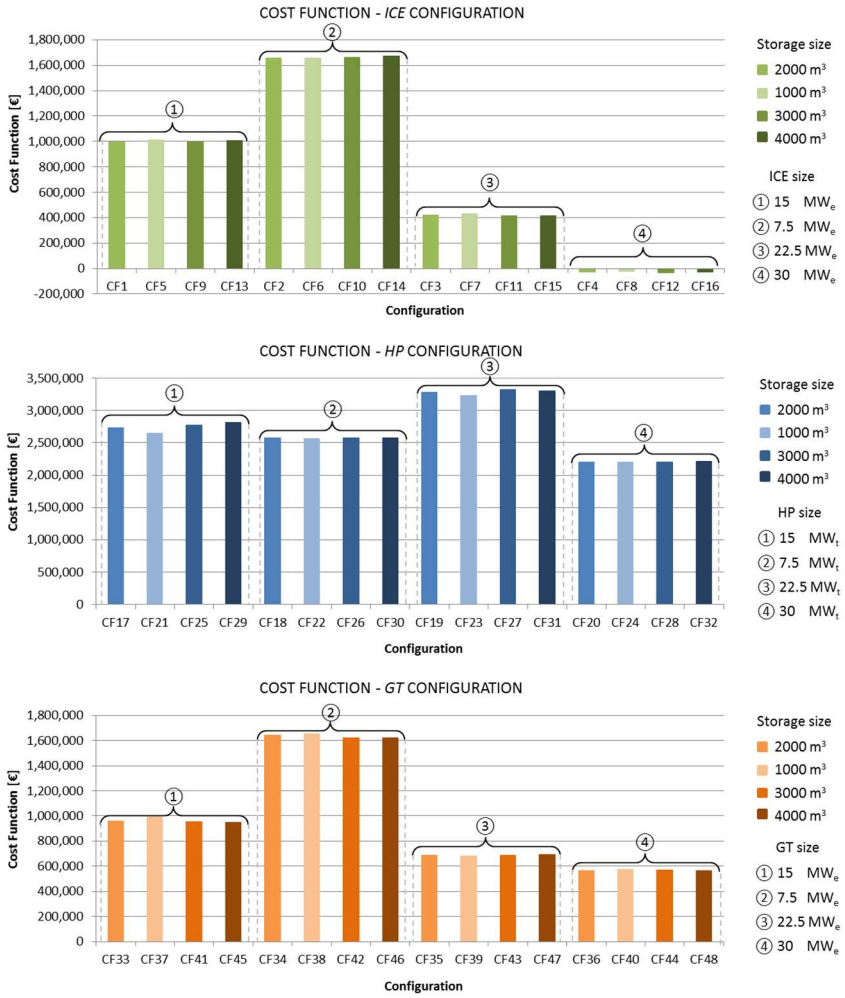

Figure 28: Annual cost functions for the ICE, HP and GT configurations of BASE scenario

As it can be noticed from this figure, the value of the cost function is strictly related to the generator size. On the contrary, the approximate repetition of levels that occurs after each group of four configurations suggests that the thermal storage size does not affect significantly the resulting cost function. This is probably due to the model and the control strategy selected for this component, which should be subject to a deeper, dedicated analysis. The *ICE* and the *GT* configurations presents decreasing values of cost function as the size of the CHP increases, turning even negative in some cases. This is coherent with the growth in electricity production, the sale of which implies higher revenues. This behaviour may be explained performing an approximate evaluation of the costs and revenues associated with the CHP and the boilers technologies. This rough estimation can be carried out assuming 1 kWh_t of thermal energy as the output of both the machines, considering the nominal values of their efficiencies and taking into account the 2014 average price for the sale of electricity in the NORD zone (PZ_{2014}) [19]. The set of parameters and the evaluation for the ICE case are respectively reported in the following Table 13 and Figure 29.

Symbol	Description	Value	Units
$\eta_{el,ICE}$	Nominal electrical efficiency of the ICE	0.44	-
$\eta_{th,ICE}$	Nominal thermal efficiency of the ICE	0.37	-
$\eta_{el,GT}$	Nominal electrical efficiency of the GT	0.348	-
$\eta_{th,GT}$	Nominal thermal efficiency of the GT	0.509	-
$\eta_{th,BOI}$	Nominal thermal efficiency of the boilers	0.93	-
PZ_{2014}	Average 2014 zonal price for the sale of electricity	50.35	€ MWh^{-1}
P_{GAS}	Price for the purchase of natural gas	0.25	€ sm^{-3}
LHV_{GAS}	Lower heating value of natural gas	$9.59*10^{-3}$	MWh sm^{-3}
R_{EL}	Revenues for the sale of electric energy to the grid	-	€
C_{GAS}	Costs for the purchase of natural gas	-	€
FC	Cost function as fuel costs minus eventual R_{EL}	-	€

Table 13: Main parameters for the approximate evaluation of the ICE cost function

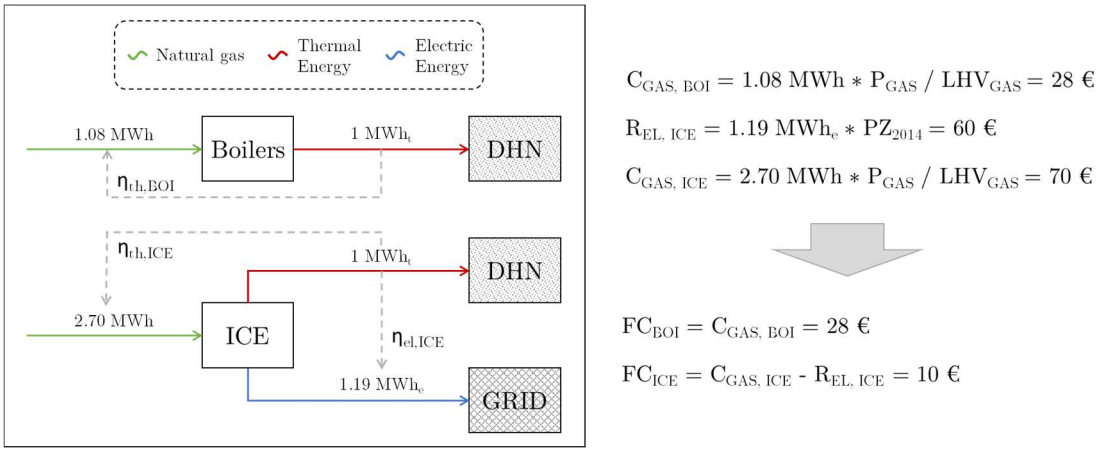

Figure 29: Approximate cost function evaluation of ICE in the BASE scenario

Thus, the cost function per unit of thermal energy output given by the combined heat and power generator is lower with respect to the one of the boilers. This of course does not mean that the ICE is always favoured over the boilers. In fact, the choice depends on the current electricity price, since it varies a lot during the year (PZ_{MIN} = 2.23 € MWh^{-1}, PZ_{MAX} = 149.66 € MWh^{-1}), and on the size of the machines, since the CHP may not be enough to satisfy the thermal load.

On the other hand, the heat pump configuration shows a different behaviour in the relationship between the size of the machine and the cost function. The following Table 14 and Figure 30 perform an evaluation similar to the one done for the *ICE* configuration.

Symbol	Description	Value	Units
COP_{HP}	HP coefficient of performance at reference conditions	2.624	-
$\eta_{th,BOI}$	Nominal thermal efficiency of the boilers	0.93	-
P_{ACQ}	Price for the purchase of electricity	140	€ MWh^{-1}
P_{GAS}	Price for the purchase of natural gas	0.25	€ sm^{-3}
LHV_{GAS}	Lower heating value of natural gas	$9.59*10^{-3}$	MWh sm^{-3}
C_{EL}	Costs for the purchase of electric energy	-	€
C_{GAS}	Costs for the purchase of natural gas	-	€
FC	Cost function as fuel costs minus eventual R_{EL}	-	€

Table 14: Main parameters for the approximate evaluation of the HP cost function

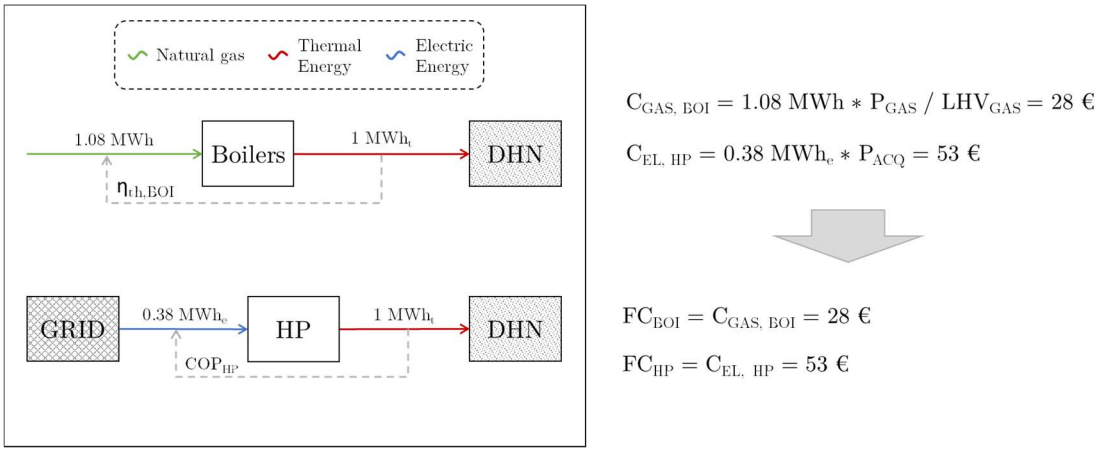

Figure 30: Approximate cost function evaluation of HP in the BASE scenario

This time, the backup boilers turn out to be more convenient with respect to the heat pump because they present a lower cost function for the same thermal output. However, since the performances of the heat pump strongly depends on the operating conditions of the systems, this result cannot be considered as the typical situation and the convenience of the two machines may frequently switch. Despite this, the trend showed by the graph is that the cost function tends to reduce as the size of the heat pump increases.

The second phase that has been carried out during the analysis is the computation of the NPV for the first three configurations. The investment costs and the operating costs and revenues has been assessed accordingly to the definitions and parameters provided in Chapter 5.1. The investment costs have been considered concentrated at the first year of the investment (year 0). Differently, the operating costs and revenues have been accounted for during every year of the generators lifetime (years from 0 to 15).

In order to provide an example, the following Table 15 and Table 16 show the main parameter and the calculation process of the net present value for the *ICE* configuration.

Symbol	Description	Units
C_{INV}	Investment costs for the machines	M€
$C_{O\&M}$	Operation and maintenance costs for the machines	M€ y^{-1}
C_F	Fuel costs for the operation of the machines	M€ y^{-1}
R_{TH}	Revenues for the sale of thermal energy to the DHN	M€ y^{-1}
R_{EL}	Revenues for the sale of electric energy to the grid	M€ y^{-1}
C_{OP}	Operating costs of the system	M€ y^{-1}
R_{OP}	Operating revenues of the system	M€ y^{-1}
NCF_{DISC}	Net Cash Flows discounted at the present value	M€
NPV	Net Present Value of the configuration	M€

Table 15: Main parameters for the computation of the NPV in the ICE configuration

			ICE CONFIGURATION															
			CF1	CF2	CF3	CF4	CF5	CF6	CF7	CF8	CF9	CF10	CF11	CF12	CF13	CF14	CF15	CF16
Investment Costs	C_{INV} - Storage	[M€]	-0.3	-0.3	-0.3	-0.3	-0.2	-0.2	-0.2	-0.2	-0.4	-0.4	-0.4	-0.4	-0.5	-0.5	-0.5	-0.5
	C_{INV} - ICE	[M€]	-15.5	-8.7	-20.9	-25.6	-15.5	-8.7	-20.9	-25.6	-15.5	-8.7	-20.9	-25.6	-15.5	-8.7	-20.9	-25.6
	C_{INV} - Boilers	[M€]	-1.8	-3.2	-0.8	-0.2	-1.9	-3.2	-0.8	-0.3	-1.8	-3.2	-0.7	-0.2	-1.8	-3.2	-0.7	-0.2
	C_{INV} - tot	**[M€]**	**-17.7**	**-12.2**	**-22.0**	**-26.1**	**-17.6**	**-12.1**	**-22.0**	**-26.1**	**-17.7**	**-12.3**	**-22.0**	**-26.2**	**-17.8**	**-12.4**	**-22.1**	**-26.3**
Operating Costs and Revenues	Cost Function (R_{EL} - C_F)	[M€/y]	-1.0	-1.7	-0.4	0.0	-1.0	-1.7	-0.4	0.0	-1.0	-1.7	-0.4	0.0	-1.0	-1.7	-0.4	0.0
	$C_{O\&M}$	[M€/y]	-0.3	-0.2	-0.4	-0.4	-0.3	-0.2	-0.4	-0.4	-0.3	-0.2	-0.4	-0.4	-0.3	-0.2	-0.4	-0.4
	R_{TH}	[M€/y]	6.0	6.0	6.0	6.0	6.0	6.0	6.0	6.0	6.0	6.0	6.0	6.0	6.0	6.0	6.0	6.0
	(R_{OP} - C_{OP}) - tot	**[M€/y]**	**4.7**	**4.1**	**5.2**	**5.6**	**4.7**	**4.1**	**5.2**	**5.6**	**4.7**	**4.1**	**5.2**	**5.6**	**4.7**	**4.1**	**5.2**	**5.6**
Net Cash Flows	Lifetime	[y]	15.0	15.0	15.0	15.0	15.0	15.0	15.0	15.0	15.0	15.0	15.0	15.0	15.0	15.0	15.0	15.0
	Discount Rate	[%]	0.1	0.1	0.1	0.1	0.1	0.1	0.1	0.1	0.1	0.1	0.1	0.1	0.1	0.1	0.1	0.1
	$NCF_{DISC}(0)$	[M€]	-13.0	-8.0	-16.8	-20.5	-12.9	-7.9	-16.8	-20.5	-13.0	-8.2	-16.9	-20.6	-13.2	-8.3	-17.0	-20.7
	$NCF_{DISC}(1)$	[M€]	4.5	3.9	4.9	5.3	4.5	3.9	4.9	5.3	4.5	3.9	4.9	5.3	4.5	3.9	4.9	5.3
	$NCF_{DISC}(2)$	[M€]	4.3	3.8	4.7	5.1	4.2	3.8	4.7	5.1	4.3	3.7	4.7	5.1	4.2	3.7	4.7	5.1
	$NCF_{DISC}(3)$	[M€]	4.1	3.6	4.5	4.8	4.0	3.6	4.5	4.8	4.1	3.6	4.5	4.8	4.0	3.6	4.5	4.8
	$NCF_{DISC}(4)$	[M€]	3.9	3.4	4.3	4.6	3.9	3.4	4.3	4.6	3.9	3.4	4.3	4.6	3.9	3.4	4.3	4.6
	$NCF_{DISC}(5)$	[M€]	3.7	3.2	4.1	4.4	3.7	3.2	4.0	4.4	3.7	3.2	4.1	4.4	3.7	3.2	4.0	4.4
	$NCF_{DISC}(6)$	[M€]	3.5	3.1	3.9	4.2	3.5	3.1	3.9	4.2	3.5	3.1	3.9	4.2	3.5	3.1	3.9	4.2
	$NCF_{DISC}(7)$	[M€]	3.3	2.9	3.7	4.0	3.3	2.9	3.7	4.0	3.3	2.9	3.7	4.0	3.3	2.9	3.7	4.0
	$NCF_{DISC}(8)$	[M€]	3.2	2.8	3.5	3.8	3.2	2.8	3.5	3.8	3.2	2.8	3.5	3.8	3.2	2.8	3.5	3.8
	$NCF_{DISC}(9)$	[M€]	3.0	2.7	3.3	3.6	3.0	2.7	3.3	3.6	3.0	2.7	3.3	3.6	3.0	2.7	3.3	3.6
	$NCF_{DISC}(10)$	[M€]	2.9	2.5	3.2	3.4	2.9	2.5	3.2	3.4	2.9	2.5	3.2	3.4	2.9	2.5	3.2	3.4
	$NCF_{DISC}(11)$	[M€]	2.7	2.4	3.0	3.3	2.7	2.4	3.0	3.3	2.7	2.4	3.0	3.3	2.7	2.4	3.0	3.3
	$NCF_{DISC}(12)$	[M€]	2.6	2.3	2.9	3.1	2.6	2.3	2.9	3.1	2.6	2.3	2.9	3.1	2.6	2.3	2.9	3.1
	$NCF_{DISC}(13)$	[M€]	2.5	2.2	2.7	3.0	2.5	2.2	2.7	3.0	2.5	2.2	2.7	3.0	2.5	2.2	2.7	3.0
	$NCF_{DISC}(14)$	[M€]	2.4	2.1	2.6	2.8	2.4	2.1	2.6	2.8	2.4	2.1	2.6	2.8	2.4	2.1	2.6	2.8
	$NCF_{DISC}(15)$	[M€]	2.3	2.0	2.5	2.7	2.3	2.0	2.5	2.7	2.3	2.0	2.5	2.7	2.3	2.0	2.5	2.7
NPV	**Net Present Value**	**[M€]**	**35.8**	**34.9**	**36.9**	**37.4**	**35.7**	**35.0**	**36.8**	**37.5**	**35.6**	**34.7**	**36.8**	**37.4**	**35.4**	**34.5**	**36.7**	**37.2**

Table 16: Computation of the NPV for the ICE configuration of the BASE scenario

A similar structure has been used to compute the NPV for the other configurations. Afterwards, the results have been collected and displayed both in the form of scatterplots, which are convenient for their immediate graphical comparison, and in the form of tables, which are useful to assess their exact value.

The results from the *ICE* configuration are reported in the following Figure 31 and Figure 32, which display two scatterplot graphs. For the NPV, both the absolute value and the value specific to the thermal energy sold to the network are reported. The second one is useful in order to make the results more general.

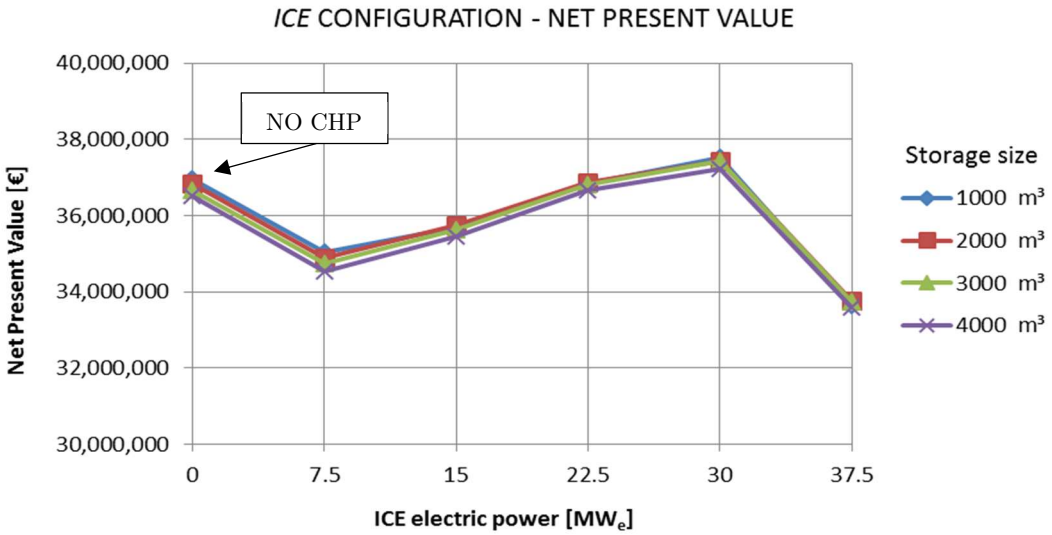

Figure 31: Absolute NPV for the ICE configuration (BASE s.)

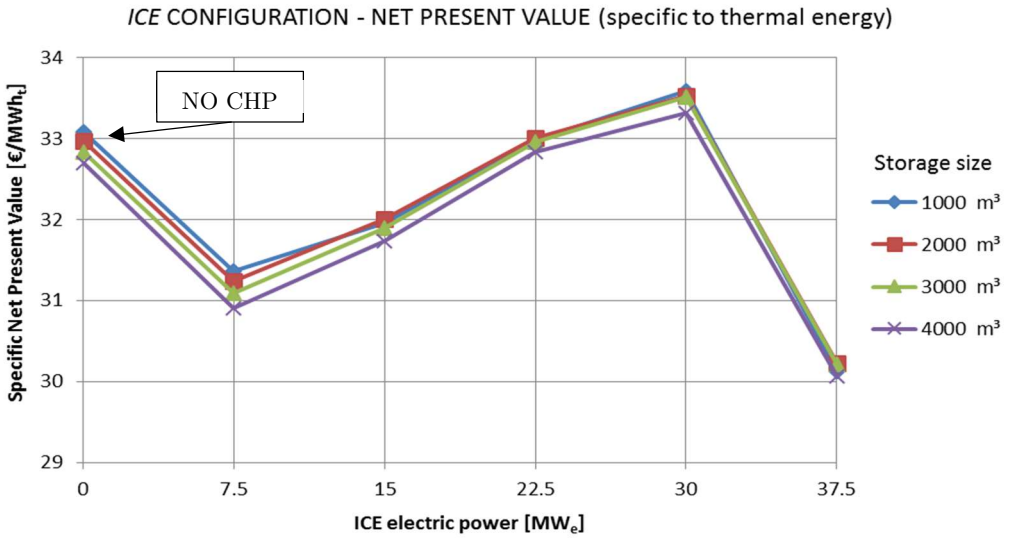

Figure 32: NPV specific to thermal energy produced for the ICE configuration (BASE s.)

Table 17 shows the results of the same configuration in numerical form, both in absolute terms and specific to the MWh_t.

		ICE CONFIGURATION - NPV [€]			
		Thermal storage size [m³]			
		1000	2000	3000	4000
ICE size [MW_e]	0	36,948,511	36,833,817	36,676,125	36,518,075
	7.5	35,024,849	34,885,674	34,729,491	34,521,867
	15	35,695,795	35,752,465	35,628,665	35,439,823
	22.5	36,839,293	36,868,968	36,809,399	36,678,225
	30	37,511,590	37,449,041	37,427,652	37,213,987
	37.5	33,656,716	33,762,295	33,750,466	33,588,675

		ICE CONFIGURATION - NPV specific to thermal energy [€/MWh_t]			
		Thermal storage size [m³]			
		1000	2000	3000	4000
ICE size [MW_e]	0	33.1	33.0	32.8	32.7
	7.5	31.4	31.2	31.1	30.9
	15	32.0	32.0	31.9	31.7
	22.5	33.0	33.0	33.0	32.8
	30	33.6	33.5	33.5	33.3
	37.5	30.1	30.2	30.2	30.1

Table 17: NPV results for the ICE configuration (BASE s.)

As illustrated in the pictures, in order to find the optimal solution two more sizes for the internal combustion engine have been considered in addition to the initial set: 0 and 37.5 MW_e. The 0 MW_e one represents the configuration that includes as generators just the boilers, which explain the initial decrease in the NPV.

With an absolute NPV of 37.5 million euros and a specific one of 33.6 euros per MWh_t, the optimal solution for the *ICE* configuration in the *BASE* scenario is given by a 30 MW_e combined heat and power engine and a 1000 m^3 thermal storage. However, confirming what was stated regarding the cost functions, the thermal storage size seems to not affect much the value of the net present value. In fact, the maximum percentage difference in the NPV value due to a variation in storage volumes is approximately 1.5%. Remember that the results are related to a variable low temperature heat network. It is possible that the influence of the storage is more considerable in a traditional network.

Similarly to the previous case, the following Figure 33 and Figure 34 reports the results of the *HP* configuration.

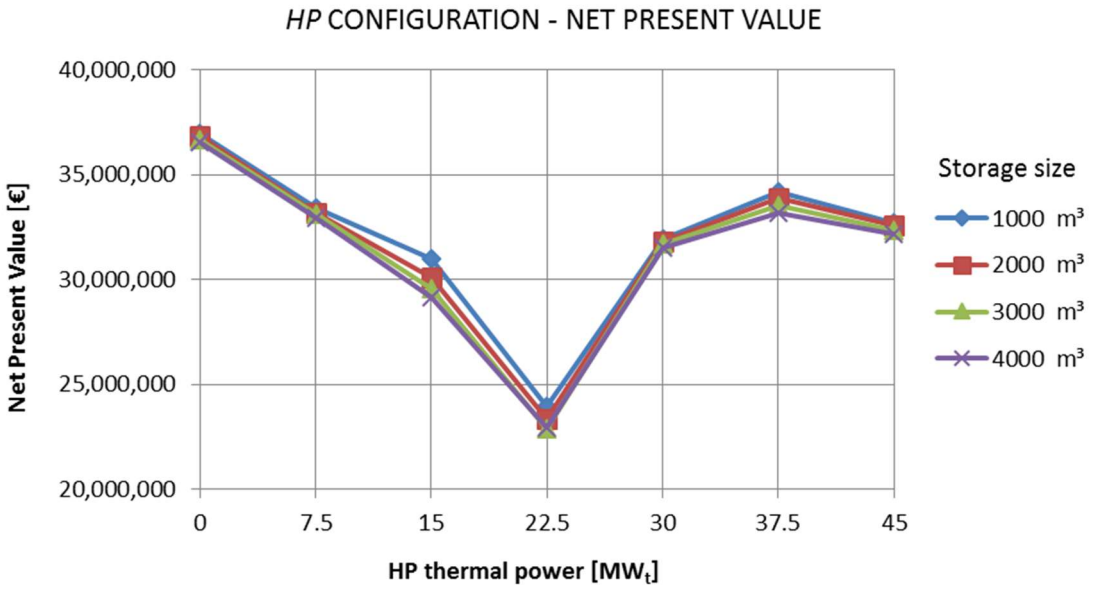

Figure 33: Absolute NPV for the HP configuration (BASE s.)

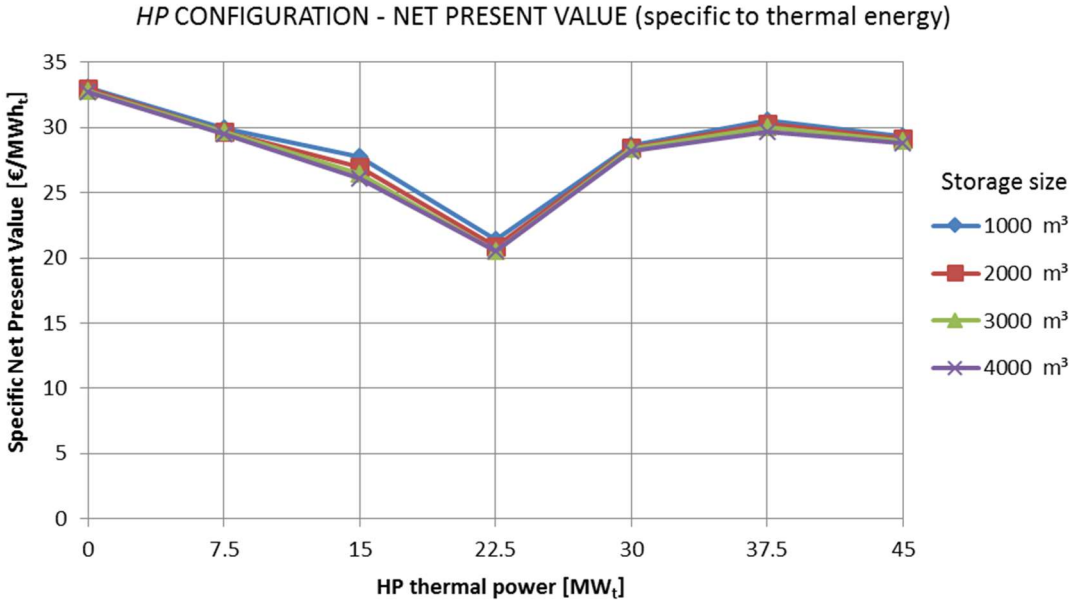

Figure 34: NPV specific to thermal energy produced for the HP configuration (BASE s.)

Table 18 shows the same results in a numerical form.

		HP CONFIGURATION - NPV [€]			
		Thermal storage size [m³]			
		1000	2000	3000	4000
HP size [MW_t]	0	36,948,511	36,833,817	36,676,125	36,518,075
	7.5	33,413,492	33,178,412	33,110,401	32,929,898
	15	30,960,012	30,081,246	29,589,019	29,122,416
	22.5	23,948,779	23,359,908	22,896,444	22,934,078
	30	31,957,044	31,806,937	31,682,375	31,508,845
	37.5	34,164,987	33,867,301	33,510,674	33,192,065
	45	32,712,180	32,563,960	32,368,754	32,138,058

		HP CONFIGURATION - NPV specific to thermal energy [€/MWh_t]			
		Thermal storage size [m³]			
		1000	2000	3000	4000
HP size [MW_t]	0	33.1	33.0	32.8	32.7
	7.5	29.9	29.7	29.6	29.5
	15	27.7	26.9	26.5	26.1
	22.5	21.4	20.9	20.5	20.5
	30	28.6	28.5	28.4	28.2
	37.5	30.6	30.3	30.0	29.7
	45	29.3	29.2	29.0	28.8

Table 18: NPV results for the HP configuration (BASE s.)

Again, three more machine sizes have been taken into account: 0, 37.5 and 45 MW_t. In particular, the boilers only solution is exactly the same of every other configuration, since the size of the boilers remains constant.

With an NPV of 36.9 million euros and a specific one of 33.1 euros per MWh_t, the optimal solution is precisely the one with boilers only and a thermal storage of 1000 m^3 size. In addition, if the boilers only solution is not allowed, a relative optimum one with a 37.5 MW heat pump and with the same storage volume is found. Once again, the variation of the thermal storage size seems to not have substantial impacts on the net present values, being the maximum percentage difference between same heat pump size solutions is around 6.3%.

Figure 35 and Figure 36 below show the results from the *GT* configuration.

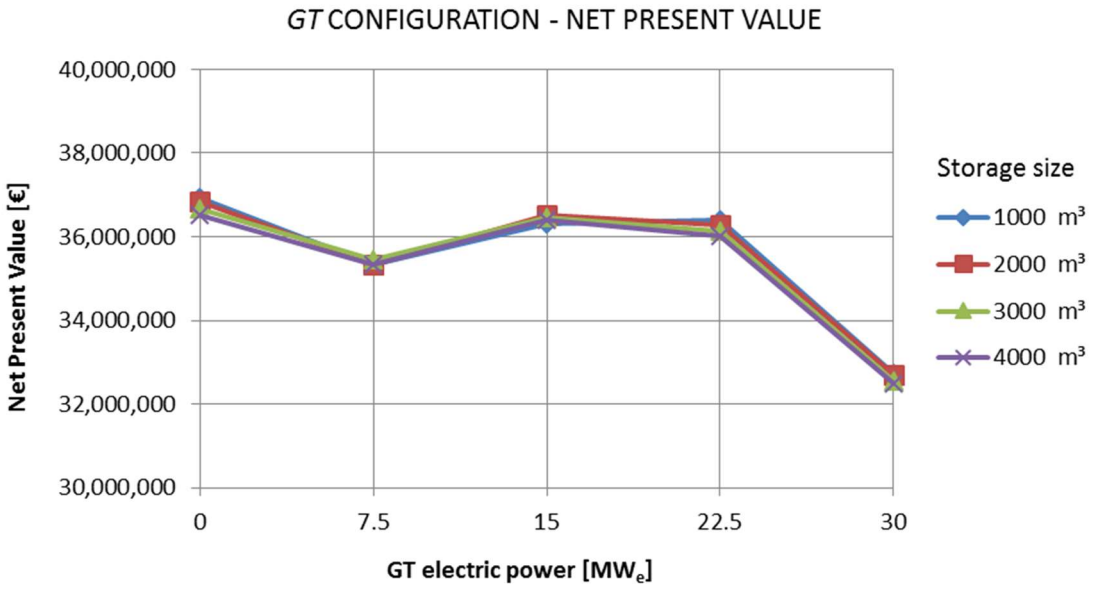

Figure 35: Absolute NPV for the GT configuration (BASE s.)

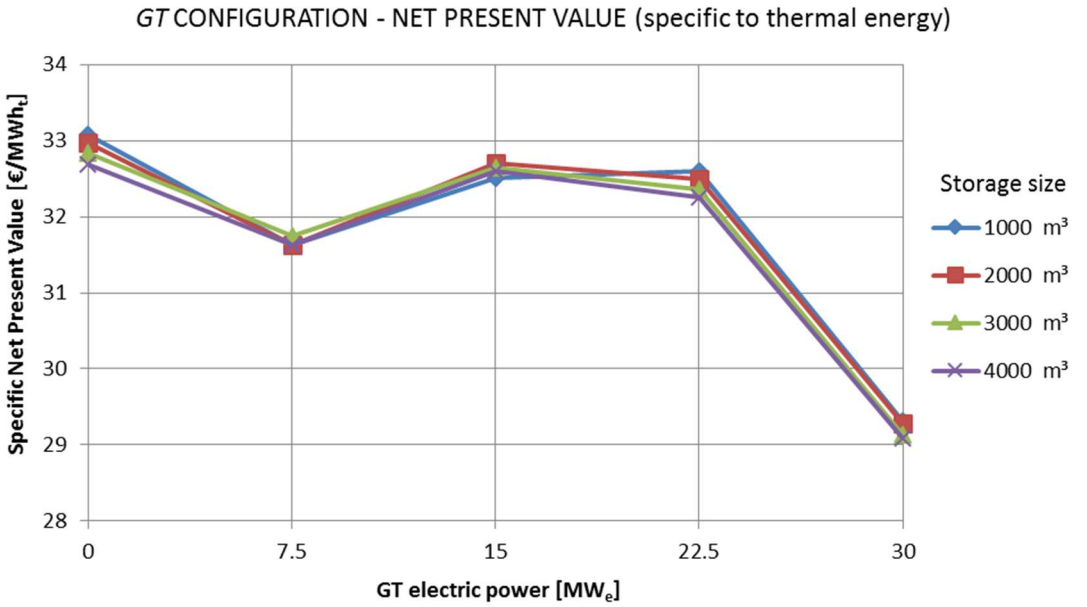

Figure 36: NPV specific to thermal energy produced for the GT configuration (BASE s.)

Once again, Table 19 reports the same results in a numerical forms, in terms of absolute and specific NPV.

		GT CONFIGURATION - NPV [€]			
		Thermal storage size [m³]			
		1000	2000	3000	4000
GT size [MW_e]	0	36,948,511	36,833,817	36,676,125	36,518,075
	7.5	35,323,043	35,329,865	35,462,507	35,329,697
	15	36,305,320	36,530,444	36,466,037	36,407,932
	22.5	36,415,804	36,290,638	36,139,912	36,019,057
	30	32,736,813	32,710,447	32,546,133	32,494,551

		GT CONFIGURATION - NPV specific to thermal energy [€/MWh_t]			
		Thermal storage size [m³]			
		1000	2000	3000	4000
GT size [MW_e]	0	33.1	33.0	32.8	32.7
	7.5	31.6	31.6	31.7	31.6
	15	32.5	32.7	32.6	32.6
	22.5	32.6	32.5	32.4	32.2
	30	29.3	29.3	29.1	29.1

Table 19: NPV results for the GT configuration (BASE s.)

The optimal solution is again the one with boilers only with a 1000 m³ thermal storage and the thermal storage volume variation have little effects on the value of the NPV. A relative optimum solution is given by a 15 MW gas turbine and a 2000 m³ thermal storage.

The last case considered is the *CHP+HP* configuration. Since the optimal solution of the internal combustion engine case have a higher NPV than the gas turbine one, this technology has been selected for the configuration in question. The following Figure 37 presents the cost functions results of this configuration.

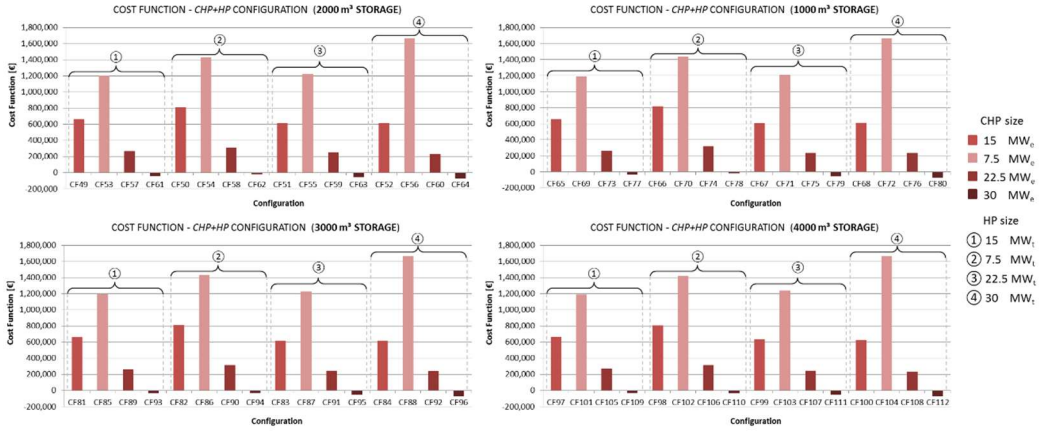

Figure 37: Annual cost functions for the CHP+HP configuration of the BASE scenario

The graphs clearly shows that the same behaviours observed for the previous cases is maintained. Moving from smaller to larger CHP generator sizes and HP sizes, we observe a decrease in the cost function. Once again, the effects of the thermal storage size appears to be negligible. Table 20 below reports the results of the NPV of the *CHP+HP* configuration.

		***CHP+HP* CONFIGURATION**						
		ICE size [Mw_e]						
		0	**7.5**	**15**	**22.5**	**30**		
HP size [MW_t]	**0**	€ 36,948,511	€ 35,024,849	€ 35,695,795	€ 36,839,293	€ 37,511,590		**Thermal storage size [m^3]**
	7.5	€ 33,413,492	€ 36,192,774	€ 36,569,323	€ 36,676,170	€ 35,879,857		
	15	€ 30,960,012	€ 38,503,294	€ 37,512,451	€ 35,872,220	€ 34,429,079	1000	
	22.5	€ 23,948,779	€ 37,361,456	€ 36,712,652	€ 34,696,939	€ 33,117,120		
	30	€ 31,957,044	€ 30,218,982	€ 35,131,027	€ 33,134,865	€ 31,683,503		
	0	€ 36,833,817	€ 34,885,674	€ 35,752,465	€ 36,868,968	€ 37,449,041		
	7.5	€ 33,178,412	€ 36,236,331	€ 36,525,053	€ 36,593,733	€ 35,770,026		
	15	€ 30,081,246	€ 38,371,104	€ 37,349,763	€ 35,661,585	€ 34,360,696	2000	
	22.5	€ 23,359,908	€ 36,990,252	€ 36,515,221	€ 34,316,972	€ 32,980,480		
	30	€ 31,806,937	€ 29,989,679	€ 35,003,960	€ 33,050,801	€ 31,546,081		
	0	€ 36,676,125	€ 34,729,491	€ 35,628,665	€ 36,809,399	€ 37,427,652		
	7.5	€ 33,110,401	€ 36,113,404	€ 36,517,190	€ 36,406,009	€ 35,746,365		
	15	€ 29,589,019	€ 38,337,107	€ 37,198,997	€ 35,558,842	€ 34,236,062	3000	
	22.5	€ 22,896,444	€ 36,775,491	€ 36,314,344	€ 34,194,741	€ 32,810,786		
	30	€ 31,682,375	€ 29,830,956	€ 34,725,397	€ 32,782,748	€ 31,449,473		
	0	€ 36,518,075	€ 34,521,867	€ 35,439,823	€ 36,678,225	€ 37,213,987		
	7.5	€ 32,929,898	€ 36,101,049	€ 36,448,741	€ 36,330,062	€ 35,696,474		
	15	€ 29,122,416	€ 38,347,821	€ 37,004,366	€ 35,321,585	€ 34,046,372	4000	
	22.5	€ 22,934,078	€ 36,472,390	€ 35,975,801	€ 34,042,191	€ 32,713,909		
	30	€ 31,508,845	€ 29,715,849	€ 34,547,580	€ 32,713,961	€ 31,338,724		

Table 20: Absolute NPV results for the CHP+HP configuration (BASE s.)

Then, Table 21 shows the same results in specific to thermal energy sold terms.

		***CHP+HP* CONFIGURATION - NPV specific to thermal energy [€/MWh_t]**						
		ICE size [Mw_e]						
		0	**7.5**	**15**	**22.5**	**30**		
HP size [MW_t]	**0**	33.1	31.4	32.0	33.0	33.6		**Thermal storage size [m^3]**
	7.5	29.9	32.4	32.7	32.8	32.1		
	15	27.7	34.5	33.6	32.1	30.8	1000	
	22.5	21.4	33.4	32.9	31.1	29.6		
	30	28.6	27.1	31.4	29.7	28.4		
	0	33.0	31.2	32.0	33.0	33.5		
	7.5	29.7	32.4	32.7	32.8	32.0		
	15	26.9	34.4	33.4	31.9	30.8	2000	
	22.5	20.9	33.1	32.7	30.7	29.5		
	30	28.5	26.9	31.3	29.6	28.2		
	0	32.8	31.1	31.9	33.0	33.5		
	7.5	29.6	32.3	32.7	32.6	32.0		
	15	26.5	34.3	33.3	31.8	30.7	3000	
	22.5	20.5	32.9	32.5	30.6	29.4		
	30	28.4	26.7	31.1	29.4	28.2		
	0	32.7	30.9	31.7	32.8	33.3		
	7.5	29.5	32.3	32.6	32.5	32.0		
	15	26.1	34.3	33.1	31.6	30.5	4000	
	22.5	20.5	32.7	32.2	30.5	29.3		
	30	28.2	26.6	30.9	29.3	28.1		

Table 21: Specific NPV results for the CHP+HP configuration (BASE s.)

With a NPV of 38.5 million euros and a specific NPV of 34.5 euros per MWh_t, the optimal solution is the configuration with a 15 MW_t heat pump, a 7.5 MW_e internal combustion engine and a 1000 m^3 thermal storage. Since this NPV is the highest one found, this solution also represents the optimum of the entire *BASE* scenario.

Since a single synthetizing graph would not be clarifying due to the large number of data and since the effects of the thermal storage size remain not substantial in the value of the NPV, the decision has been taken to show just two, more illustrative graphs concerning the 1000 m^3 thermal storage size configuration. These two scatterplots are reported in Figure 38 here below in absolute terms.

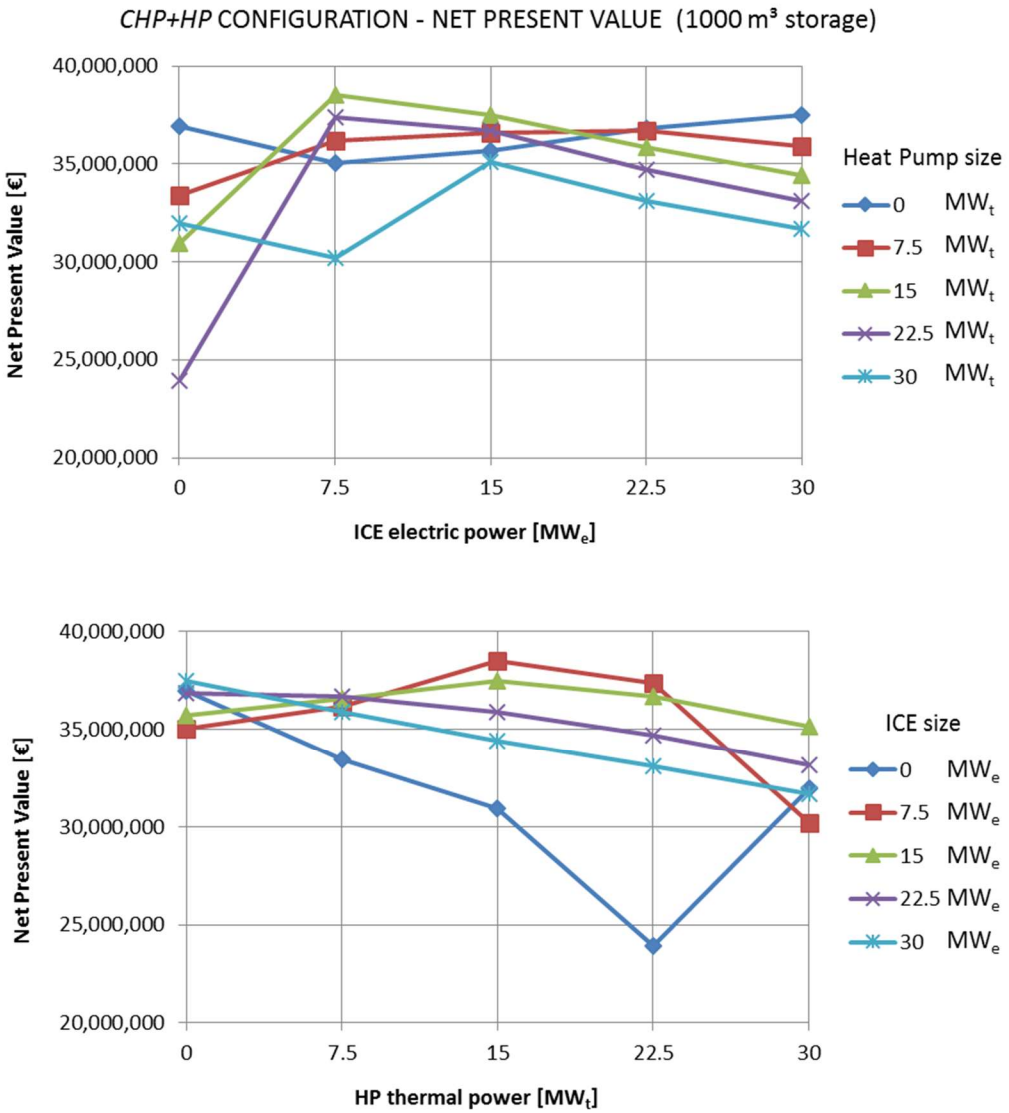

Figure 38: Absolute NPV for the CHP+HP configuration (BASE s.)

The two graphs represents two of the cross sections of the three-dimensional curve given by the value of the NPV for each combination of the ICE and the HP sizes. The 0 MW line in the first graph represents the *ICE* configuration with the same storage size, since the heat pump size is precisely zero. Likewise, in the second graph the 0 MW line represents the *HP* configuration. These graphs demonstrate the consistency of the optimal solution found. In fact, the only curves that are still growing passing from a 22.5 to a 30 MW machine are the ones representing the *ICE* and *HP* configurations and their trends outside the graph interval is known. The same graphs in terms specific to thermal energy sold are reported in the following Figure 39. As it can be noticed, the trends remains the same as in the absolute NPV representation.

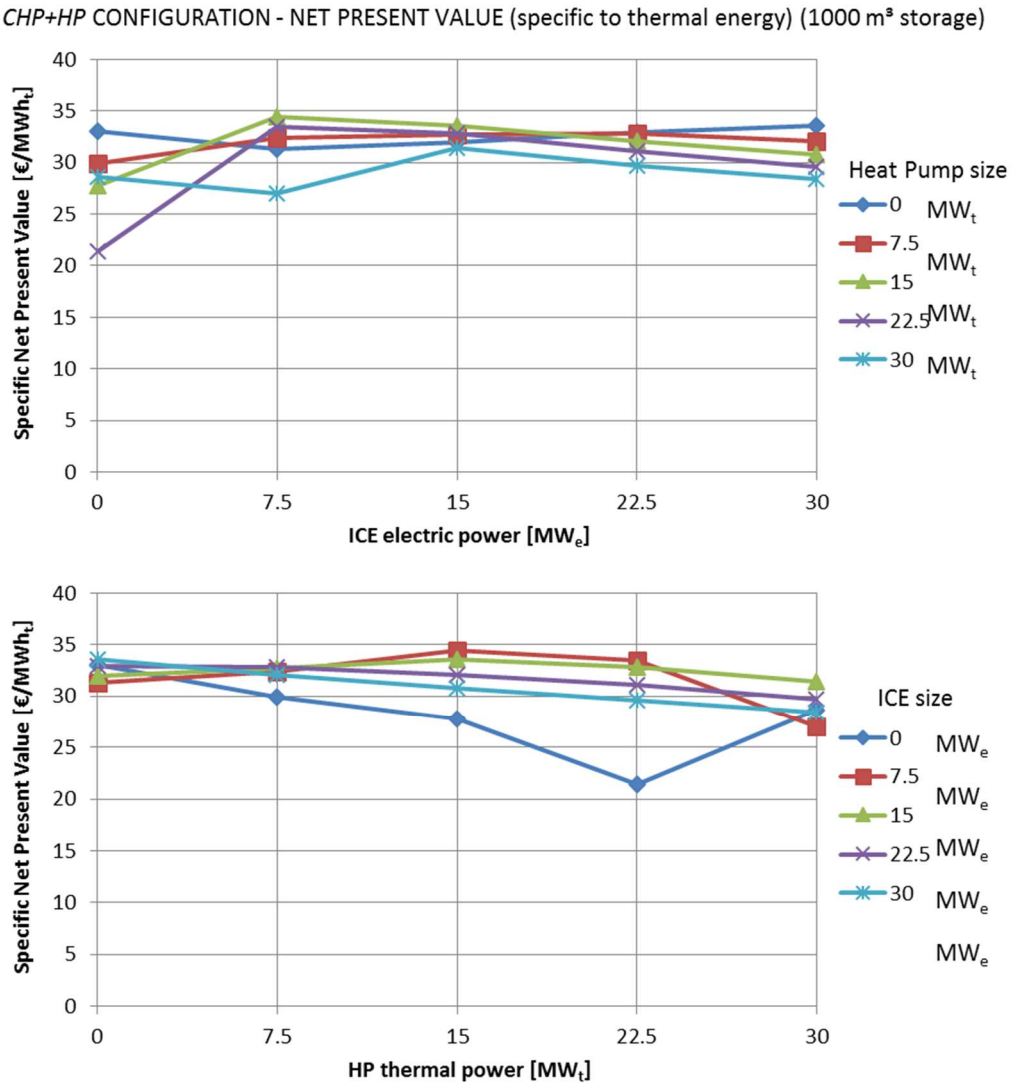

Figure 39: NPV specific to thermal energy produced for the CHP+HP configuration (BASE s)

5.3.2 Results and analysis of *2017* scenario

Since, during the previous scenario, the impact of the thermal storage dimension resulted negligible in each configuration considered, for the subsequent scenarios the decision was made to consider just the 1000 m^3 size for the storage tank. However, in order to be sure about the validity of this assumption, a test has been made for at least one configuration of each subsequent scenario. The results positively confirmed this hypothesis. The implementation of the system for the initial set of configurations gives as a result the cost functions reported in Figure 40.

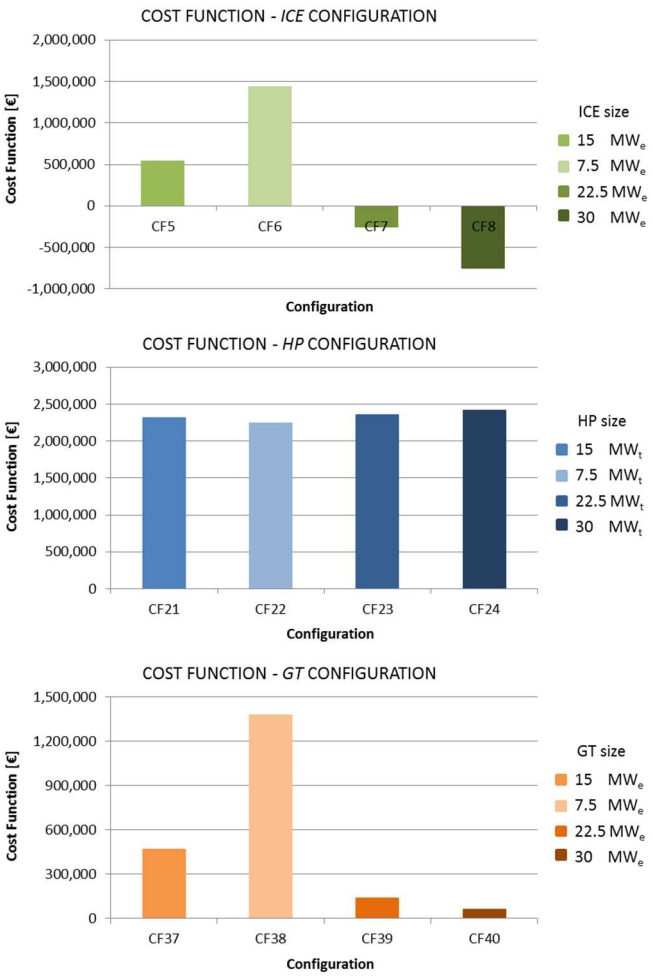

Figure 40: Annual cost functions for the ICE, HP and GT configurations of the 2017 scenario

The relative variation of cost functions as the size of the machines changes is very similar to the one of the previous scenario. On the other hand, the absolute value of the cost functions in the *ICE* and *GT* configurations is very much lower than the corresponding ones for the previous scenario. This can be explained by the fact that the average price for the sale of electricity is higher, passing from a value of 50.35 € MWh^{-1} to a value of 54.41 € MWh^{-1}. In fact, zonal prices higher than 80 € MWh^{-1} are much more frequent in the *2017* scenario and they reach a maximum value of 206.12 € MWh^{-1}. Similarly, the *HP* configuration shows absolute values of cost function lower than the ones of the previous price scenario. This can be explained by the fact that the average price for the PUN, being around a value of 86.32 € MWh^{-1}, is much lower than the constant one of the *BASE* case.

Repeating the same approximate evaluation made in the *BASE* scenario using the new average prices for the sale and purchase of electricity, the results are coherent with what was stated in the previous paragraph. These results are reported in Figure 41.

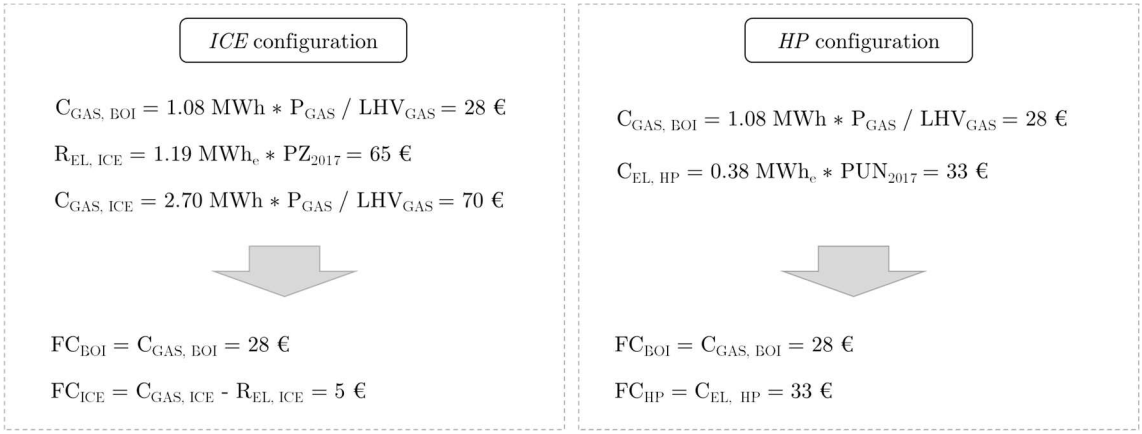

Figure 41: Approximate cost function evaluation of ICE and HP in the 2017 scenario

The use of the combined heat and power generator is even more favored with respect to the boilers, due to the higher average PZ. Once again, the heat pump and the boilers have similar effects in terms of cost function. On the other hand, this time the convenience of the HP over the boilers depends not only on the operating conditions, which have effects on its performances, but also on the variability of the PUN, which is very high (PUN_{MIN} = 16 € MWh^{-1}, PUN_{MAX} = 272 € MWh^{-1}).

The computation of the NPV proceeded as in the previous case. Again, the absolute results and the ones specific to the MWh of thermal energy sold have been collected both in graphical and numerical forms. The results for the *ICE* configurations are represented in Figure 42.

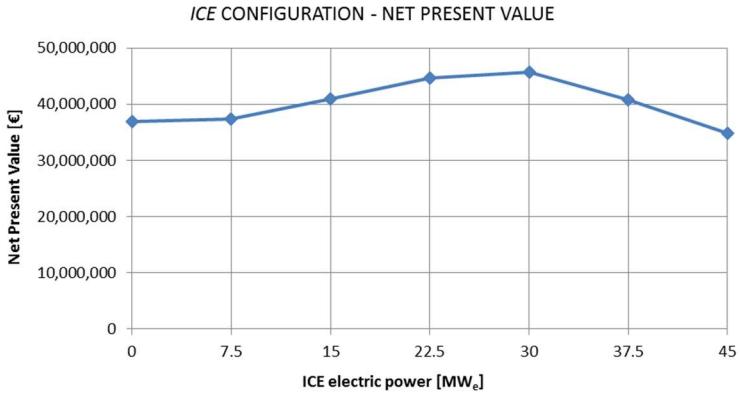

ICE size [MWe]	ICE CONFIGURATION Absolute NPV [€]
0	36,949,106
7.5	37,417,956
15	40,948,210
22.5	44,649,455
30	45,755,648
37.5	40,747,587
45	34,850,504

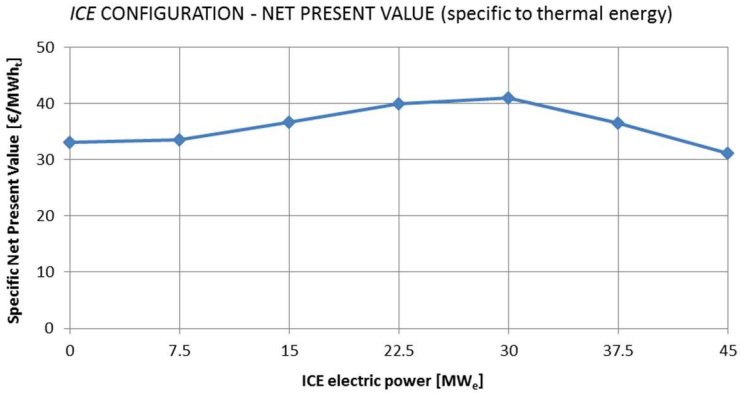

ICE size [MWe]	ICE CONFIGURATION Specific NPV [€/MWht]
0	33.1
7.5	33.5
15	36.7
22.5	40.0
30	41.0
37.5	36.5
45	31.2

Figure 42: Absolute and specific NPV for the ICE configuration (2017 s.)

With an absolute NPV of 45.8 million euros and a specific one of 41 euros per MWh_t, the optimal size for this configuration is the 30 MW engine with a storage tank of 1000 m^3.

The results for the *HP* configuration can be seen in Figure 43.

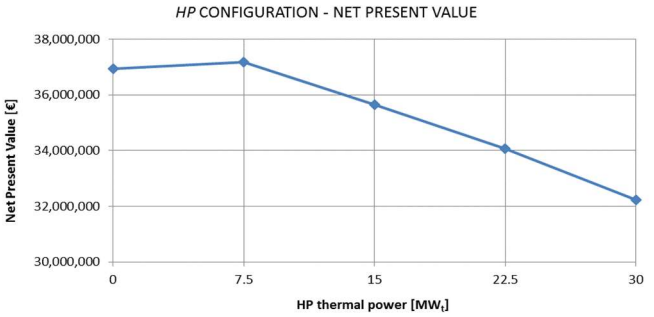

HP size [MWt]	HP CONFIGURATION Absolute NPV [€]
0	36,949,106
7.5	37,184,330
15	35,655,984
22.5	34,069,074
30	32,229,479

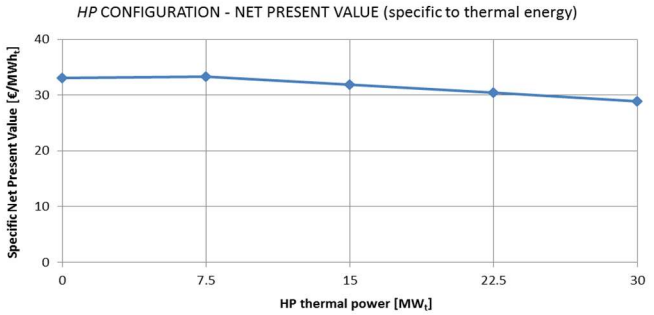

HP size [MWt]	HP CONFIGURATION Specific NPV [€/MWht]
0	33.1
7.5	33.3
15	31.9
22.5	30.5
30	28.9

Figure 43: Absolute and specific NPV for the HP configuration (2017 s.)

The optimal solution for this configuration is the 7.5 MW heat pump with a 1000 m^3 thermal storage, having an absolute NPV of 37.2 million euros and a specific NPV of 33.3 euros per MWh_t.

Figure 44 shows the results for the *GT* configuration.

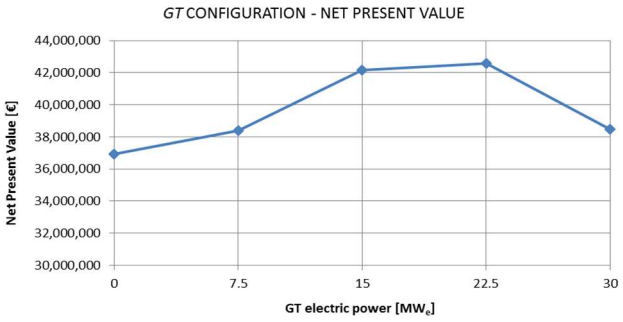

GT size [MWe]	GT CONFIGURATION Absolute NPV [€]
0	36,942,554
7.5	38,405,470
15	42,173,610
22.5	42,599,515
30	38,492,972

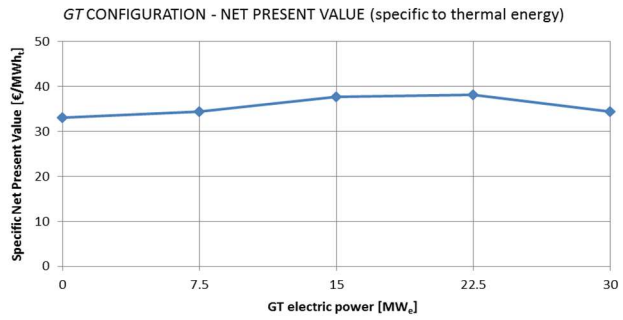

GT size [MWe]	GT CONFIGURATION Specific NPV [€/MWht]
0	33.1
7.5	34.4
15	37.8
22.5	38.1
30	34.5

Figure 44: Absolute and specific NPV for the GT configuration (2017 s.)

Thus, the optimal solution is given by the 22.5 MW gas turbine with a 1000 m^3 thermal storage, having an absolute NPV of 42.6 million euros and a specific one of 38.1 euros per MWh_t.

Once again, the choice for the CHP generator of the last configuration fell on the ICE, being this solution better than the GT one in terms of NPV. Figure 45 below reports the cost functions for the initial set of configurations for the *CHP+HP* scenario.

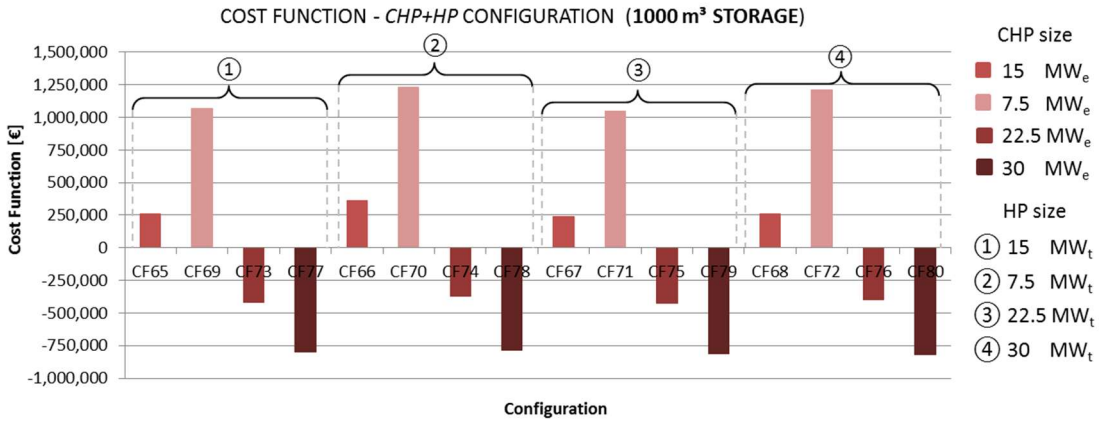

Figure 45: Annual cost functions for the CHP+HP configuration of the 2017 scenario

The same effects observed in the single generator cases can be observed here, with the joint use of the engine and the heat pump. The best configurations in terms of cost function are identified by the use of a 30 MW CHP generator, while the size of the heat pump does not seems to have big impacts on the result.

Moving to the NPV computation, Table 22 reports the results of the economic analysis of this configuration, both in absolute and specific terms.

Net Present Value		*CHP+HP* CONFIGURATION						
		ICE size [Mw_e]						
		7.5	15	22.5	30	37.5	45	
	Absolute [€]	37,417,956	40,948,210	44,649,455	45,755,648	40,747,587	34,850,504	0
		38,552,690	41,799,976	44,523,816	44,684,001	39,753,415	34,169,686	7.5
		39,729,099	41,955,571	43,668,107	43,286,814	38,278,346	33,089,031	15
		38,851,860	40,730,591	42,140,405	41,851,821	36,871,331	31,166,927	23
		35,391,668	38,897,490	40,283,382	40,226,673	35,345,290	29,729,005	30
	Specific [€/MWh_t]	33.5	36.7	40.0	41.0	36.5	31.2	0
		34.5	37.4	39.9	40.0	35.6	30.6	7.5
		35.6	37.6	39.1	38.8	34.3	29.6	15
		34.8	36.5	37.7	37.5	33.0	27.9	23
		31.7	34.8	36.1	36.0	31.6	26.6	30

HP size [MW$_t$]

Table 22: Absolute and specific NPV for the CHP+HP configuration (2017 s.)

Even though two higher CHP sizes have been investigated, the optimal solution remains the 30 MW combined heat and power engine with no heat pumps, which is the same solution found in the *ICE* case. The HP optimal size (0 MW) suggests that the cost function improvements given by the use of a heat pump are not high enough to recover the increase in the investment costs. The optimal solution has an absolute NPV of 45.8 million euros and a specific one of 41 euros per MWh_t.

The optimal solution for the *2017* price scenario is then given by the *ICE* configuration with a 30 MW engine and a 1000 m^3 thermal storage, having this solution the highest NPV.

The graphical representation of the CHP+HP configurations considered can be seen in Figure 46, which reports both the absolute and specific NPVs.

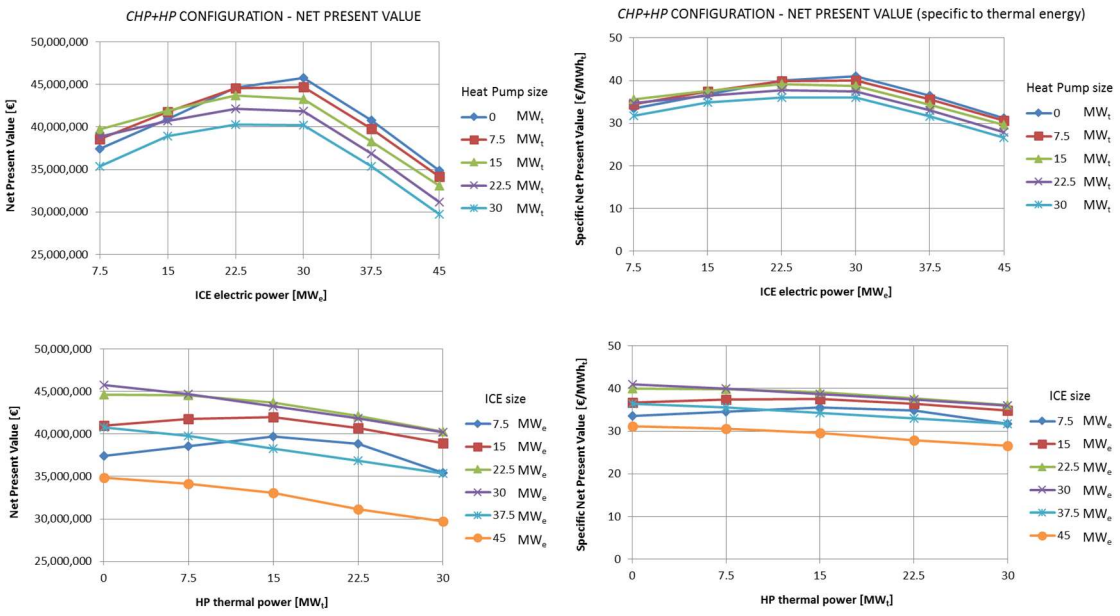

Figure 46: Absolute and specific NPV for the CHP+HP configuration (2017 s.)

5.3.3 Results and analysis of *SEN* scenario

The implementation of this scenario proceeded as like as the previous ones: the implementation of the model made gave as results the value of the cost functions, which have been later used to compute the NPV of each configuration to find the optimal solution. During the analysis of this scenario, the variation of size of the thermal storage has been neglected once again. A constant size of 1000 m^3 was considered for the storage tanks of every configuration. Figure 47 reports the cost functions resulting from the implementation of the first three configurations.

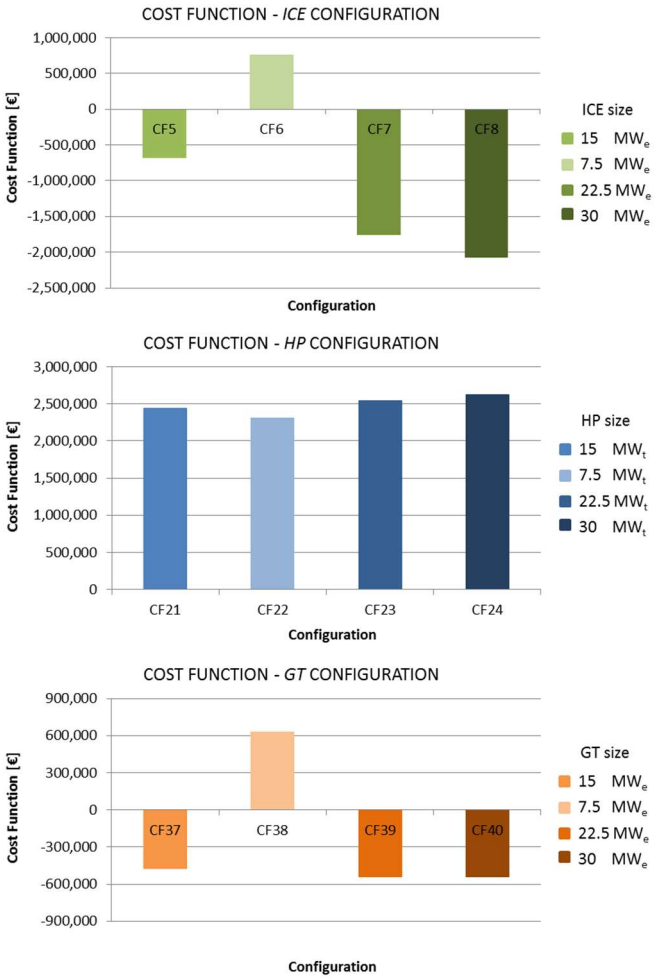

Figure 47: Annual cost functions for the ICE, HP and GT configurations of the SEN scenario

The results, in terms of relative values of the cost functions, are pretty similar to the *2017* scenario. The decrease in the absolute values for the *ICE* and the *GT* cases can be justified by a further increase in the average zonal price for the sale of electricity, which reaches the value of 73.65 € MWh^{-1}. The increase in the average PUN with respect to the *2017* case may be the explanation for the increase of the cost functions for the *HP* configuration. The average PUN reaches the value of 113.42 € MWh^{-1}. Using the new average values for the purchase and sell of electricity to make the same evaluation of the previous cases, the results are reported in Figure 48.

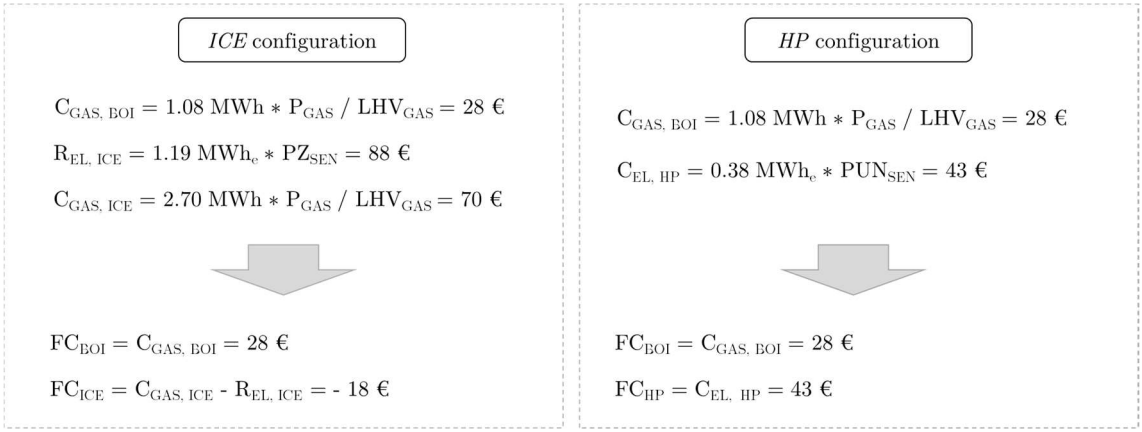

Figure 48: Approximate cost function evaluation of ICE and HP in the SEN scenario

Evidently, since the average price for selling electricity increases, the ICE becomes even more convenient. In fact, if the assumed conditions are achieved, the CHP generator is able to even present a negative cost function when producing 1 MWh_t of thermal energy, meaning that the system is gaining money even before the earnings for the sale of thermal energy are considered. On the other hand, once again the heat pump is less convenient than the boilers, in the reference conditions. Still, the variability of the PUN and of the heat pump operating conditions may switch the generators convenience.

The NPV resulting from the implementation of the model for the *ICE* configuration are reported in Figure 49, both in graphical and numerical form.

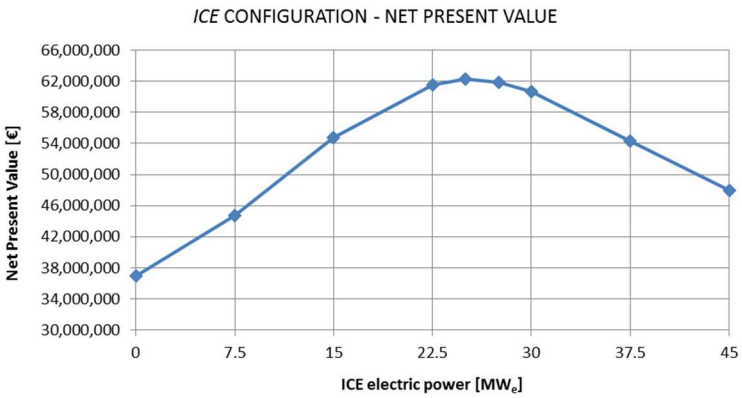

ICE size [MWe]	ICE CONFIGURATION Absolute NPV [€]
0	36,949,106
7.5	44,694,826
15	54,693,231
22.5	61,515,581
25	62,288,767
27.5	61,895,642
30	60,673,011
37.5	54,321,517
45	47,901,721

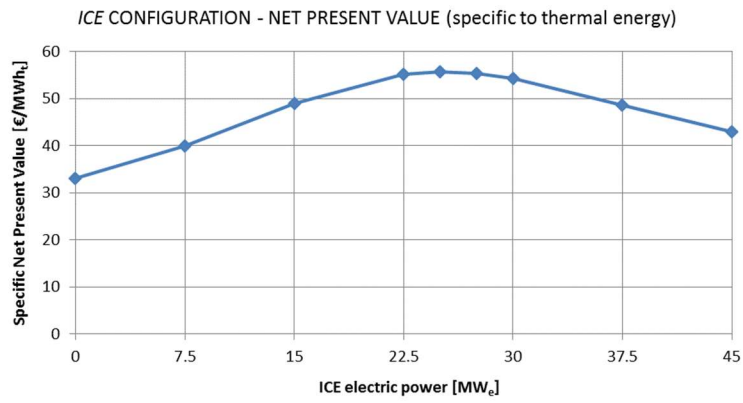

ICE size [MWe]	ICE CONFIGURATION Specific NPV [€/MWht]
0	33.1
7.5	40.0
15	49.0
22.5	55.1
25	55.8
27.5	55.4
30	54.3
37.5	48.6
45	42.9

Figure 49: Absolute and specific NPV for the ICE configuration (SEN s.)

In addition to the initial set of configurations, five more sizes of the ICE have been investigated. The 25 and 27.5 MW generators have been analysed in order to better locate the optimal solution, since the difference in NPV between the 22.5 and the 30 MW machines is much smaller compared to the differences between the other solutions. The optimum is found as the configuration with the 25 MW engine with a thermal storage of 1000 m^3, having an absolute NPV of 62.3 million euros and a specific one of 55.8 euros per MWh_t of thermal energy sold.

The results for the *HP* configuration are reported in Figure 50 below.

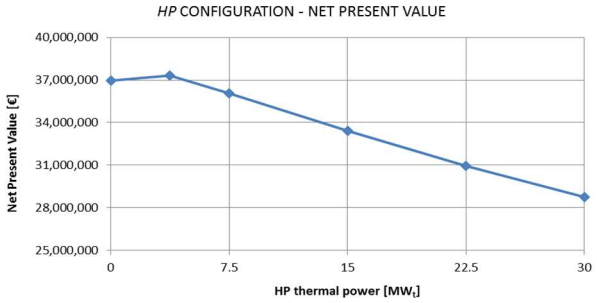

HP size [MWt]	HP CONFIGURATION Absolute NPV [€]
0	36,949,106
3.75	37,292,872
7.5	36,071,700
15	33,420,250
22.5	30,950,046
30	28,737,888

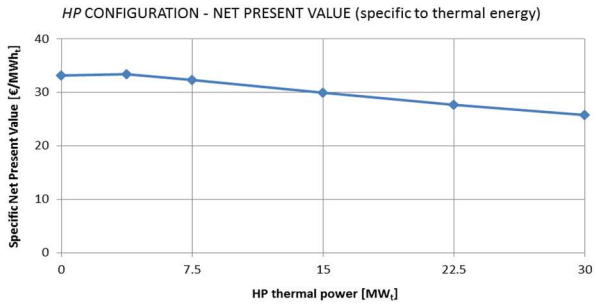

HP size [MWt]	HP CONFIGURATION Specific NPV [€/MWht]
0	33.1
3.75	33.4
7.5	32.3
15	29.9
22.5	27.7
30	25.7

Figure 50: Absolute and specific NPV for the HP configuration (SEN s.)

Two additional sizes for the heat pump have been considered: the boilers only solution, with a 0 MW heat pump, and a 3.75 MW heat pump. The latter, which derives from the choice of a 0.25 multiplying factor, results to be the optimal solution, having an absolute NPV of 37.3 million euros and a specific one of 33.4 euros per MWh_t.

The results of the GT configuration are reported in Figure 51.

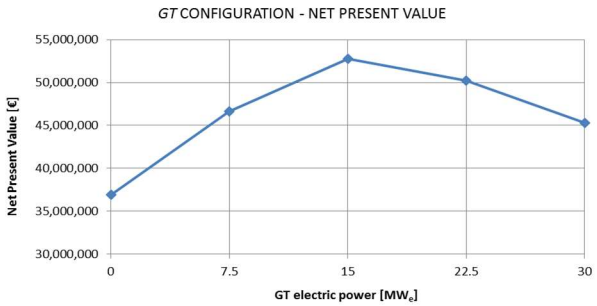

GT size [MWe]	GT CONFIGURATION Absolute NPV [€]
0	36,949,106
7.5	46,672,168
15	52,752,758
22.5	50,221,170
30	45,325,147

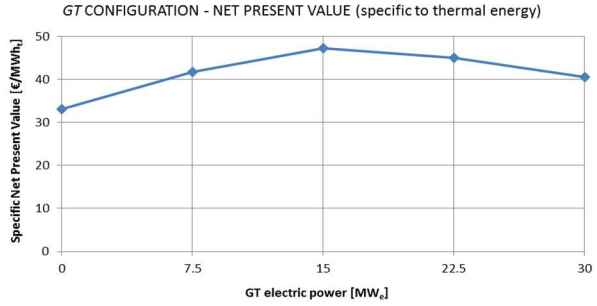

GT size [MWe]	GT CONFIGURATION Specific NPV [€/MWht]
0	33.1
7.5	41.8
15	47.2
22.5	45.0
30	40.6

Figure 51: Absolute and specific NPV for the GT configuration (SEN s.)

The optimal solution for the *GT* configuration is the one with a 15 MW gas turbine and a 1000 m^3 thermal storage. The optimum NPV amounts to 52.8 million euros, while the optimum specific NPV amounts to 47.2 euros per MWh_t.

Once more, for the last configuration, the choice for the CHP technology saw the prevailing of the ICE over the GT, since the optimal solution of the first one is characterized by a higher NPV. The following Figure 52 reports the results for the *CHP+HP* configuration in terms of cost functions.

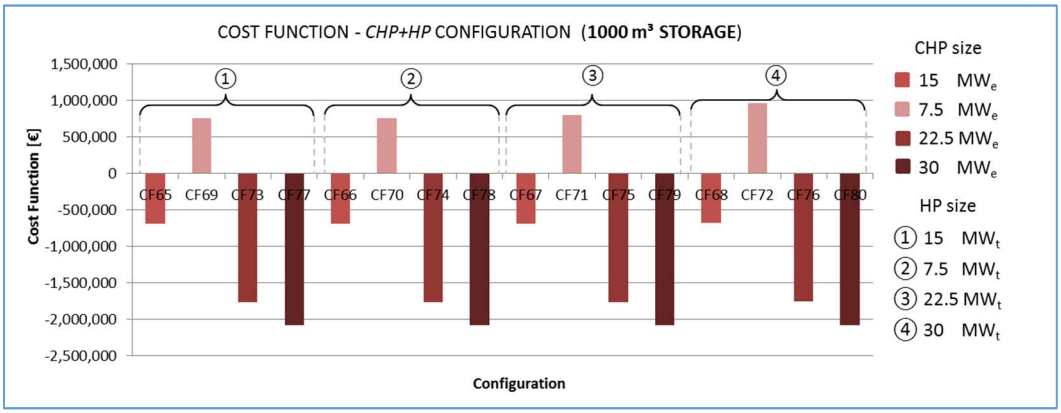

Figure 52: Annual cost functions for the CHP+HP configuration of the SEN scenario

The cost function variation as the CHP and the HP sizes increase shows the same behaviour of the previous scenarios. The effect of the higher electricity selling average price is clearly visible in the very low cost function values.

The results in terms of NPV are reported in Table 23 below.

Net Present Value		*CHP+HP* CONFIGURATION ICE size [Mw_e]							HP size [MW_t]
		0	7.5	15	22.5	30	37.5	45	
Absolute [€]		36,949,106	44,694,826	54,693,231	61,515,581	60,673,011	54,321,517	47,901,721	0
		35,632,872	43,824,442	53,445,801	59,892,330	58,966,934	52,579,577	46,190,985	7.5
		33,050,024	43,077,748	52,393,806	58,393,557	57,281,094	50,986,241	44,949,081	15
		30,950,046	40,736,571	50,572,551	56,795,876	55,702,477	49,354,754	42,922,096	23
		28,737,888	37,780,026	49,073,368	55,148,404	54,119,765	47,757,182	41,341,552	30
Specific [€/MWh_t]		33.1	40.0	49.0	55.1	54.3	48.6	42.9	0
		31.9	39.2	47.8	53.6	52.8	47.1	41.4	7.5
		29.6	38.6	46.9	52.3	51.3	45.7	40.2	15
		27.7	36.5	45.3	50.9	49.9	44.2	38.4	23
		25.7	33.8	43.9	49.4	48.5	42.8	37.0	30

Table 23: Absolute and specific NPV for the CHP+HP configuration (SEN s.)

The optimal solution for the *CHP+HP* configuration is composed by a 22.5 MW internal combustion engine with a thermal storage of 1000 m^3 and no heat pumps, which is of course one of the solutions of the *ICE* case.

The graphical form of the NPV results is reported in Figure 53.

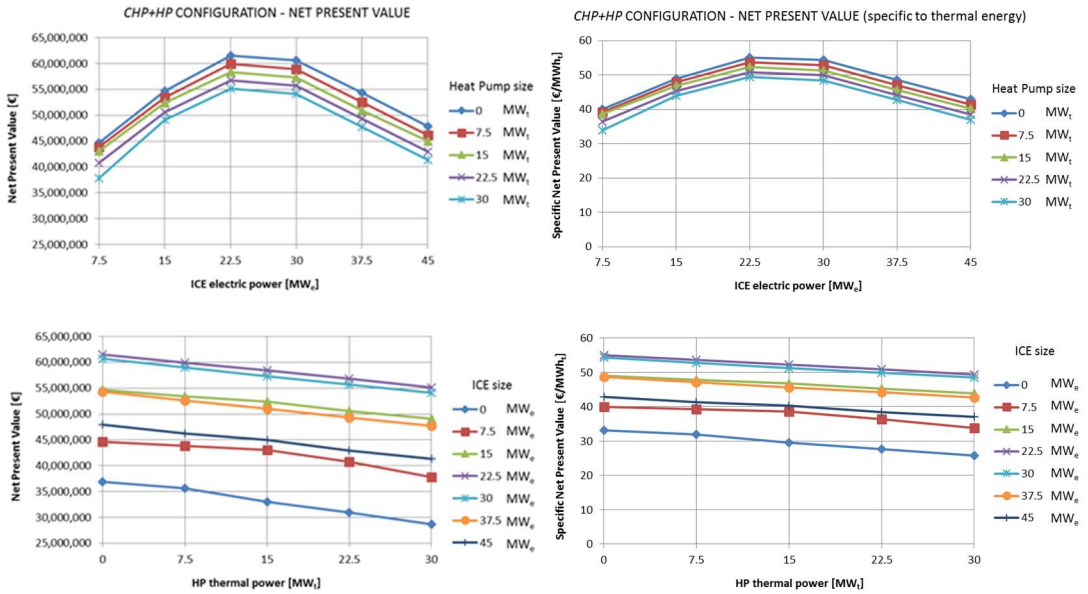

Figure 53: Absolute and specific NPV for the CHP+HP configuration (SEN s.)

The optimal solution for the *SEN* scenario is hence given by the ICE configuration one, which is made of a 25 MW internal combustion engine and a 1000 m^3 storage tank.

5.3.4 Results and analysis of *MSD* scenario

As pointed out in Chapter 5.2, the *MSD* scenario considers 75% of the CHP nominal power as participating in the day-ahead market, selling electricity at a price equal to the zonal price for the NORD zone. The remaining part of the nominal capacity is devoted to the participation to the MSD market. The reference year for the prices is again 2017.

Since this scenario requires a CHP generator, among the possible configurations only three options are available: the *ICE* configuration, the *GT* configuration and the *CHP+HP* configuration. Furthermore, as pointed out by the previous scenarios, the ICE

solution has always been preferred over the GT one. For this reason, the CHP technology selected for this last scenario is precisely the internal combustion engine one. Then, since the ICE configuration can be seen as a particular case of the CHP+HP configuration, only the latter have been evaluated during the analysis. The results, in terms of cost function, are reported in Figure 54.

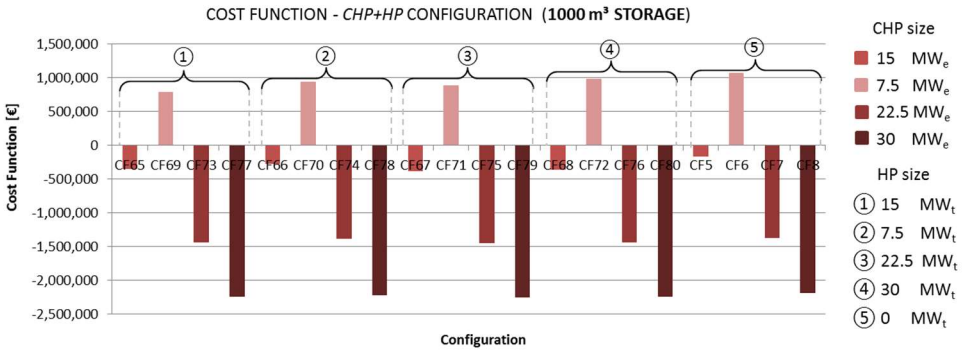

Figure 54: Annual cost functions for the CHP+HP configurations of the MSD scenario

Evidently, the same observations made during the previous scenarios still holds. The influence of the CHP size is substantial: as the size increases, the cost function value decreases considerably. The effects of the variation of the HP size, on the other hand, are much less important. Despite this, the increase of the heat pump size seems to positively influence the value of the cost function, at least for the small sizes of the machine. The cost function absolute value is generally lower with respect to the previous cases. This can be explained by the fact that the average price for the sale of electricity on the MSD market is higher than the one for the sale on the MGP market, which remains the same as in the *2017* scenario. The average MSD price for 2017 amounts to a value of 86.66 € MWh^{-1}. Figure 55 reports the usual evaluation that considers a 1 MWh output of the machines, which help to understand this positive effect on the cost function. Only the ICE is considered in the evaluation, since its interaction with the heat pump depends on the relative value of the electricity purchasing and selling prices.

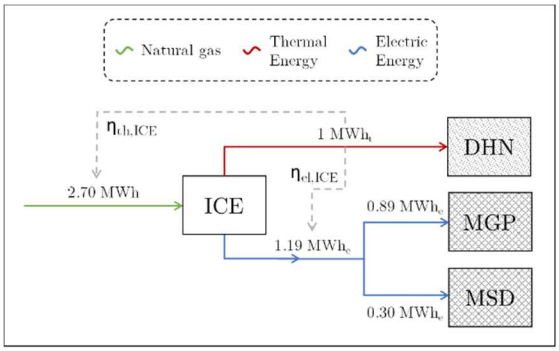

$$R_{EL\ MGP,\ ICE} = 0.89\ MWh_e * PZ_{2017} = 49\ €$$

$$R_{EL\ MSD,\ ICE} = 0.30\ MWh_e * P_{MSD,\ 2017} = 26\ €$$

$$C_{GAS,\ ICE} = 2.70\ MWh * P_{GAS} / LHV_{GAS} = 70\ €$$

$$FC_{ICE} = C_{GAS,\ ICE} - R_{EL\ MGP,\ ICE} - R_{EL\ MSD,\ ICE} = -5\ €$$

Figure 55: Approximate cost function evaluation of ICE in the MSD scenario

The results of the NPV computation is reported in the following Table 24, both in absolute and specific to the thermal energy sold forms.

		CHP+HP CONFIGURATION						
		ICE size [Mw_e]						
		7.5	15	22.5	30	37.5	45	
Net Present Value	Absolute [€]	41,610,197	48,980,545	57,286,121	62,087,468	60,787,767	58,670,384	0
		42,051,755	49,239,014	56,206,010	61,061,109	59,060,226	57,367,808	7.5
		43,208,062	49,083,479	55,392,841	59,764,740	57,910,456	55,916,356	15
		40,801,634	48,148,818	54,122,183	58,255,810	56,289,011	54,185,161	23
		38,065,710	46,293,558	52,337,302	56,593,897	54,434,273	52,707,018	30
	Specific [€/MWh_t]	37.3	43.8	51.3	55.6	54.4	52.5	0
		37.6	44.0	50.2	54.5	52.9	51.4	7.5
		38.6	43.8	49.5	53.4	51.9	50.1	15
		36.4	43.0	48.3	52.0	50.4	48.5	23
		34.0	41.3	46.7	50.6	48.7	47.2	30

HP size [MW_t]

Table 24: Absolute and specific NPV for the CHP+HP configuration (MSD s.)

The graphical form of the NPV results is reported in Figure 56.

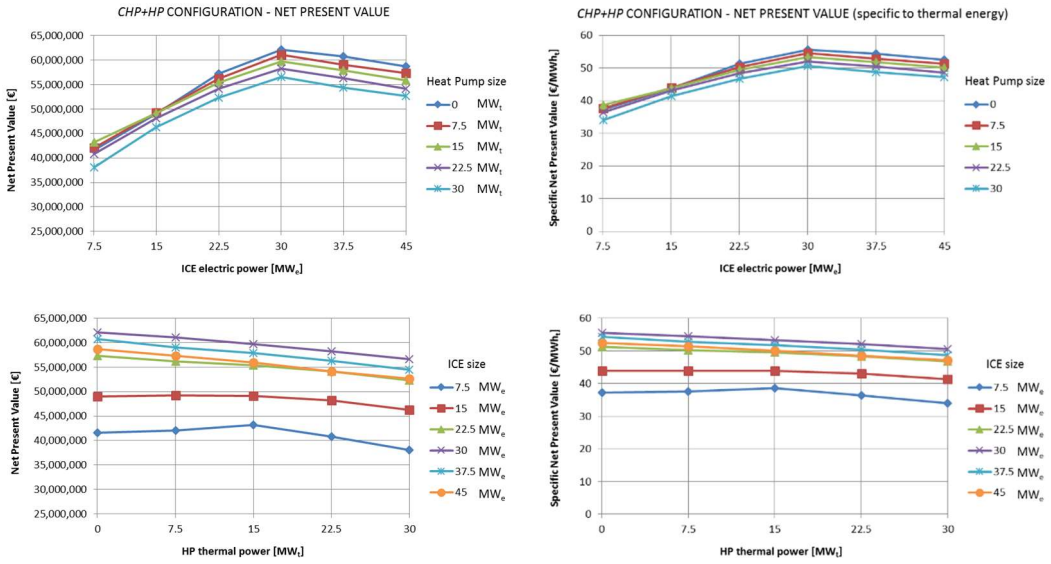

Figure 56: Absolute and specific NPV for the CHP+HP configuration (MSD s.)

The optimal solution for the *MSD* scenario is given by a 30 MW internal combustion engine with a 1000 m^3 thermal storage and no heat pumps. The optimum NPV is 62.1 million euros and the optimum specific NPV is 55.6 euros per MWh_t of thermal energy. It is worth noting that the optimal solution is exactly the same of the *2017* scenario. The NPV, on the other hand, is much higher, despite facing the same investment costs.

5.3.5 Optimal solutions analysis

The following Table 25 is useful to summarize the optimal solutions found for the four considered price scenarios. The first line of the table reports the same data for the reference (*REF*) configuration, which is the *BASE* configuration with the same machines sizes of the power station currently in operation in *Canavese*.

		OPTIMAL SOLUTIONS											
		Configuration	Internal Combustion Engine		Heat Pump		Storage		Boilers		NPV		Specific NPV	
SCENARIO	*REF*	*CHP+HP*	MW_e	15	MW_t	15	m^3	2,000	MW_t	45	€	37,349,763	€/MWh_t	33.4
	BASE	*CHP+HP*	MW_e	7.5	MW_t	15	m^3	1,000	MW_t	45	€	38,503,294	€/MWh_t	34.5
	2017	*ICE*	MW_e	30	-		m^3	1,000	MW_t	45	€	45,755,648	€/MWh_t	41.0
	SEN	*ICE*	MW_e	25	-		m^3	1,000	MW_t	45	€	62,288,767	€/MWh_t	55.1
	MSD	*ICE*	MW_e	30	-		m^3	1,000	MW_t	45	€	62,087,468	€/MWh_t	55.6

Table 25: Comparison between the optimal solutions of the selected scenarios

The starting point for the comparison between the optimal solutions found and the reference configuration is the analysis of how their thermal energy production is allocated during each day. In order to do this, every day has been divided into six, equally distributed time bands and the annual thermal energy production for each band has been computed. The results of this operation for all the scenarios are reported in Figure 57.

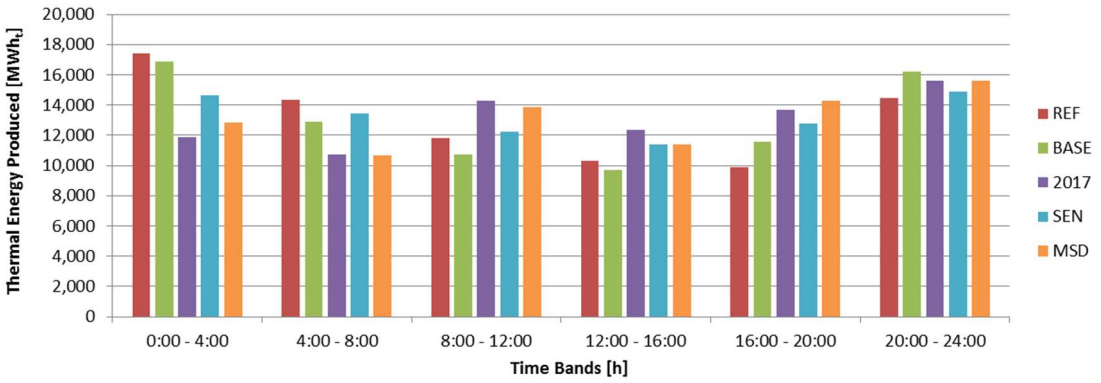

Figure 57: Total thermal energy produced during each time band of the day

The trends of the *REF* and *BASE* configurations are quite similar, as well as those of the *2017* and *MSD* cases. This indicates that the electricity prices may have a significant impact on the operation of the system, possibly making the difference in deciding whether to produce or not during each time slot. In order to investigate this analysis, the following Figure 58 reports three graphs representing the annual thermal energy production of each machine type (respectively CHP, HP and boilers) divided between the time bands considered. In addition, the graph represented in the following Figure 59 can help to understand the correlation with the electricity prices. This figure reports the average electricity prices of each time band, for every considered price scenario. As it can be noticed, the impact of the electricity prices results particularly meaningful for the operation of the combined heat and power generator: the CHP produces more energy in the bands where the zonal price for selling electricity is higher. On the other hand, to understand the impact of the electricity price on the operation of the heat pump, a more in-depth analysis has to be made. As a first thing, it is worth noting that, even though the only two cases that include a heat pump in the generation plant (*REF* and *BASE*) are characterized by the same price scenario (the *BASE* one), their thermal energy production results very different. The most probable cause of this is the different size of the CHP generator, the thermal production of which has to be integrated with the other available machines.

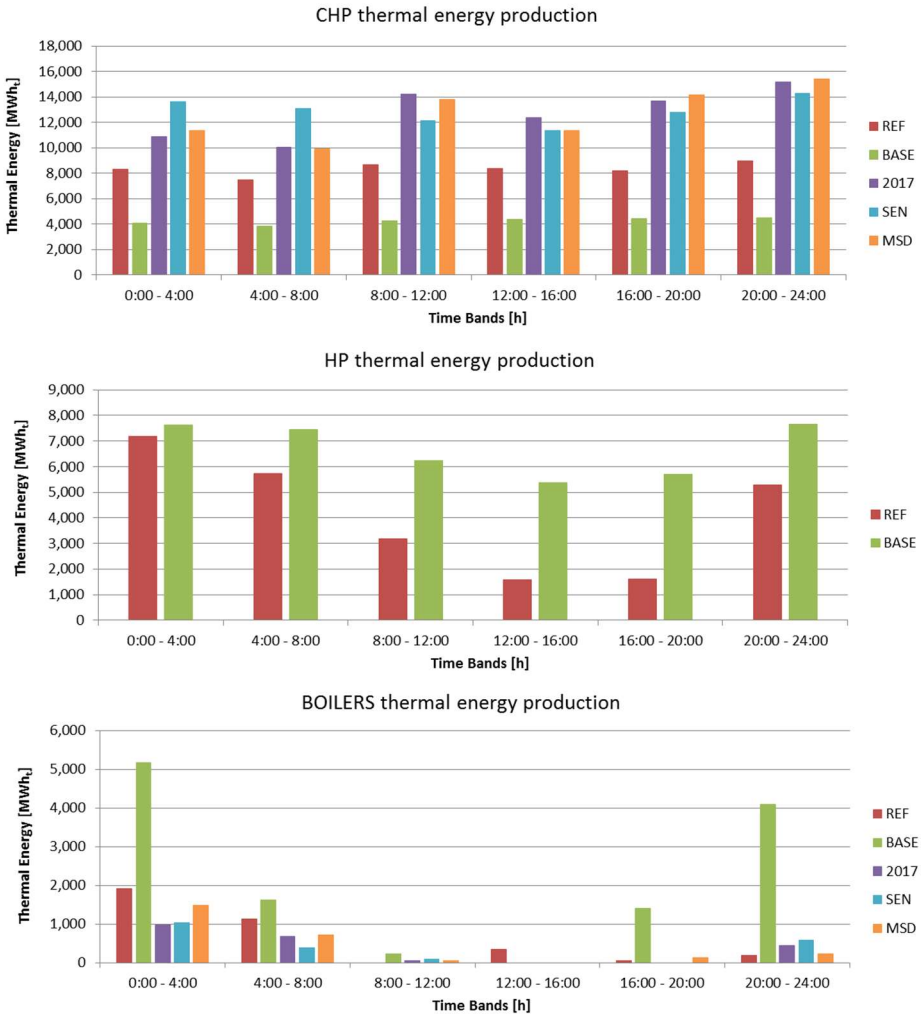

Figure 58: Comparison, based on scenario and technology, of the thermal energy produced

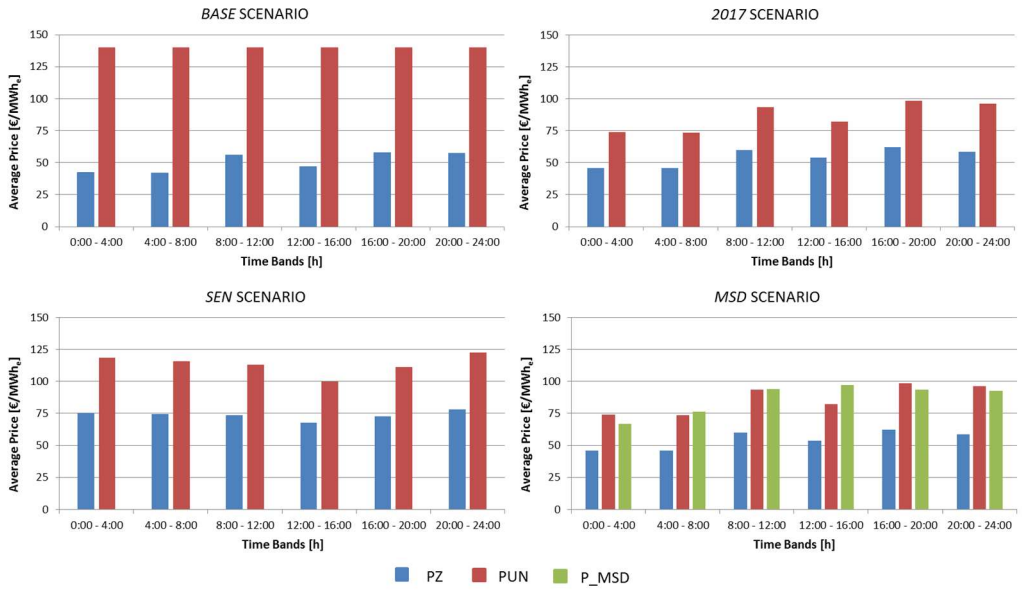

Figure 59: Annual average electricity buying and selling prices for each scenario

A confirmation of this can be found observing the different thermal energy production of the boilers. Furthermore, since the heat pump is coupled with a CHP in the considered configurations, its operation is affected not only by the electricity purchase price, but also by the difference between the purchase and the sale prices. The *BASE* price scenario is characterized by a constant electricity purchase price, equal to 140 € MWh^{-1}. From the Figure 26 it can be seen that, in general, this purchase price can be considered higher than the zonal price for the sale of electricity. Thus, it is reasonable to expect that, most of the time, the heat pump tends to feed on the electricity produced by the CHP, when both the machines are switched on. Then, the higher is the difference between the purchase and the sale prices, the higher are the savings due to the self-consumption of electricity (see Chapter 5.1).

Another fundamental factor that can influence the operation of the system is the thermal energy demand of the users, which is reported in the next Figure 60. However, even though the load remains the same for each price scenario, the system still holds a certain level of discretion in deciding when to produce the thermal energy required because the available range for the supply temperature is quite broad. This is important because it allows, along with the presence of the thermal storage, to decouple the production and the consumption of thermal energy, at least up to a certain point. In fact, as pointed out during the definition of the model, the network itself behaves like a thermal energy storage.

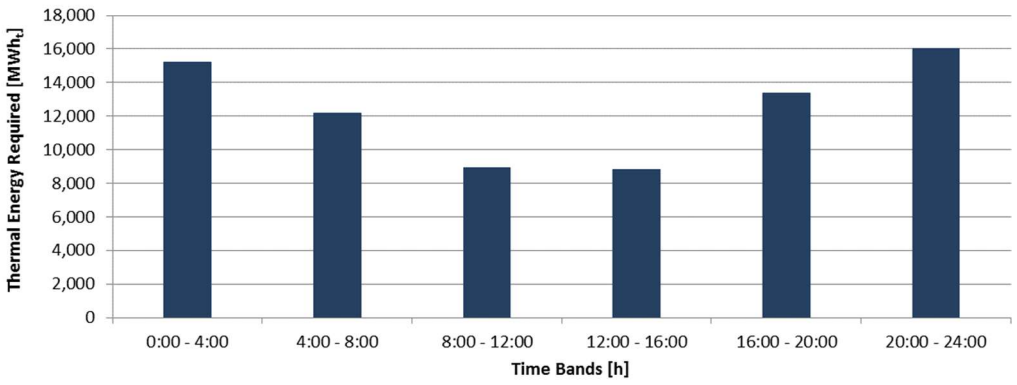

Figure 60: Thermal energy demand of the users for each time band of the day

The following Figure 61 is helpful to compare immediately how the annual thermal load has been satisfied by each optimal configuration.

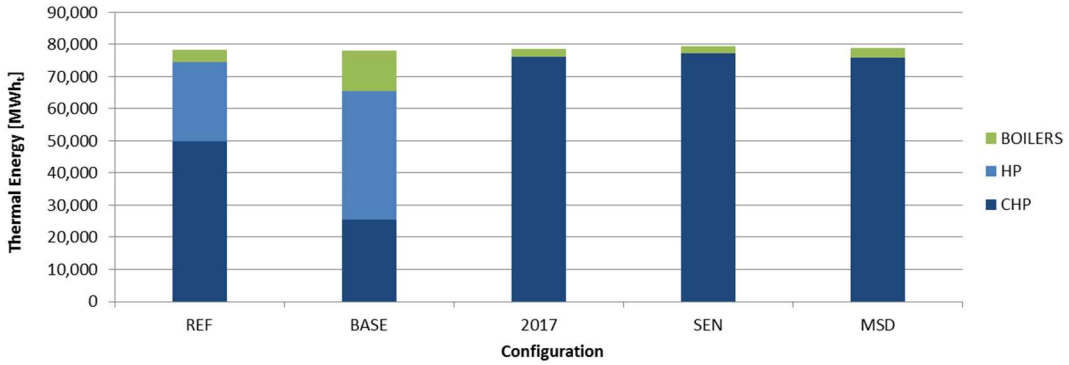

Figure 61: Thermal energy production by technology in each scenario

As expected from the evaluations made in the previous paragraphs on the convenience of the boilers and the ICE, the last three configurations produce approximately 97% of the annual thermal energy with the CHP technology, while the remaining part comes from the backup boilers. Coherently with the previous observations, the *REF* and the *BASE* configurations make an extensive use of the heat pumps. The *REF* case produces the annual thermal energy in the following proportions: 64% ICE, 31% HP and 5% boilers. The proportions of the *BASE* optimal solution are: 33% ICE, 51% HP and 16% boilers.

Another important aspect to consider in the comparison is the electrical energy produced and consumed by the system, which is reported in Figure 62.

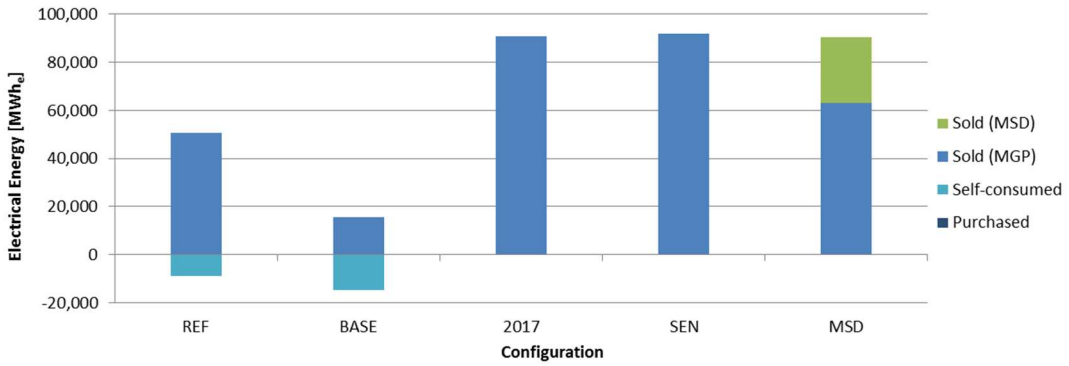

Figure 62: Electrical energy sold, self-consumed and purchased by the plant in each scenario

A positive ordinate represents the electrical energy sold, while a negative one represents the electricity consumed by the system. Confirming the observation that the buying price is in general higher than the sale one, the quantity of electricity purchased in the first two configurations is almost negligible (less than 1% of the consumed electricity) while the self-consumed quantity is much more substantial. Naturally, the *2017* and the *SEN* configurations, which only have the CHP technology and only interact with the day-ahead market, sell the entire electricity production to the MGP. On the other hand, the *MSD* configuration is able to sell roughly one third of its electrical production to the ancillary services market, with 25% of the available electrical power.

It is worth noting that, even if the electricity and thermal energy production of the *2017* and the *MSD* configurations is approximately equivalent, even if their machines sizes are identical and even if the price scenario for the PZ and the PUN remains the same, the *MSD* optimal solution has an NPV much larger than the *2017* one. The first one has an NPV approximately 36% higher than the second one. This means that the participation of a plant to the MSD market is able alone to boost its economical results in a substantial way.

In order to complete the analysis on the electricity production it is useful to compute the weighted average electricity prices: one for the sale and one for the purchase of electricity. These mean prices has been weighted for the actual quantities of electrical energy sold/purchased to the market; two distinct prices have been considered for the *MSD* sale case, one for the day-ahead market and one for the ancillary services market.

Of course, since the only two configurations in which the electricity is purchased are the *REF* and the *BASE* ones, the weighted average price for the buying is simply equal to 140 € MWh^{-1}, being this value constant for the *BASE* price scenario. On the other hand, the weighted average prices for the sale of electricity are reported in the Figure 63, along with the annual average value for the corresponding prices.

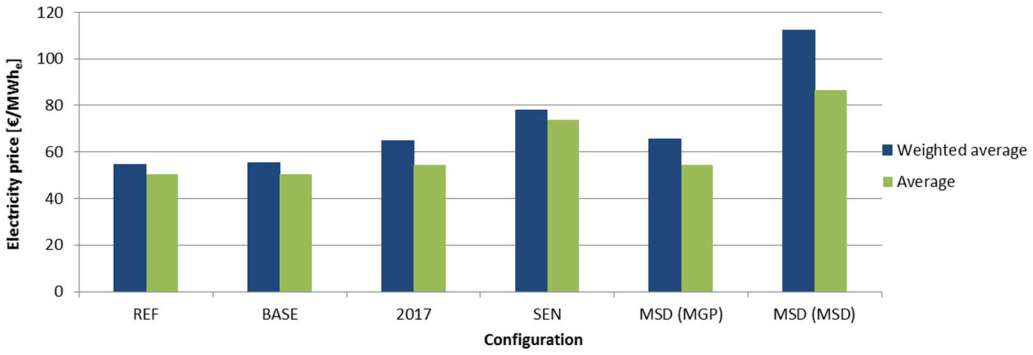

Figure 63: Average price for the sale of electricity vs annual average sale price of the market

As it can be noticed, the weighted average prices results higher than the average ones. This means that the system, equipped with a MPC controller and optimizer, is able to produce and sell electricity during the most favourable hours, in terms of price. This also confirms the reasoning at the base of the first attempt evaluations of the previous paragraphs on the convenience comparison between the ICE and the boilers technologies.

At last, an interesting consideration can be made analysing the optimal configurations, referring them to the typical user of the network. In accordance with Table 1, the average user results very close to the condominium type and requires approximately 137 kWh of thermal energy every year. If we refer the optimal solutions to this typical user, dividing the results by the total number of users connected to the system, it is possible to obtain valuable first-attempt indications for the design of a larger DHN. These specific optimal solutions are reported in Table 26.

		OPTIMAL SOLUTIONS (specific to the number of users connected)									
		Configuration	**Internal Combustion Engine**		**Heat Pump**		**Storage**		**Boilers**		**Expected NPV**	
SCENARIO	***REF***	*CHP+HP*	kW$_e$/us	27	kW$_t$/us	27	m^3/us	4	kW$_t$/us	81	€/us	67
	BASE	*CHP+HP*	kW$_e$/us	13	kW$_t$/us	27	m^3/us	2	kW$_t$/us	81	€/us	69
	2017	*ICE*	kW$_e$/us	54	-		m^3/us	2	kW$_t$/us	81	€/us	82
	SEN	*ICE*	kW$_e$/us	45	-		m^3/us	2	kW$_t$/us	81	€/us	111
	MSD	*ICE*	kW$_e$/us	54	-		m^3/us	2	kW$_t$/us	81	€/us	111

Table 26: Optimal configurations referred to a typical average user of the network

5.4 Sensitivity analysis

In order to determine the impact of some of the system variables on the results found in the previous paragraph, the decision was made to perform a sensitivity analysis. The evaluation has been made considering some fundamental economic variables and the effect of their variation on the NPV of the system.

The first important economic parameter to be considered has been the discount rate at which the value of the system net cash flows have been discounted to their present value. For the sensitivity analysis, a $\pm 2\%$ variation on the discount rate has been taken into account. Since the base discount rate has been set to 5%, the two new values considered have been 7% and 3%. The optimal configuration for each price scenario is reported in Table 27, where the variations in the optimal configuration have been highlighted with a thicker contour.

		DISCOUNT RATE 5%				DISCOUNT RATE 7%			
		ICE	HP	Storage	NPV	ICE	HP	Storage	NPV
		[MW]	[MW]	[m^3]	[M€]	[MW]	[MW]	[m^3]	[M€]
SCENARIO	*BASE*	7.5	15	1000	38.5	7.5	15	1000	32.9
	2017	30	0	1000	45.8	30	0	1000	37.7
	SEN	25	0	1000	62.3	25	0	1000	52.8
	MSD	30	0	1000	62.1	30	0	1000	52.2

		DISCOUNT RATE 5%				DISCOUNT RATE 3%			
		ICE	HP	Storage	NPV	ICE	HP	Storage	NPV
		[MW]	[MW]	[m^3]	[M€]	[MW]	[MW]	[m^3]	[M€]
SCENARIO	*BASE*	7.5	15	1000	38.5	30	0	1000	46.2
	2017	30	0	1000	45.8	30	0	1000	55.6
	SEN	25	0	1000	62.3	25	0	1000	73.9
	MSD	30	0	1000	62.1	30	0	1000	74.1

Table 27: Results of the sensitivity analysis on the discount rate

Because of its definition, an increase in the discount rate causes the NPV to decrease and vice versa. The only optimal solution altered in terms of plant configuration by the variation of this economic parameter is the *BASE* price scenario with a discount rate of 3%. This is due to the fact that, for the NPV computation, a low discount rate

favours those investments with higher net cash flows, since their present value results closer to the future one. The new optimal configuration (30 MW ICE) is characterized by higher net cash flows compared to the previous one and hence, despite facing higher investment costs, it benefits more from the lower discount rate.

In addition to the evaluation of the possible variation in the optimal solution, it is interesting to analyse the percentage change of the NPV as the parameters considered vary. Figure 64 below shows this percentage change for each of the selected scenarios.

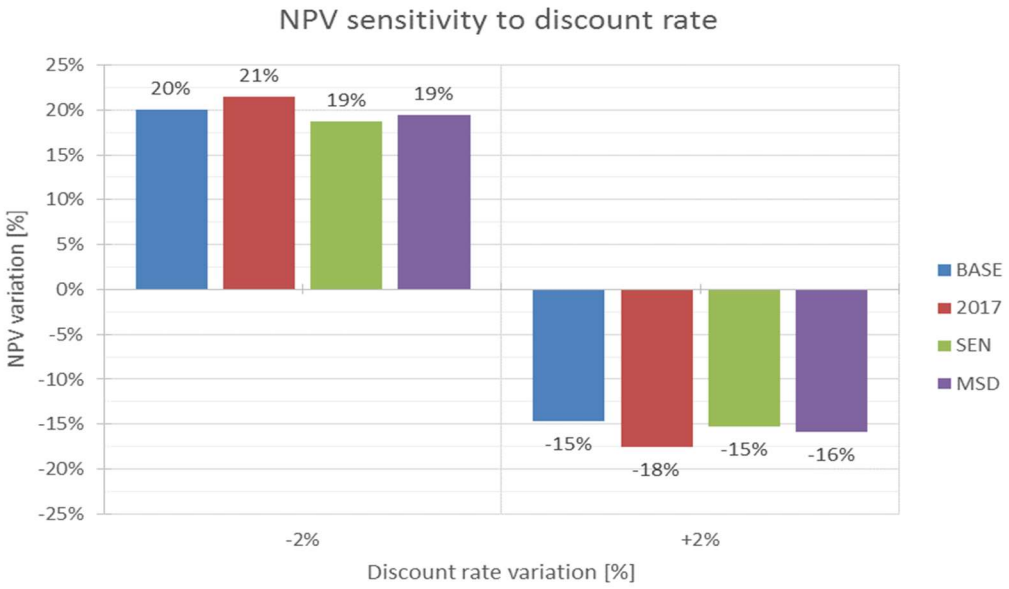

Figure 64: Percentage change in the NPV in response to a change in the discount rate

The percentage change is very similar for all scenarios and is around +20% for a -2% change in the discount rate and around -15% for a +2% change. As a result, the NPV appears to be very sensitive to a variation of this parameter and, consequently, particular attention must be paid to its definition. While the observable trend of the 2017, SEN and MSD scenarios is justified by the non-linear relationship between the discount rate and the NPV, the change in the BASE one derives also from the modification of the optimal solution configuration. This circumstance will also recur in the subsequent cases in a more evident way.

The next step in the sensitivity analysis has been the variation of the investment costs for the primary generators. The assessment of the impact of the change in these

parameters on the result is very important, as they constitute the largest of the cost items, as far as the investment costs of the installation are concerned. Since none of the optimum configurations involved the use of gas turbine technology and since the investment cost of thermal storage and backup boilers is lower (and, in any case, constant throughout all configurations) than that of the primary generators, the only costs that have been considered in the analysis were those for the ICE and the HP generators.

As regards the ICE investment costs, a ±20% variation has been performed. The results are shown in Table 28, once again highlighting the new optimal solutions.

		ICE INVESTMENT COST 100%				ICE INVESTMENT COST 120%			
		ICE	HP	Storage	NPV	ICE/GT	HP	Storage	NPV
		[MW]	[MW]	[m^3]	[M€]	[MW]	[MW]	[m^3]	[M€]
SCENARIO	*BASE*	7.5	15	1000	38.5	0	0	1000	36.9
	2017	30	0	1000	45.8	(GT) 22.5	0	1000	42.6
	SEN	25	0	1000	62.3	25	0	1000	57.8
	MSD	30	0	1000	62.1	30	0	1000	57.0

		ICE INVESTMENT COST 100%				ICE INVESTMENT COST 80%			
		ICE	HP	Storage	NPV	ICE	HP	Storage	NPV
		[MW]	[MW]	[m^3]	[M€]	[MW]	[MW]	[m^3]	[M€]
SCENARIO	*BASE*	7.5	15	1000	38.5	30	0	1000	42.6
	2017	30	0	1000	45.8	30	0	1000	50.9
	SEN	25	0	1000	62.3	25	0	1000	66.8
	MSD	30	0	1000	62.1	30	0	1000	67.2

Table 28: Results of the sensitivity analysis on the ICE investment cost

The impact of this parameter results more significant, compared to the ones of the discount rate, in terms of optimal configuration. Naturally, the increase in the ICE investment cost disfavours this technology, as it is evident in the optimal solution change in the *BASE* scenario, where the configuration with the boilers alone results the best one, and in the *2017* scenario, where the higher zonal prices allows to employ a CHP technology in the form of a gas turbine. The decrease in the investment cost, on the other hand, results less relevant, as the ICE is already the best technology. The only optimal solution change is found in the *BASE* price scenario, where the heat pump disappears and a bigger ICE is selected.

Figure 65 below shows the percentage change in the NPV that results from the change in the ICE investment cost.

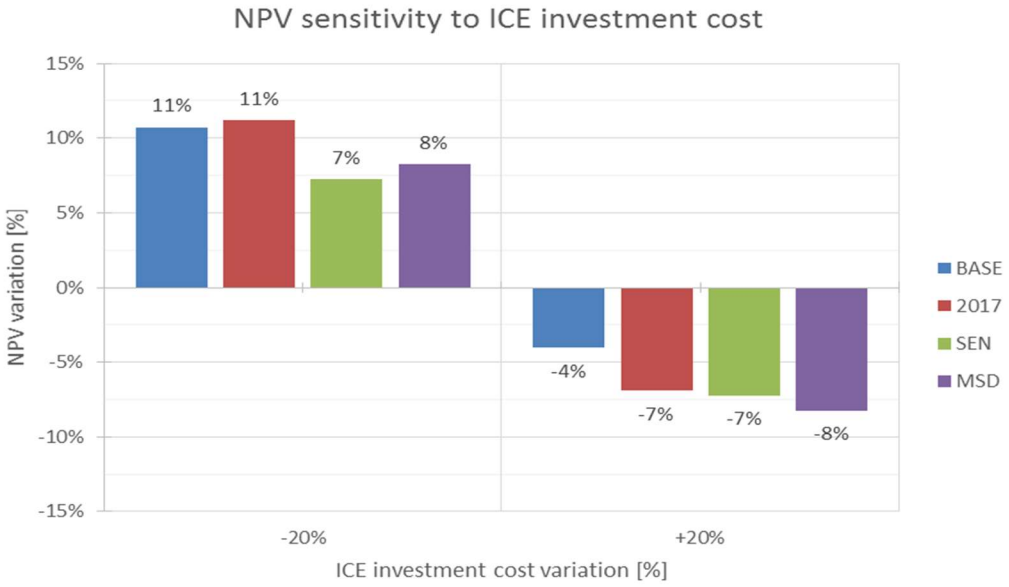

Figure 65: Percentage change in the NPV in response to a change in the ICE investment cost

The sensitivity of the NPV on this parameter turns out to be lower than in the previous case, but still not negligible. The linearity of the relationship between the ICE investment cost and the NPV is clearly visible in the trend of the SEN and MSD scenarios (∓7% and ∓8% respectively). On the other hand, the optimal solution variation affects the inclination of the curves in the BASE and in the 2017 scenarios. The first one, in particular, shows a steep change in the NPV variation at increased investment costs, due to the complete elimination of the ICE generator from the optimal solution.

As regards the heat pump investment costs, the same ±20% variation has been considered, with the goal to determine any eventual variation of the competitiveness of this technology with respect to the ICE. The results are reported in Table 29.

		HP INVESTMENT COST 100%				HP INVESTMENT COST 120%			
		ICE	HP	Storage	NPV	ICE	HP	Storage	NPV
		[MW]	[MW]	[m^3]	[M€]	[MW]	[MW]	[m^3]	[M€]
SCENARIO	*BASE*	7.5	15	1000	38.5	7.5	15	1000	38.0
	2017	30	0	1000	45.8	30	0	1000	45.8
	SEN	25	0	1000	62.3	25	0	1000	62.3
	MSD	30	0	1000	62.1	30	0	1000	62.1

		HP INVESTMENT COST 100%				HP INVESTMENT COST 80%			
		ICE	HP	Storage	NPV	ICE	HP	Storage	NPV
		[MW]	[MW]	[m^3]	[M€]	[MW]	[MW]	[m^3]	[M€]
SCENARIO	*BASE*	7.5	15	1000	38.5	7.5	15	1000	39.0
	2017	30	0	1000	45.8	30	0	1000	45.8
	SEN	25	0	1000	62.3	25	0	1000	62.3
	MSD	30	0	1000	62.1	30	0	1000	62.1

Table 29: Results of the sensitivity analysis on the HP investment cost

As it is immediately evident, none of the optimal configuration changes. The reason behind this may be that the heat pump investment costs considered are much lower than the other technologies ones, thus not resulting in big differences in the NPV variation. Moreover, as shown in Figure 66, the effect on the NPV is evident only in the BASE scenario, since this is the only one that includes a heat pump in the optimal solution.

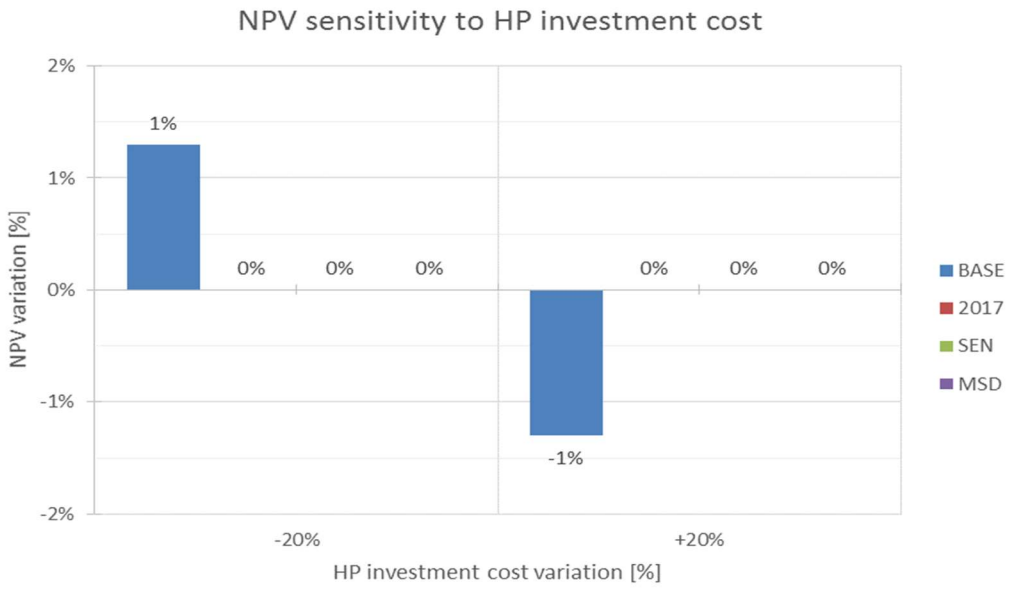

Figure 66: Percentage change in the NPV in response to a change in the HP investment cost

The last parameter considered in the implementation of the sensitivity analysis has been the cost of natural gas, the price of which has been changed by ±20% compared to the reference value of 0.25 € sm^{-3}. From this analysis, the expectation was to find out whether low natural gas costs would result in optimum solutions with higher sizes of gas-powered generators and, on the contrary, whether high costs would instead favour heat pump technology. The following Table 30 illustrates the results of this investigation.

		NATURAL GAS PRICE 100%				NATURAL GAS PRICE 120%			
		ICE	HP	Storage	NPV	ICE	HP	Storage	NPV
		[MW]	[MW]	[m^3]	[M€]	[MW]	[MW]	[m^3]	[M€]
SCENARIO	*BASE*	7.5	15	1000	38.5	7.5	15	1000	33.5
	2017	30	0	1000	45.8	7.5	22.5	1000	34.7
	SEN	25	0	1000	62.3	25	0	1000	49.7
	MSD	30	0	1000	62.1	30	0	1000	49.9

		NATURAL GAS PRICE 100%				NATURAL GAS PRICE 80%			
		ICE	HP	Storage	NPV	ICE	HP	Storage	NPV
		[MW]	[MW]	[m^3]	[M€]	[MW]	[MW]	[m^3]	[M€]
SCENARIO	*BASE*	7.5	15	1000	38.5	30	0	1000	51.1
	2017	30	0	1000	45.8	30	0	1000	57.4
	SEN	25	0	1000	62.3	30	0	1000	72.8
	MSD	30	0	1000	62.1	30	0	1000	73.7

Table 30: Results of the sensitivity analysis on the natural gas price

As regards the first hypothesis, the results seems to confirm the switch to natural gas powered machines as fuel price decreases. Specifically, the optimal sizes all converge towards the 30 MW ICE-only solution. However, the response to an increase in gas prices is less evident: it emerges that the only optimal solution that varies is the 2017 scenario ones, which varies according to the second hypothesis expressed. There may be several reasons why the other solutions remain unchanged. The most likely explanation is that the high price for electricity purchase that characterizes the BASE, SEN and MSD scenarios, results in higher heat pump sizes being disadvantaged. Added to this is the fact that the selling price of electricity is progressively increasing in these scenarios, favouring the gas-powered technology, which has electricity as a by-product of the thermal energy production.

The percentage variation of NPV in response to the variation in natural gas price is reported in the following Figure 67.

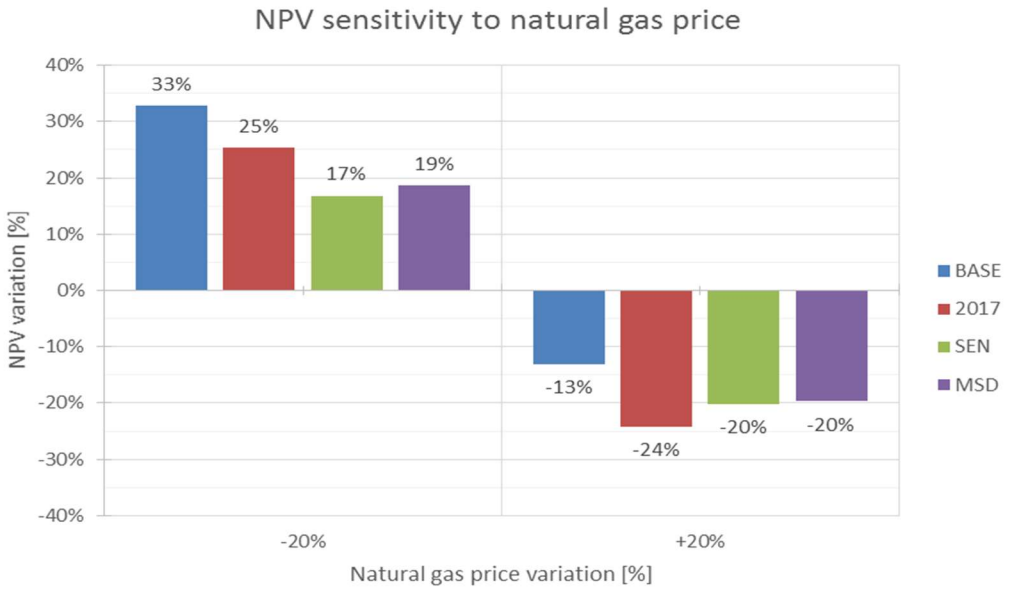

Figure 67: Percentage change in the NPV in response to a change in the natural gas price

As expected, this parameter not only affects the optimal configuration but also greatly influences the NPV value. It can be noted that the configuration that is most negatively affected in percentage terms by an increase in the price of gas is the 2017, which is also the only one to face a change in the optimal solution. On the other hand, the BASE configuration suffers less from this condition, due to the predominant presence of the heat pump in the optimal plant. The decrease in natural gas price is instead highly beneficial in terms of NPV, especially for the BASE scenario.

Chapter 6

Conclusions and future developments

The conclusions of the thesis are reported in this chapter, followed by some indications that provide possible starting points for potential future developments.

6.1 Conclusions

This thesis work focused on the evaluation of the possible exploitation of the synergies between a 4GDH system and the electrical network, developing the design of an advanced thermal plant. For this purpose a controller, based on model predictive control, has been developed, allowing the optimal design and operation of the generation section of a multi-generator district heating system. The simplified network model that was employed as the forecasting basis for the operation of the MPC-based optimizer that manages the system proved to be sufficiently precise in determining the subsequent states of the network, even for large prediction horizons. This indicates that, in the event that there are sufficiently accurate forecasts on the load and the environmental conditions of the following hours, the model is able to predict discreetly the temperatures of the system, thus allowing the optimal management of the machines.

The optimizer has been subsequently employed to perform an in-depth analysis on the economically optimal configuration of the generation section for the reference district heating network of Canavese (*A2A Milano*), in view of changes in electricity prices. The design of the plant, both in terms of generation technology and sizing of the machines, has been performed considering four different scenarios of interaction with the electrical network:

1. BASE scenario, in which electricity is sold at the zonal price (MGP market) and is purchased at a fixed price.
2. 2017 scenario, in which both the electricity buying and selling prices are the result of the participation in the day-ahead market (MGP), with reference to the 2017 market data.
3. SEN scenario, in which both the electricity buying and selling prices are the result of the participation in the day-ahead market (MGP), with reference to projected market data to 2030 and considering the SEN strategy as fulfilled.
4. MSD scenario, in which 75% of the available power is dedicated to participation in the day-ahead market (MGP), while the remaining 25% is dedicated to the dispatching services market (MSD), with reference to the 2017 market data.

The optimization has been carried out in view of the NPV of the plant at the end of the useful life of the machines (15 years) and many possible combinations for the generators size and technology have been considered.

The results of the design phase show that, except for the BASE scenario, the preferable solution is the use of only CHP, in the form of internal combustion engines, integrated with backup boilers and by a 1000 m^3 thermal storage. The use of a configuration with both combined heat&power and heat pump technologies has proved to be economically competitive, but only for a rather small HP size, which allows it to run just with the electricity produced by the CHP. Moreover, the size of the thermal storage does not seem to have particular impact on the definition of the optimum. As regards the size of the CHP generators, the general trend indicates an optimal size of about 30 MW_e. This value is consistent with the thermal demand of the reference network, which for over 93% of the operating time requires a power equal to or less than this value.

Another important result that can be drawn is that participation in both the electricity markets, MGP and MSD, seems to be highly desirable. The margins that can be obtained by dedicating a fraction of the available power to the dispatching services market are in fact very significant, indicating that it is possible to achieve much higher profits even with the same plant configuration. This is evidenced by the fact that the

most profitable solution is that of the MSD scenario, which, despite having the same configuration and operating with the same prices for the sale and purchase of electricity on the MGP market as in the 2017 scenario, manages to obtain an NPV that is 36% higher: 62.1 M€ (MSD s.) vs 45.8 M€ (2017 s.).

The optimized management of the plant and the network, which favours high electricity selling prices, together with the shape of the thermal demand curve, has led the system to sell electricity to the grid mainly during the peak hours of the electrical network. For the same reasons, the purchase of the electricity consumed by the HP is concentrated during the hours with the lowest buying price, which corresponds to the off-peak ones. This means that the system operates in an anti-cyclical manner with respect to the electricity load curve, thus determining a stabilizing effect to the benefit of the electrical network. This stabilizing effect is certainly beneficial for the electrical system, which has the possibility to reduce the production from less convenient plants.

The work has been completed by carrying out a sensitivity analysis on a number of significant variables to assess their impacts on the results of the study. The selected parameters were the following: the discount rate of the investment, the investment costs for the ICE and the HP, and the natural gas price. The changes in the value of the NPV were in line with expectations. While the optimal configuration proved to be robust with respect to a variation in the discount rate or in the HP investment cos, it resulted much more affected by variations in the ICE investment cost and in the gas price.

6.2 Future developments

The possible future developments of this thesis work can be summarized as follows:

1. Evaluation of the possible implementation in the system of non-traditional technologies, such as: electric boilers, power-to-gas systems, fuel cells, smart thermal networks, etc.. This study would require a possible introduction of faster intervention times of the control system compared to the current ones, in line with the selected technologies.
2. Evaluation of the effects on the optimization process of the presence of forecasting errors on system variables.
3. Evaluation of the influence of the district heating network characteristics on the optimization process.

Appendix A - TRNSYS Model

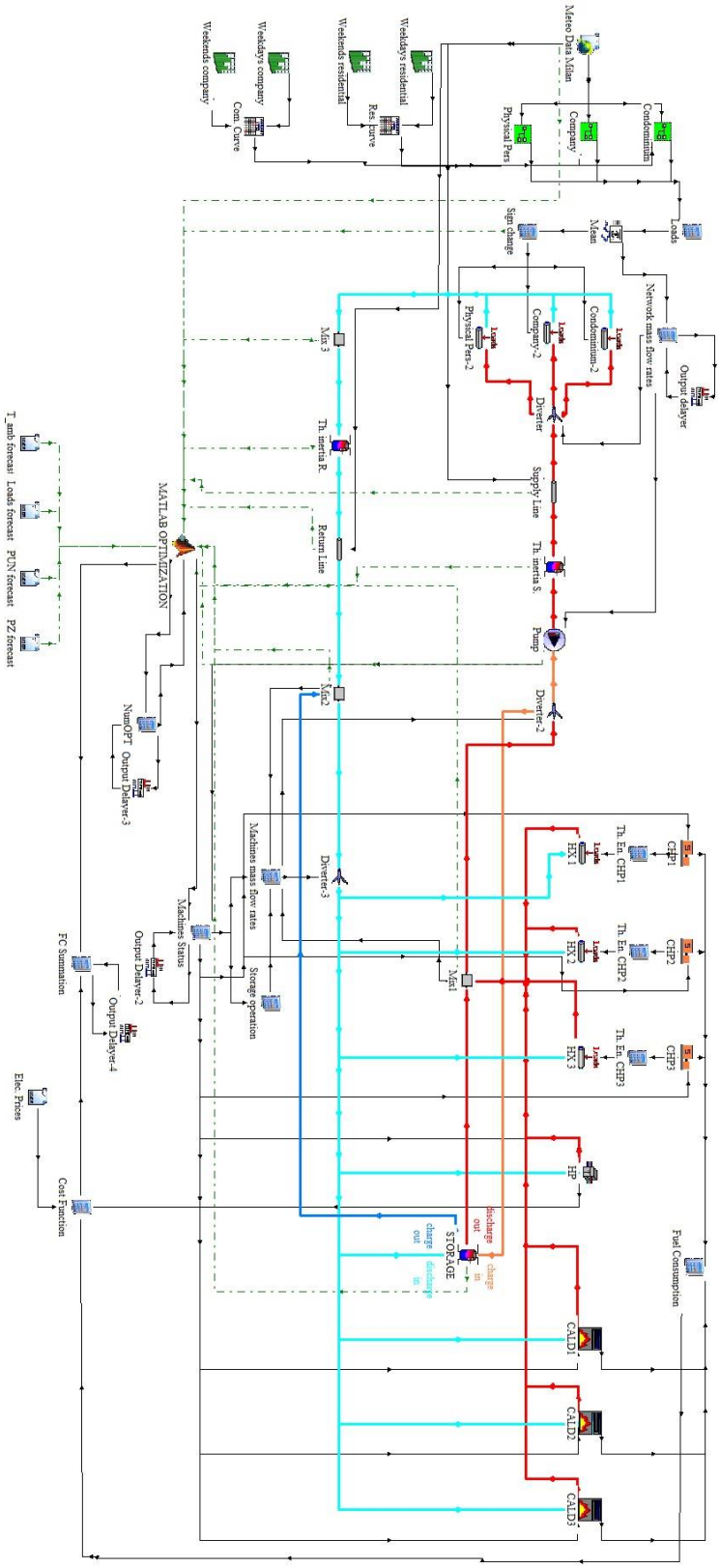

Bibliography

[1] IPCC, "*Climate Change 2014: Synthesis Report. Contribution of Working Groups I, II and III to the Fifth Assessment Report of the Intergovernmental Panel on Climate Change*". [Core Writing Team, R.K. Pachauri and L.A. Meyer (eds.)]. IPCC, Geneva, Switzerland, 2014.

[2] http://unfccc.int/paris_agreement/items/9444.php

[3] Communication from the Commission to the European Parliament, the Council, the European Economic and Social Committee and the Committee of the Regions on "A*n EU Strategy for Heating and Cooling.*". Brussels, 2016.

[4] European Commission, "*EU Energy in figures - Statistical pocketbook 2018*". 2018.

[5] "*Direttiva 2012/27/UE del Parlamento europeo e del Consiglio, del 25 ottobre 2012, sull'efficienza energetica, che modifica le direttive 2009/125/CE e 2010/30/UE e abroga le direttive 2004/8/CE e 2006/32/CE*". 2012.

[6] Jiang XS, Jing ZX, Li YZ, Wu QH, Tang WH. "*Modelling and operation optimization of an integrated energy based direct district water-heating system.*". Energy 2014;64:375-88.

[7] Lund H. "*Renewable energy systems: a smart energy systems approach to the choice and modeling of 100% renewable solutions."* 2nd ed. Burlington, USA: Academic Press; 2014. ISBN: 978-0-12-410423-5.

[8] Lund, H., Werner, S., Wiltshire, R., Svendsen, S., Thorsen, J.E., Hvelplund, F., Mathiesen, B.V. "*4th Generation District Heating (4GDH): Integrating smart thermal grids into future sustainable energy systems.*". 2014. Energy 68, 1–11.

[9] Castellazzi P., "*Efficienza energetica nelle Smart Cities: l'integrazione delle reti elettrica e termica. Predisposizione di un modello di rete di teleriscaldamento reale.*". RSE 16002202, 2015.

[10] www.a2acaloreservizi.eu/home/cms/a2a_caloreservizi/area_clienti/prezzi/

[11] U.S. Environmental Protection Agency Combined Heat and Power Partnership, "*Catalog of CHP Technologies*". 2017.

[12] Pardo Garcia N.; Vatopoulos K.; Krook-Riekkola A.; Perez Lopez A.; Olsen L., "*Best available technologies for the heat and cooling market in the European Union*". Publications Office of the European Union. 2012

[13] IEA-ETSAP, "*IEA-ETSAP - Technology Brief E16 – January 2013*". 2013

[14] Gudmundsson O., Thorsen J. E., Zhang L., "*Cost analysis of district heating compared to its competing technologies*". Denmark, 2013.

[15] IEA-ETSAP, IRENA, "*IEA-ETSAP and IRENA © Technology-Policy Brief E17 – January 2013*". 2013.

[16] F. Lanati, A. Gelmini, D. Moneta, G. Viganò, A. Iaria, M. Rapizza, "*Studi a supporto della Governance dei sistemi elettrici.*". RSE 18001055, 2017. Rapporto Ricerca di Sistema

[17] www.mercatoelettrico.org/It/download/DownloadDati.aspx?val=MSD_ServiziDispacciamento

[18] www.energy.siemens.com/us/pool/hq/power-generation/gas-turbines/downloads/Industrial%20Gas%20Turbines/E50001-G430-A100-V1-4A00_Gas%20Turbine_Broschuere_E_LR.pdf

[19] www.mercatoelettrico.org/it/Download/DatiStorici.aspx